THE QUARTERLY JOURNAL OF
MECHANICS AND APPLIED MATHEMATICS

VOLUME XIII PART 1
FEBRUARY 1960

OXFORD
AT THE CLARENDON PRESS
1960

Price 18*s. net*

PRINTED IN GREAT BRITAIN BY VIVIAN RIDLER AT THE UNIVERSITY PRESS, OXFORD

THE QUARTERLY JOURNAL OF MECHANICS AND APPLIED MATHEMATICS

THE QUARTERLY JOURNAL OF MECHANICS AND APPLIED MATHEMATICS is published at 18*s.* net for a single number with an annual subscription (for four numbers) of 60*s.* post free.

NOTICE TO CONTRIBUTORS

1. *Communication.* Papers should be communicated to Dr. D. M. A. Leggett, Department of Mathematics, King's College, Strand, London, W.C. 2.

If possible, to expedite publication, papers should be submitted in duplicate.

2. *Presentation.* Papers should be typewritten (double spacing) and should be preceded by a summary not exceding 300 words in length. References to literature should be given in standard order, *author, title of journal, volume number, date, page.* These should be placed at the end of the paper and arranged according to the order of reference in the paper.

3. *Diagrams.* The number of diagrams should be kept to the minimum consistent with clarity. The lines of the figures should be drawn in ink either on draughtsman's paper or on good quality white paper. Each individual line in the figure should bear reducing to one-half of the size of the original, and great care should be exercised to see that the lines are regular in thickness, especially where they meet. Lettering of the figure should be in pencil and should be sufficient to define clearly the lines and curves in it. The writing of formulae or of explanations on the diagram itself should be avoided. All explanations of symbols, etc., should be given in underline. Contributors should indicate on their manuscripts where figures should be inserted.

4. *Tables.* Tables should preferably be arranged so that they can be printed with the columns parallel to the longer edge of the page.

5. *Notation.* All single letters used to denote vectors in the manuscript should be marked by underlining with a wavy line. Scalar and vector products should be denoted by $\underset{\sim}{a} . \underset{\sim}{b}$ and $\underset{\sim}{a} \wedge \underset{\sim}{b}$ respectively. Real and imaginary parts of complex quantities should be denoted by re and im respectively.

6. *Offprints.* Authors of papers will be entitled to 25 free offprints. This number is available for sharing between authors of joint papers.

7. All correspondence other than that dealing with contributions should be addressed to the publishers:

OXFORD UNIVERSITY PRESS
AMEN HOUSE, LONDON, E.C. 4

[1 *front*]

THE QUARTERLY JOURNAL OF MECHANICS AND APPLIED MATHEMATICS

THE QUARTERLY JOURNAL OF MECHANICS AND APPLIED MATHEMATICS is published at 18*s.* net for a single number with an annual subscription (for four numbers) of 60*s.* post free.

NOTICE TO CONTRIBUTORS

1. *Communication.* Papers should be communicated to Dr. D. M. A. Leggett, Department of Mathematics, King's College, Strand, London, W.C.2.

If possible, to expedite publication, papers should be submitted in duplicate.

2. *Presentation.* Papers should be typewritten (double spacing) and should be preceded by a summary not exceeding 300 words in length. References to literature should be given in standard order, *author, title of journal, volume number, date, page.* These should be placed at the end of the paper and arranged according to the order of reference in the paper.

3. *Diagrams.* The number of diagrams should be kept to the minimum consistent with clarity. The lines of the figures should be drawn in ink either on draughtsman's paper or on good quality white paper. Each individual line in the figure should bear reducing to one-half of the size of the original, and great care should be exercised to see that the lines are regular in thickness, especially where they meet. Lettering of the figure should be in pencil and should be sufficient to define clearly the lines and curves in it. The writing of formulae or of explanations on the diagram itself should be avoided. All explanations of symbols, etc., should be given in underline. Contributors should indicate on their manuscripts where figures should be inserted.

4. *Tables.* Tables should preferably be arranged so that they can be printed with the columns parallel to the longer edge of the page.

5. *Notation.* All single letters used to denote vectors in the manuscript should be marked by underlining with a wavy line. Scalar and vector products should be denoted by $g \cdot h$ and $g \wedge h$ respectively. Real and imaginary parts of complex quantities should be denoted by re and im respectively.

6. *Offprints.* Authors of papers will be entitled to 25 free offprints. This number is available for sharing between authors of joint papers.

7. All correspondence other than that dealing with contributions should be addressed to the publishers:

OXFORD UNIVERSITY PRESS
AMEN HOUSE, LONDON, E.C.4

THE LARGE-SCALE CRUMPLING OF THIN CYLINDRICAL COLUMNS

By SIR ALFRED PUGSLEY *and* M. MACAULAY
(*The University, Bristol*)

[Received 11 December 1958]

SUMMARY

When a very thin metal tube of cylindrical section is compressed between parallel platens, its walls tend to buckle in and out to form a diamond pattern of deformation around the tube. This paper considers the subsequent behaviour of such tubes when the compression is continued to cause large-scale crumpling of the tube walls. The nature and mode of this crumpling is examined in the light of experimental results and, guided by an approximate theory for an idealized case, an empirical expression for the load required to effect the crumpling is obtained.

1. THE elastic buckling of very thin tubes subject to axial compression has been the subject of extensive study (**1**, **2**), both theoretical and experimental, during the first half of this century. As a result, it has become well known that for such cylindrical columns:

(*a*) The critical buckling load, as determined by experiment, is much below (roughly one-third of) that given by the classical theory based on small deflexions.

(*b*) The local buckling of the tube walls, as observed by experiment, does not conform in size or pattern with the results of classical theory. In general, the walls buckle into a diamond pattern,† each diamond being approximately square with its diagonals in the longitudinal and circumferential directions. The diamonds so formed tend to be appreciably larger than suggested by classical theory and to favour inward rather than outward deformation.

The departures from classical theory represented by (*a*) and (*b*) are now thought to be due partly to initial geometrical irregularities in the curvature of the tube walls, and partly—perhaps largely—to the non-linear support that longitudinal elements or strips of the tube walls receive from the circular circumferential strips. A circular ring provides decreasing resistance to radial compression as the inward deflexion proceeds. On this basis, a physical explanation of the preferential inward deformation of a thin cylindrical column is forthcoming, together with a qualitative explanation of the lowering of the critical buckling load and the increase in the size of the individual 'diamonds'.

2. Most of the experimental work done to date has concentrated on

† The symmetrical, concertina-like buckling characteristic of rather thicker tubes is not dealt with here.

the features (*a*) and (*b*) above, and as a result few compression tests on thin tubes have been carried to large axial strains. In recent years, however, the authors have been concerned† with studying the energy absorbed by thin tubes when they are compressed by amounts sensible in relation to their radii and/or lengths. When this is done, following upon initial buckling into the well-known diamond pattern, these buckles first become accentuated and then tend (at least over a length of the tube) to

FIG. 1 (*a*)

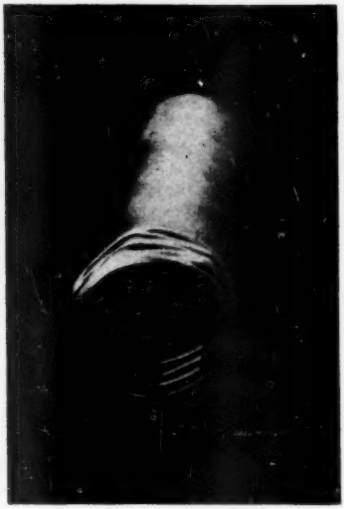

FIG. 1 (*b*)

increase in size by 'swallowing' adjoining buckles, usually until a final stage is reached when there are only three or four large diamonds around any circumference of the tube. Further compression then 'folds' these large diamonds to a closed pattern, so shortening the column in the region of the folds very considerably. This large-scale crumpling process is illustrated by the pictures given in Fig. 1.

The purpose of the present paper is to obtain a physical understanding of the crumpling process and thence, guided by a theoretical analysis of a simplified version of this process, an empirical expression for the work done in crumpling a thin tube under axial compression; and, incidentally, also an estimate of the average resistance to crumpling. It is thought that the bulk of the work done must arise from plastic deformation of the metal

† With the support of the Aluminium Development Association and the British Transport Commission.

of the tube walls; no account, therefore, will be taken of any residual elastic strain energy stored in the tube.

3. We have first to consider the geometry of the crumpling process,† and so if possible establish an idealized process embodying the main features of the practical deformations illustrated by Fig. 1. When the large-scale diamonds are established, and before any further folding or crumpling has occurred, the tube, originally circular in section, will appear essentially

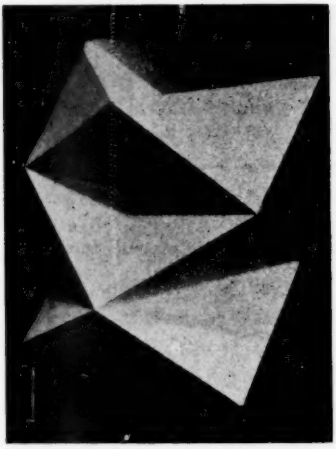

FIG. 2 (*a*)

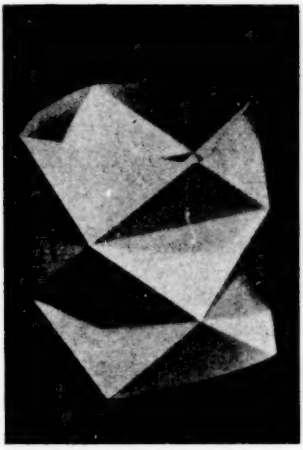

FIG. 2 (*b*)

in one or other of the forms shown in Fig. 2, accordingly as there are three or four diamonds ($n = 3$ or 4) around its circumference. At this stage, a little plastic work will have been stored along the rather sharp edges and diagonals of the diamonds and the tube will have shortened somewhat (19 per cent for $n = 3$; 8 per cent for $n = 4$). At this stage too, the plan form of the tube will appear as in Fig. 3, and if no appreciable stretching of the tube material has occurred it is evident that if d is the length of a circumferential diagonal, then

$$nd = 2\pi R, \tag{1}$$

where R is the radius of the undeformed tube.

With further compression the large 'square' diamonds collapse on themselves by folding across their circumferential diagonals and along their sides. In doing so they tend to maintain their initial plan form, so that, for example, the tube of Fig. 2 (*a*) and Fig. 3 (*a*) appears, when its diamonds

† Since this paper went to print, the authors' attention has been drawn to an interesting early contribution to this subject by A Mallock (**3**).

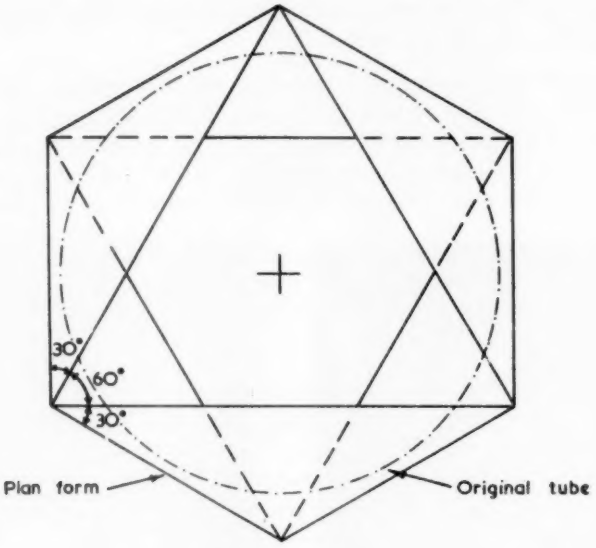
30°
60°
30°
Plan form
Original tube

(a) n = 3

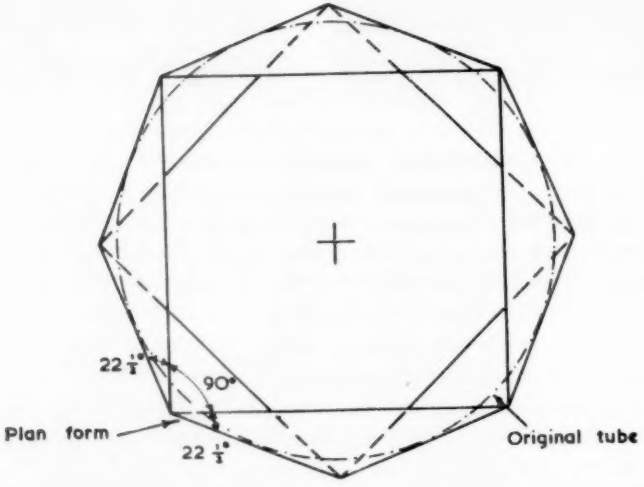
22 ½°
90°
Plan form
22 ½°
Original tube

(b) n = 4

FIG. 3

are folded flat, with a plan geometry still approximating to that of Fig. 3 (*a*). The great resistance of the metal to circumferential extension has, in effect, caused the crumpling process to be executed as though the metal walls were guided axially down rods at each of the corners of the hexagonal pattern of Fig. 3 (*a*). To a first order, therefore, the plan form of the tube when the large diamonds are first formed is also that of the tube when fully crumpled.

In this process, if the folding were perfect, the actual area of the metal walls would necessarily have been greatly reduced. Such an impossibly large reduction of area (it would be down to 59 per cent of the original area for $n = 3$ and 41 per cent for $n = 4$) is in practice avoided by the fact that the diamonds do not fold really flat along their edges and circumferential diagonals. A section at right angles to an edge or diagonal shows a finite region of circular bending and not a sudden localized fold; this is, of course, consistent with experience when one tries to bend any strip of metal locally—it develops a finite curvature in preference to a sudden kink. As a result, an appreciable part of the original wall area has, when a tube is crumpled nearly flat, gone into the roll-like edges formed, as well as into the triangular shaped flat areas.

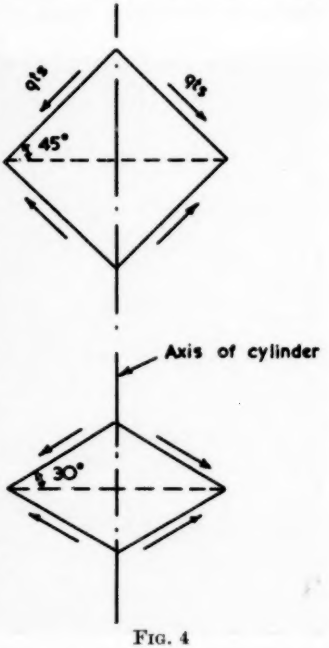

FIG. 4

It is necessary to notice also that this restricted folding process, coupled with curvature at the edges, cannot occur if the metal remains continuous without considerable shear deformation of the metal in its plane, particularly in the region of the corners of each of the flat triangles formed in plan. On the simplest view, each large diamond, originally of square shape, has, by the crumpling process, become a folded rhomboid as though sheared in the manner indicated in Fig. 4. However, on account of the way this process is restricted circumferentially, as already explained, and because it is complicated by the resulting formation of 'rolled' edges to the triangles formed, this simple shear view of the deformation is very rough indeed and the large-scale plastic deformation in shear, as indicated in Fig. 5, tends to be concentrated in the corner regions. In these regions also it is clear that some plastic extension, as well as shear, must occur.

4. Whatever the number of folded diamonds that are finally produced around the tube circumference, each diamond will have started as a square one and ended as a rhomboid folded about its circumferential diagonal. The effective length of this diagonal, initially given by equation (1) above, will remain approximately the same throughout the crumpling process; but the angle between it and any side, initially about 45°, will fall to 30° when $n = 3$ and $22\frac{1}{2}°$ when $n = 4$, as illustrated in Fig. 3.

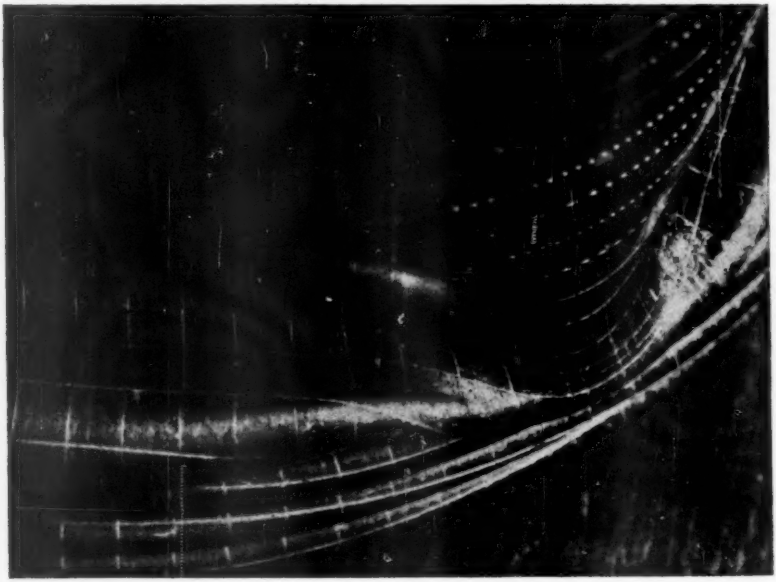

FIG. 5

On this simple geometrical basis we can now assess the energy absorbed by the deformation of the diamond pattern to the folded rhomboid pattern.

First as to the work done in plastic bending along the lines of the *final* folds. Coupled with the folding along a diagonal of length d there will also be folding along each side s of the diamond. If we consider a length of the undeformed tube equal to $\frac{1}{2}d$, corresponding to half the height of the original square diamonds, there will be foldings along two sides to be accounted for per diamond in addition to one diagonal fold, making a fold of length $(d+2s)$ in all. Now the work done per unit length of fold will be given by the product of the full plastic moment required to bend the wall plating (per unit length) freely and of the angle (π radians) through

which it is turned. On this basis, if p is the yield stress for the wall material the above plastic moment is $\frac{1}{4}pt^2$ and the total plastic work done in the folding process around the tube is given by

$$U_1 = \tfrac{1}{4}(\pi n)pt^2(d+2s) = k_1 npt^2 d, \tag{2}$$

where k_1 is a coefficient depending on the relation between s and d. For $n = 3$, $s = 0{\cdot}58d$, and $k_1 = 1{\cdot}70$; for $n = 4$, $s = 0{\cdot}54d$, and $k_1 = 1{\cdot}64$.

If we now consider the deformation of the shape of the diamonds from square to rhomboid this, as indicated in Fig. 4, can be regarded as a plastic shear distortion under forces along the sides of each diamond. If q is the average shear stress concerned, the force along any side will be qts and the work done by this action, for an angle change of θ as between square and rhomboid, will be, for the diamonds in a length of tube equal to $\frac{1}{2}d$,

$$U_2 = n\theta qts^2 = k_2 nqtd^2, \tag{3}$$

where k_2 is a coefficient depending on the relation between s and d. For $n = 3$, $k_2 = 0{\cdot}18$; for $n = 4$, $k_2 = 0{\cdot}23$.

If we now write P as the average compressive force acting on this tube during the crumpling process, we can equate the internal and external work thus:

$$\tfrac{1}{2}Pd = U_1 + U_2 = k_1 npt^2 d + k_2 nqtd^2, \tag{4}$$

and so derive

$$P = 2k_1 npt^2 + 2k_2 nqtd. \tag{5}$$

In equation (5), since k_1 and k_2 vary only slowly with n, the first term will be least when n is least; and since nd is (from (1)) constant, the second term hardly varies with n, though it is least when k_2 is least, corresponding to n being small. But n must be an integer not less than 3; hence P will be least when $n = 3$. With the appropriate values for k_1 and k_2 in (5), this becomes

$$P = 10{\cdot}2pt^2 + 1{\cdot}08qtd. \tag{6}$$

It will be convenient to compare this load P with the end load P_0 that would cause simple yielding of the tube in direct compression. With the same notation

$$P_0 = 2\pi Rtp, \tag{7}$$

and the ratio of these two loads is thus given by

$$\frac{P}{P_0} = C_1\frac{t}{R} + C_2, \tag{8}$$

where

$$C_1 = 1{\cdot}62, \qquad C_2 = 0{\cdot}36\frac{q}{p}.$$

It remains to consider the value of q/p. This ratio of yield stresses, for most metals, is of the order of 0·5; but it may well be, because of the distribution of shear noted in section 3, that q/p is effectively less than $\frac{1}{2}$. Taking $q/p = \frac{1}{3}$ as a tentative estimate,

$$\frac{P}{P_0} = 1{\cdot}6\frac{t}{R} + 0{\cdot}12. \tag{9}$$

Before proceeding to consider (8) and (9) in the light of experimental results, we have first to recall that they are based on $n = 3$ and to consider how they would be affected were n larger than 3. For $n = 4$, for example, k_1 and k_2 have already been evaluated, and (5) and (7) give at once

$$\frac{P}{P_0} = 2{\cdot}1\frac{t}{R} + 0{\cdot}15, \tag{10}$$

which is substantially greater than (9) for any value of t/R.

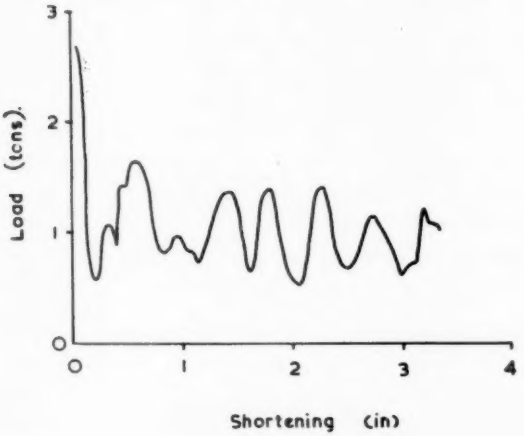

FIG. 6

5. When a thin-walled tube is slowly crushed between parallel platens, it crumples progressively in the manner illustrated by the photographs of Fig. 1. At the same time its resistance varies with the amount of shortening of the tube in the manner illustrated by the curve of Fig. 6. In order to compare experimental results with expressions such as (8) or (9), we have first to integrate the area under the curve of Fig. 6 and thence, by dividing by the total shortening of the tube, derive an average value for the resistance of the tube to crumpling. This average resistance, based on the work done in shortening the tube, will be a direct experimental measure of P in our equations.

This has now been done for a number of tubes with various values of t/R and with materials (stainless steel and soft aluminium) for which the yield stress p (taken as the 0·2 per cent proof stress) has been measured. As a result the ratio P/P_0 so determined experimentally, has been plotted against t/R in Fig. 7. Two curves are shown on the diagram against the background of the experimental points thus obtained. One corresponds

to (9) directly and the other corresponds to (8) with C_1 and C_2 chosen to give a close fit to the experimental points. It will be seen that (9) itself gives a rough approximation to the experimental results and that (8), rewritten as

$$\frac{P}{P_0} = 5\frac{t}{R} + 0{\cdot}13, \tag{11}$$

fits very well.

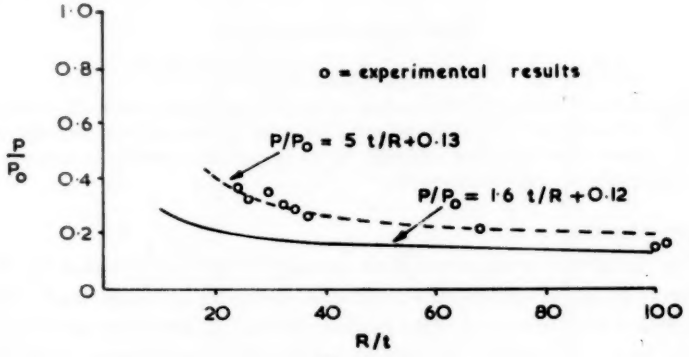

FIG. 7

6. The foregoing simple theory is given as a first approach to the problem of determining the energy absorbed in the crumpling of a very thin circular tube in compression. It has led to a form (equation (8)) capable of fitting our experimental results, but the theoretical coefficients (in equations (9) and (10)), though of the right order, clearly require to be replaced by others established experimentally. It is of interest to note that in (9) the coefficient of t/R appears more inaccurate than the constant term. This may be due partly to theoretical error, arising, for example, from the extra work done in folding at the diamond corners, but partly also to the fact that the empirical value in (11) depends largely upon experimental results for high t/R values. Here the mode of buckling is approaching a transition to the symmetrical concertina-like form typical of rather thicker tubes, for which it is known (from work by the second author, for publication elsewhere) that P/P_0 tends to vary with $\sqrt{(t/R)}$ rather than t/R. Further work bearing on these points is in hand.

REFERENCES

1. A. ROBERTSON, *The Strength of Tubular Struts*, A.R.C., R. and M. 1185 (1927).
2. G. GERARD and H. BECKER, *Handbook of Structural Stability, Part III—Buckling of Curved Plates and Shells*, N.A.C.A. Tech. Note 3783 (1957).
3. A. MALLOCK, 'Note on the instability of tubes subjected to end pressure and on the folds in a flexible material', *Proc. Roy. Soc.* A, **81** (1908).

AN APPROXIMATE ANALYSIS OF THE COLLAPSE OF THIN CYLINDRICAL SHELLS UNDER AXIAL LOADING

By J. M. ALEXANDER

(*Imperial College of Science and Technology*)

[Received 29 January 1959]

SUMMARY

An approximate theory for the process is derived, leading to a solution of the type $P = Ct^{1.5}\sqrt{D}$, where P is the collapse load, t the shell thickness, D the shell diameter, and C a constant for any given material. Good agreement is exhibited between this relationship and experimental results.

1. Introduction

In the design of nuclear reactors having vertical fuel channels, it is necessary to guard against the accidental dropping of components, either in these fuel channels, or in other vertical channels containing, for example, control rods. To absorb the energy consequent on dropping some component, it is usual to provide energy-absorbing devices. One such device takes the form of a thin cylindrical shell arranged to buckle lengthwise when hit by the dropped component.

Considerations of damage to the components set limits on the allowable loads which can be sustained during this absorption of energy. It is therefore necessary to determine a relationship which will allow prediction of the dimensions of a shell to give the required resisting load. An empirical relationship can be determined by experiment—the following note gives an approximate theory for the process, to provide a guide for the choice of the empirical formula.

2. Theory

A simple mode of collapse of the tube is assumed, and the work required to achieve this mode determined. The mean collapse load is determined by equating this work to the mean collapse load multiplied by the distance through which the load operates.

There are two *actual* modes of collapse, one in which the tube forms symmetrical convolutions so that it takes up the appearance of a bellows, the other in which both transverse and longitudinal waves are formed. This latter mode is the general mode of collapse for thin tubes, but is too complicated to use for the present purpose. A simplified version of the 'bellows' type of collapse mode is adopted, it being assumed that the shell

collapses in the form of a 'concertina' with straight-sided convolutions. One of these convolutions is illustrated diagrammatically in Fig. 1, the symbols used for the various dimensions being also shown on that figure.

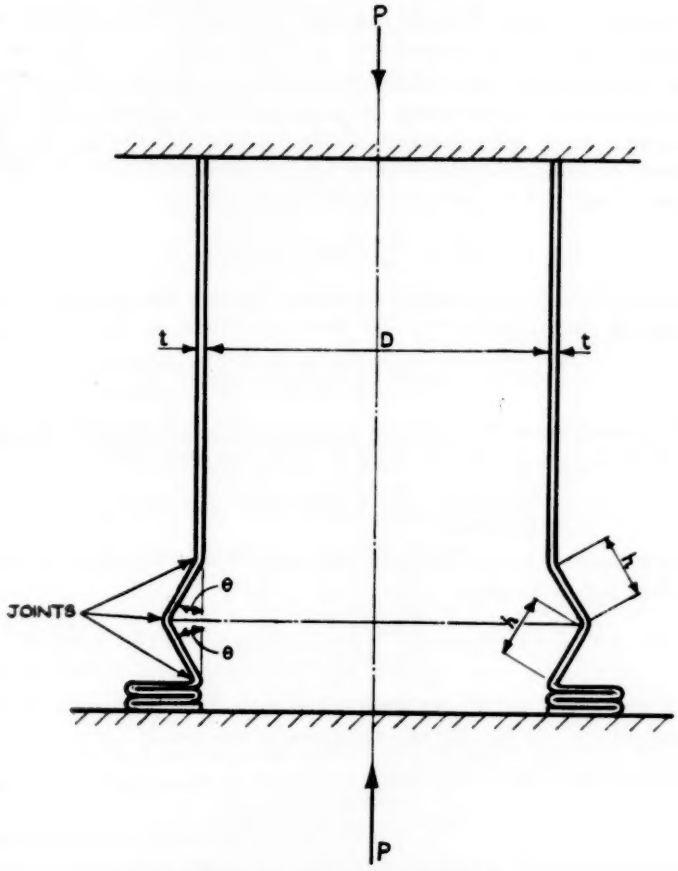

FIG. 1. Assumed collapse mode.

The work done in deforming the metal into one such convolution can be split into two parts, namely that required for bending at the circular 'joints', and that required for stretching the metal between the joints.

To simplify the analysis, elastic strains and work hardening of the material are neglected, i.e. a 'plastic-rigid' material is assumed.

During an increment $d\theta$ of the angle θ, the increment of work done at the

three joints shown is

$$dW_1 = 4M\,d\theta\,\pi(D+h\sin\theta), \tag{1}$$

where M is the collapse moment per unit circumferential length of the joint.

For a narrow beam M would be equal to $Yt^2/4$, Y being the yield stress in uniaxial tension or compression (assumed equal). In this case the 'beam' is essentially very wide and may be regarded as being deformed under substantially plane strain conditions during the incremental change $d\theta$. Under these circumstances, if the material obeys the von Mises criterion of yielding the direct stress will be raised to $(2/\sqrt{3})Y$, so that the collapse moment M will become $(2/\sqrt{3})(Yt^2/4)$. Thus

$$dW_1 = \frac{2\pi}{\sqrt{3}}Yt^2\,d\theta(D+h\sin\theta). \tag{2}$$

The mean strain in extending the metal between the joints, during the incremental change $d\theta$, is

$$\frac{\pi[D+h\sin(\theta+d\theta)]-\pi[D+h\sin\theta]}{\pi(D+h\sin\theta)} = \frac{h\,d\theta\cos\theta}{D+h\sin\theta}. \tag{3}$$

The stress in these fibres will be equal to Y, the yield stress of the metal, so that the increment of work done in stretching them will be

$$dW_2 = \frac{Yh\,d\theta\cos\theta}{D+h\sin\theta}\pi(D+h\sin\theta).2ht = 2\pi Yh^2t\,d\theta\cos\theta. \tag{4}$$

The total work done in collapsing one convolution, i.e. for θ increasing from 0 to 90°, is therefore

$$W = \int (dW_1+dW_2) = \int_0^{\frac{1}{2}\pi} \left[\frac{2\pi}{\sqrt{3}}Yt^2(D+h\sin\theta)+2\pi Yh^2t\cos\theta\right] d\theta. \tag{5}$$

This must be equal to the mean axial load $\bar{P}$ multiplied by its total displacement $2h$ (neglecting the thickness of the metal).

Hence, integrating equation (5),

$$\frac{\bar{P}}{Y} = \frac{\pi t^2}{\sqrt{3}}\left(\frac{\pi D}{2h}+1\right)+\pi ht; \tag{6}$$

h is now determined, by minimizing this expression, to give

$$h = \sqrt{\left(\frac{\pi}{2\sqrt{3}}\right)}\sqrt{(Dt)} \doteq 0{\cdot}953\sqrt{(Dt)}. \tag{7}$$

It is interesting to compare this value of h with that derived from the elastic analysis for the buckling of thin cylindrical shells,† namely

$$h = \frac{\pi\sqrt{(Dt)}}{2\{3(1-\nu^2)\}^{\frac{1}{4}}} \tag{8}$$

† Timoshenko, S., *Theory of Elastic Stability*, p. 441.

where ν = Poisson's ratio. Substituting $\nu = 0{\cdot}25$ gives

$$h = 1{\cdot}213\sqrt{(Dt)}. \tag{9}$$

Substituting $h = k\sqrt{(Dt)}$ in equation (6),

$$\frac{\overline{P}}{Y} = \left(\frac{\pi^2}{2\sqrt{3}k} + \pi k\right)t^{1{\cdot}5}\sqrt{D} + \frac{\pi t^2}{\sqrt{3}}. \tag{10}$$

An alternative mode of collapse is to assume that the convolutions are formed internally instead of externally as shown in Fig. 1. If the analysis is repeated for this case there results the following variation of equation (10):

$$\frac{\overline{P}}{Y} = \left(\frac{\pi^2}{2\sqrt{3}k} + \pi k\right)t^{1{\cdot}5}\sqrt{D} - \frac{\pi t^2}{\sqrt{3}}. \tag{11}$$

Bearing in mind the approximate nature of this analysis, and also that the true deformation mode lies somewhere between these two cases, it seems reasonable to adopt the mean value between equations (10) and (11), i.e.

$$\frac{\overline{P}}{Y} = \left(\frac{\pi^2}{2\sqrt{3}k} + \pi k\right)t^{1{\cdot}5}\sqrt{D}. \tag{12}$$

Substituting $k = 0{\cdot}953$ from equation (7) gives

$$\frac{\overline{P}}{Y} = 5{\cdot}99t^{1{\cdot}5}\sqrt{D}, \tag{13}$$

and substituting $k = 1{\cdot}213$ from equation (9) gives

$$\frac{\overline{P}}{Y} = 6{\cdot}16t^{1{\cdot}5}\sqrt{D}. \tag{14}$$

Thus, the final solution becomes of the form

$$\overline{P} = KYt^{1{\cdot}5}\sqrt{D}, \tag{15}$$

where $K \simeq 6{\cdot}08$, Y = yield strength of the material (assumed perfectly plastic), t = thickness of the cylindrical shell, D = mean diameter.

3. Comparison with experiment

Table 1 gives data relating to experiments carried out to determine the mean collapse loads for mild steel tubes.

The data are shown plotted in Fig. 2, on which the ordinates are $\overline{P}$ and the abscissae $t^{1{\cdot}5}\sqrt{D}$. The mean straight line drawn through these points and the origin has a slope $KY = 434{,}000$ lb/in.^{2} A reasonable value for the yield strength of a plastic rigid material simulating mild steel would be $Y = 70{,}000$ lb/in.^{2} giving a value of 6·2 for K, compared with 6·08 from the theoretical analysis.

TABLE 1

D (*in.*)	t (*in.*)	$t^{1\cdot5}\sqrt{D}$ (*in.*^{2})	$\bar{P}$ (*lb*)
1·43	·03	·006216	2,600
1·43	·04	·009572	4,260
1·43	·05	·013375	6,650
2·12	·03	·007569	3,450
2·12	·04	·011652	4,990
2·12	·05	·016290	6,980
2·66	·03	·008481	3,700
2·66	·04	·013052	5,610
2·66	·05	·018250	7,480

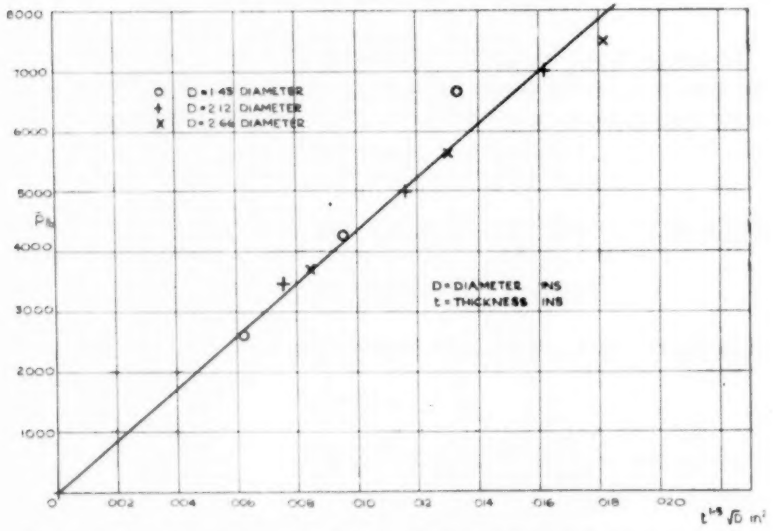

FIG. 2. Plot of mean collapse load $\bar{P}$ vs. $t^{1\cdot5}\sqrt{D}$ from tests on mild steel tubes of various diameters and thicknesses.

4. Discussion

In view of the approximate nature of the analysis presented, it is surprising that there is such good agreement with experiment. The form of solution obtained agrees well, and the numerical magnitude is of the right order. The simple theory developed here does not take into account the effect of the superimposed axial stresses on the yield criterion, or detailed consideration of the deformation mode and equilibrium conditions. In effect, the methods used are those of upper bound techniques in limit analysis, which are not generally applicable to problems in which

large deformation or buckling occurs. No attempt has been made to determine the values of maxima and minima of the load during formation of the convolutions, since it is thought that a more realistic model of the true deformation mode would be necessary to give any realistic estimate.

The main conclusion to be drawn from this analysis is that $\bar{P} = Cl^{1\cdot5}\sqrt{D}$, where C is a constant best determined by a few experiments.

5. Acknowledgement

Grateful acknowledgement is made to the English Electric Co. Ltd. for permission to publish this report, and to Mr. H. H. Heath and staff of the Experimental Section of the Atomic Power Division of that company for the experimental results quoted.

ON THE BUCKLING OF AN ANNULAR PLATE

By E. H. MANSFIELD

(*Royal Aircraft Establishment, Farnborough*)

[Received 29 January 1959]

SUMMARY

This paper considers the buckling of an infinite plate supported along two concentric circles and subjected to a uniform radial compression, or tension, along the inner circle. The solution is also applicable to a similarly loaded finite annular plate if there is a member of the requisite tensile stiffness supporting the outer circle. The effect of regularly spaced diametral supporting members is also investigated.

1. List of symbols

E	Young's modulus.
ν	Poisson's ratio, taken as 0·3 for numerical purposes.
t	plate thickness.
D	$Et^3/\{12(1-\nu^2)\}$.
r, θ	polar coordinates.
r_0, r_1	inner and outer radii.
σ_r, σ_θ	radial and hoop stresses (positive if compressive).
σ_0	radial stress at $r = r_0$ causing buckling.
w	deflexion of plate normal to surface.
β	buckling stress parameter, $t\sigma_0 r_0^2/D$.
ρ	r/r_0.
μ	r_1/r_0.
n	number of diametral nodal lines.
m	number of diametral supporting members.
f	radial variation of w (see equation (4)).
A_i	constants.
γ_i	indices defined by equation (7).
ϕ	$(\beta-1)^{\frac{1}{2}}$.
χ, λ, ψ	indices defined by equations (21), (22), (26).

2. Introduction

When a uniform radial compressive stress is applied to the circumference of a circular hole in an infinite plate, the resulting radial stresses in the plate decay inversely as the square of the distance from the centre of the circle; there are also tensile hoop stresses of the same magnitude and varying in the same way. An identical stress distribution exists in a similarly loaded annular plate, of thickness t, say, and bounded by circles of radii r_0 and r_1, if the outer circle is supported by a member

of section area $r_1 t/(1+\nu)$. Such an annular plate will buckle when the applied radial stress reaches a certain critical value, depending on the boundary conditions. If the radial stress is compressive the mode of buckling will have rotational symmetry, but if the radial stress is tensile the plate will buckle into a number of circumferential waves due to the fact that the hoop stresses are now compressive. The present paper determines the magnitude of such critical compressive and tensile radial stresses and also considers the influence of regularly spaced diametral supporting members. The analysis throws light on certain buckling phenomena due to thermal or manufacturing stresses and on the buckling behaviour of highly tapered panels.

The buckling of an annulus compressed along one boundary and free from stress along the other has been considered by Meissner (**1**), and the buckling of a uniformly compressed annulus by Yamaki (**2**).

3. Differential equation of the buckled plate

The differential equation of the buckled plate may be written in the form

$$D\nabla^4 w + t\sigma_r \frac{\partial^2 w}{\partial r^2} + t\sigma_\theta \left(\frac{1}{r}\frac{\partial w}{\partial r} + \frac{1}{r^2}\frac{\partial^2 w}{\partial \theta^2} \right) = 0, \tag{1}$$

where compressive stresses are regarded as positive. Now the radial and hoop stresses in the plate are given by

$$\sigma_r = -\sigma_\theta = \left(\frac{r_0}{r}\right)^2 \sigma_0 \tag{2}$$

so that we finally obtain

$$\left(\frac{\partial^2}{\partial r^2} + \frac{1}{r}\frac{\partial}{\partial r} + \frac{1}{r^2}\frac{\partial^2}{\partial \theta^2} \right) \left(\frac{\partial^2 w}{\partial r^2} + \frac{1}{r}\frac{\partial w}{\partial r} + \frac{1}{r^2}\frac{\partial^2 w}{\partial \theta^2} \right) + \frac{\beta}{r^2} \left(\frac{\partial^2 w}{\partial r^2} - \frac{1}{r}\frac{\partial w}{\partial r} - \frac{1}{r^2}\frac{\partial^2 w}{\partial \theta^2} \right) = 0 \tag{3}$$

where the buckling stress parameter β is given by

$$\beta = t\sigma_0 r_0^2 / D.$$

The solution of equation (3) can be expressed in the form

$$w = f(r)\cos n\theta \tag{4}$$

where n represents the number of diametral nodal lines and $f(r)$ satisfies the equation

$$\frac{d^4 f}{dr^4} + \frac{2}{r}\frac{d^3 f}{dr^3} - \frac{(1+2n^2-\beta)}{r^2}\frac{d^2 f}{dr^2} + \frac{(1+2n^2-\beta)}{r^3}\frac{df}{dr} - \frac{n^2(4-n^2-\beta)}{r^4} f = 0. \tag{5}$$

The particular case of buckling with rotational symmetry can be obtained by taking n equal to zero in equation (5).

3.1. *Integration of the differential equation*

Equation (5) is homogeneous in r and the solution may be expressed in the form

$$f = \sum_{i=1}^{4} A_i \rho^{1+\gamma_i} \tag{6}$$

where $\rho = r/r_0$

and, after some simplification,

$$\gamma_i^2 = 1+n^2-\tfrac{1}{2}\beta \pm (4n^2-2\beta n^2+\tfrac{1}{4}\beta^2)^{\frac{1}{2}}. \tag{7}$$

When there is rotational symmetry n is zero and, as β is generally greater than unity, the indices γ_i can be expressed in the simple form

$$\left.\begin{aligned} \gamma_i &= \pm 1, \pm i\phi \\ \phi &= (\beta-1)^{\frac{1}{2}} \end{aligned}\right\}. \tag{8}$$

where

3.2. *Boundary conditions*

The following different conditions along the circular boundaries are considered:

(i) zero displacement,
(ii) zero radial slope,
(iii) zero radial moment,
(iv) zero shear resultant (i.e. the shear in the plate equals the component of the applied load normal to the deflected plate).

Expressed in terms of $f(r)$, these conditions are

$$\left.\begin{aligned} &\text{(i)} \quad f = 0, \\ &\text{(ii)} \quad \frac{df}{dr} = 0, \\ &\text{(iii)} \quad \frac{d^2f}{dr^2}+\frac{\nu}{r}\frac{df}{dr}-\frac{\nu}{r^2}n^2 f = 0, \\ &\text{(iv)} \quad \frac{d^3f}{dr^3}+\frac{1}{r}\frac{d^2f}{dr^2}-(1+2n^2-\nu n^2-\beta)\frac{1}{r^2}\frac{df}{dr}+\frac{n^2(3-\nu)}{r^3}f = 0. \end{aligned}\right\} \tag{9}$$

4. Buckling with rotational symmetry

We consider here the simplest case of buckling, with rotational symmetry, which occurs when σ_0 is positive (i.e. compressive) and there are no diametral supporting members. From equations (6) and (8) we can express f (or w) in the form:

$$f = A_1+A_2\rho^2+A_3\rho\sin(\phi\ln\rho)+A_4\rho\cos(\phi\ln\rho). \tag{10}$$

For any particular buckling problem there are four boundary conditions from which four equations connecting the relative magnitudes of A_1, A_2, A_3, and A_4 may be obtained; an expression for the buckling stress is found

from the vanishing of the determinantal equation. For example, if the inner and outer circular boundaries are clamped, conditions (i) and (ii) apply; whence, writing $\mu = r_1/r_0$,

$$(\mu^2-1)(\phi^2-1)\sin(\phi \ln \mu)-2\phi\{2\mu-(\mu^2+1)\cos(\phi \ln \mu)\} = 0. \qquad (11)$$

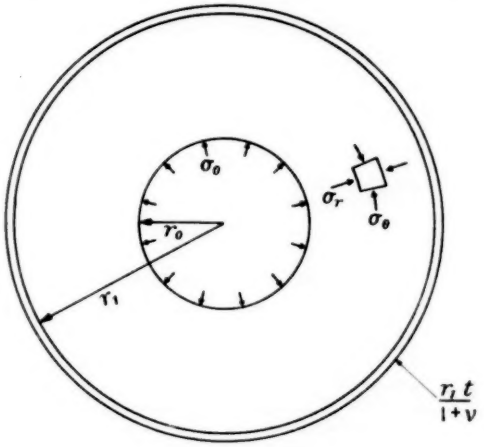

FIG. 1

Similarly, if the boundaries are simply supported, conditions (i) and (iii) apply, whence

$$(\mu^2-1)\left\{\phi^2-1+\left(\frac{\phi^2+1}{1+\nu}\right)^2\right\}\sin(\phi \ln \mu)-2\phi\{2\mu-(\mu^2+1)\cos(\phi \ln \mu)\} = 0. \qquad (12)$$

If the boundaries are free from rotation but are free to move axially, conditions (ii) and (iv) apply, whence

$$\beta = 1+\left(\frac{\pi}{\ln \mu}\right)^2. \qquad (13)$$

The buckling mode for this 'freely clamped' case is given by

$$f \propto \rho\left[\cos\left\{\pi\left(\frac{\ln \rho}{\ln \mu}\right)\right\}-\frac{\ln \mu}{\pi}\sin\left\{\pi\left(\frac{\ln \rho}{\ln \mu}\right)\right\}\right]-1. \qquad (14)$$

If the boundaries are completely free, conditions (iii) and (iv) apply, whence

$$\beta = 1-\nu^2 \qquad (15)$$

and the buckling stress is thus independent of r_1. This surprising result can be explained by a consideration of the buckling mode which is given by

$$f \propto \rho^{1-\nu}-1. \qquad (16)$$

Substituting into equation (9, iii) it will be seen that the radial bending moment is zero *everywhere*; furthermore, from simple equilibrium, if there is no shear resultant at either boundary the shear resultant is zero *everywhere*. It follows that the precise location of the outer boundary is, for this 'free-free' case, immaterial.

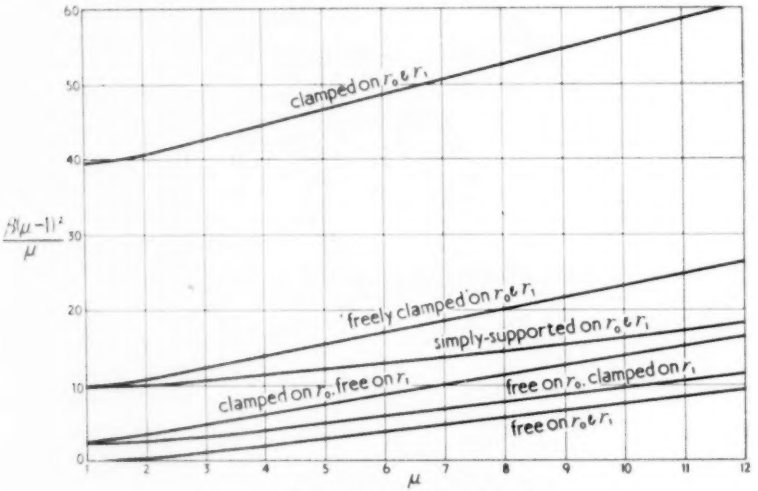

Compressive buckling of annulus

FIG. 2

If conditions (ii) and (iv) apply along the inner boundary and conditions (iii) and (iv) along the outer boundary, we find

$$\phi\cos(\phi\ln\mu)+\nu\sin(\phi\ln\mu)=0, \tag{17}$$

while if (iii) and (iv) apply to the inner boundary and (ii) and (iv) to the outer:

$$\phi\cos(\phi\ln\mu)-\nu\sin(\phi\ln\mu)=0. \tag{18}$$

The variation of the buckling stress with μ for the six cases considered in this section is plotted in Fig. 2. The ordinate in Fig. 2 has been taken to be $\beta(\mu-1)^2/\mu$, rather than β, for ease of presentation.

4.1. *Buckling stresses for infinite plate*

As r_1 tends to infinity the buckling stress depends only on the inner boundary conditions (ii) or (iii); if there is zero radial slope

$$\sigma_0 \to \frac{E}{12(1-\nu^2)}\left(\frac{t}{r_0}\right)^2 \tag{19}$$

and if there is zero radial bending moment

$$\sigma_0 \to \frac{E}{12}\left(\frac{t}{r_0}\right)^2. \tag{20}$$

5. Buckling with diametral nodal lines

If there are m regularly spaced diametral members supporting the plate and σ_0 is compressive, the buckling mode is of the form given by equation (4) with n equal to m. If σ_0 is tensile the buckling mode exhibits diametral nodal lines naturally, i.e. even if there are no supporting members.

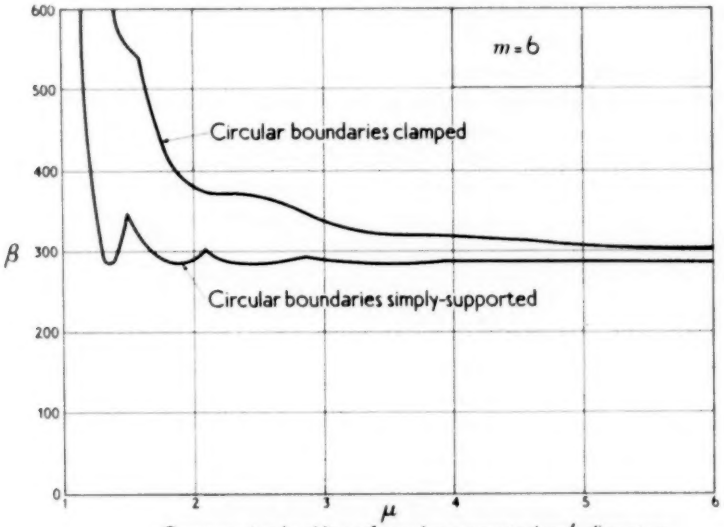

FIG. 3

5.1. *Compressive radial stresses*

Consider first the case of σ_0 compressive (i.e. positive). For this case it can be shown that the indices γ_i given by equation (7) are all imaginary and accordingly it is convenient to introduce the following symbols which are real and positive:

$$\chi = \{\tfrac{1}{2}\beta - 1 - n^2 + (4n^2 - 2\beta n^2 + \tfrac{1}{4}\beta^2)^{\frac{1}{2}}\}^{\frac{1}{2}} \tag{21}$$

and

$$\lambda = \{\tfrac{1}{2}\beta - 1 - n^2 - (4n^2 - 2\beta n^2 + \tfrac{1}{4}\beta^2)^{\frac{1}{2}}\}^{\frac{1}{2}}. \tag{22}$$

The buckling stress may now be determined by standard methods. For example, if the inner and outer circular boundaries are clamped the buckling stress is determined by

$$(\chi^2+\lambda^2)\sin(\chi \ln \mu)\sin(\lambda \ln \mu) - 2\chi\lambda\{1-\cos(\chi \ln \mu)\cos(\lambda \ln \mu)\} = 0. \tag{23}$$

Similarly, if the boundaries are simply supported

$$\left\{\chi^2+\lambda^2+\left(\frac{\chi^2-\lambda^2}{1+\nu}\right)^2\right\}\sin(\chi\ln\mu)\sin(\lambda\ln\mu)- \\ -2\chi\lambda\{1-\cos(\chi\ln\mu)\cos(\lambda\ln\mu)\}=0. \quad (24)$$

The variation of the buckling stress with μ for these two cases is plotted in Fig. 3 for the case when $n\ (=m)=6$.

As μ tends to infinity it can be shown that β is determined by the vanishing of the term in parentheses in equations (21) and (22), whence, for $m \geqslant 1$,

$$\sigma_0 \to \frac{Em^2}{3(1-\nu^2)}\left(\frac{t}{r_0}\right)^2\left\{1+\left(1-\frac{1}{m^2}\right)^2\right\}. \quad (25)$$

5.2. *Tensile radial stresses*

When σ_0 is tensile (i.e. negative), it can be shown that two of the indices γ_i given by equation (7) are imaginary and two are real. Because of this

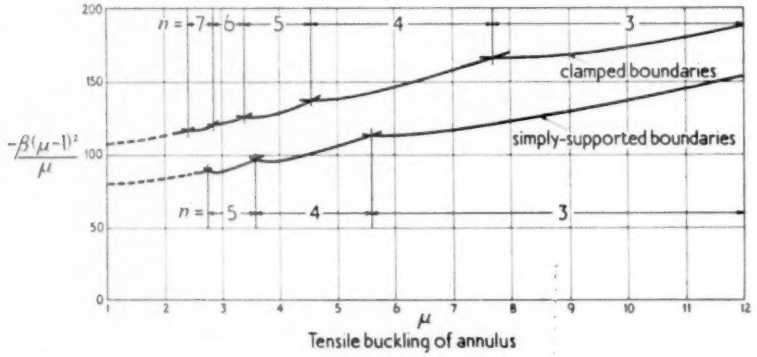

FIG. 4

we introduce the symbols χ and ψ which are real and positive, χ being given by equation (21) and ψ by

$$\psi=\{1+n^2-\tfrac{1}{2}\beta+(4n^2-2\beta n^2+\tfrac{1}{4}\beta^2)^{\frac{1}{2}}\}^{\frac{1}{2}}. \quad (26)$$

If the inner and outer boundaries are clamped the buckling stress is then given by the equation

$$(\chi^2-\psi^2)\sin(\chi\ln\mu)\sinh(\psi\ln\mu)-2\chi\psi\{1-\cos(\chi\ln\mu)\cosh(\psi\ln\mu)\}=0. \quad (27)$$

If the inner and outer boundaries are simply-supported the buckling stress is given by the equation

$$\left\{\chi^2-\psi^2+\left(\frac{\chi^2+\psi^2}{1+\nu}\right)^2\right\}\sin(\chi\ln\mu)\sinh(\psi\ln\mu)- \\ -2\chi\psi\{1-\cos(\chi\ln\mu)\cosh(\psi\ln\mu)\}=0. \quad (28)$$

If there are no diametral supporting members the method of solution of equations (27) and (28) is to assume various integral values of n for each value of μ, and solve for β; the envelope of the resulting family of curves gives the true value of β (and n). Fig. 4 shows the result of such calculations. As μ tends to infinity it can be shown that for both clamped and simply supported cases

$$\left.\begin{aligned} n &= 2 \\ \text{and} \qquad \sigma_0 &\to \frac{-E}{4(1-\nu^2)}\left(\frac{t}{r_0}\right)^2 \end{aligned}\right\}. \tag{29}$$

A comparison of this result with the corresponding result for compressive σ_0, e.g. equation (19), shows that the buckling tensile stress is three times the buckling compressive stress.

If there are m regularly spaced diametral supporting members the method of solution of equations (27) and (28) is to assume, for each value of μ, various values of n which are integral multiples of m. The envelope of the resulting family of curves gives the true value of β (and n). As μ tends to infinity it can be shown that, for $m \geqslant 2$,

$$\sigma_0 \to -\frac{E(m^2-1)}{12(1-\nu^2)}\left(\frac{t}{r_0}\right)^2. \tag{30}$$

6. Conclusions

This paper considers the buckling of an annular plate in which the radial and hoop stresses vary inversely as the square of the distance from the centre. The presence of diametral nodal lines, either imposed or occurring naturally, has been allowed for, and this has enabled the buckling behaviour under tensile, as well as compressive, radial stresses to be determined. Figures are presented giving the buckling stress as a function of the geometrical proportions of the plate for a variety of boundary conditions.

The class of problems considered is unusual in that exact solutions are available in terms of elementary functions despite the fact that the stresses are varying throughout the plate.

REFERENCES

1. E. Meissner, 'Über das Knicken kreisring-förmiger Scheiben', *Schweizerische Bauzeitung*, **101** (1933) 87–89.
2. N. Yamaki, 'Buckling of a thin annular plate under uniform compression', *J. Appl. Mech.* **25** (1958) 267–73.

THE THIN-WALLED CIRCULAR CYLINDER SUBJECTED TO CONCENTRATED RADIAL LOADS

By L. S. D. MORLEY

(*Royal Aircraft Establishment, Farnborough*†)

[Received 7 May 1959]

SUMMARY

Using a new equation governing the radial displacement of a thin-walled circular cylinder, expressions are obtained for this displacement and the resultants in an infinitely long cylinder subjected to equal and opposite concentrated radial loads. In addition, a method of numerical approximation is presented which enables the calculations to be carried out with rapidity and yet retaining an accuracy usually associated with Flügge's equations.

1. Introduction

PROBLEMS of equilibrium of thin-walled circular cylinders under various loading conditions have attracted the attention of many authors. The solution of some of these problems has required quite complex analyses, but it is significant that when numerical values are needed, resort is usually made, notwithstanding loss in accuracy, to simple approximations so that the computations are not prohibitively laborious.

For example, during the last few years, Hoff (**1**, **2**) and his collaborators have employed a simple approximation which was introduced by Donnell (**3**) in 1933 whilst investigating the torsional stability of thin-walled cylinders. Unfortunately, however, the error in this approximation becomes intolerable beyond a certain wavelength of circumferential distortion and, recognizing this, Hoff (**4**) later examined the accuracy of the trigonometric eigenfunctions arising from the equation which governs the behaviour of the radial displacement. For this purpose a more accurate, and more complex, equation derived by Flügge (**5**) was used as the standard for comparison and Hoff found that it was necessary to restrict the range of application of his previous equilibrium solutions.

Earlier, in 1946, Yuan (**6**) had used the same Donnell equation to determine the radial displacements in an infinitely long and thin-walled circular cylinder subjected to equal and opposite concentrated radial loads. However, this equation is particularly inaccurate for this purpose and so, in 1957, Yuan and Ting (**7**) presented another solution to the same problem but this time using the more accurate Flügge equation. This second

† Paper prepared whilst attending the 'Post Graduate Course in Structures and Materials', Cambridge University.

solution is much more complex but, although he found the computation tedious, Yuan discovered that his first solution gave a result some 25 per cent in error for a particular numerical example.

More recently a new equation has been introduced (**8**) and, although it has the simplicity associated with Donnell's equation, it has been demonstrated that its trigonometric eigenfunctions are in close agreement with those calculated from Flügge's equation. Now the purpose of this paper is to present an application of the new equation to the solution of Yuan's (**6**, **7**) equilibrium problem which has just been described. The analysis follows that employed by Yuan but, in addition to presenting an expression for the radial displacement, expressions are here given for the stress and moment resultants. It is further shown that important simplifications can be made to these expressions which enable the numerical calculations to be carried out with rapidity and accuracy. In the example it is shown that a brief slide rule calculation yields a value for the maximum radial displacement which is only 0·5 per cent different from that obtained by Yuan (**7**) in his second and accurate solution. The method of carrying out these simplifications is not confined to the present problem, but provides a basis for the ready and accurate solution of many further problems of thin-walled circular cylinders.

Finally, Flügge's equations are used for the stress and moment resultants although, as Hildebrand, Reissner, and Thomas (**9**) have pointed out, they contain terms of small order whose retention is not justified by the basic assumptions. However, the inclusion of such terms does not reduce the accuracy, and it is a simple matter to discard them as and when the numerical analysis shows that this is justified.

2. Notation

a	mean radius of the thin-walled cylinder.
D	flexural rigidity, $D = Eh^3/12(1-\nu^2)$.
E	Young's modulus of elasticity.
h	wall thickness.
i	$\sqrt{(-1)}$.
K	non-dimensional structural parameter, $4K^4 = 12(1-\nu^2)(a/h)^2$.
m	first even integer satisfying $5m^2(2m^2-1)^2 > 16K^4$.
M_x	bending moment resultant along a generator.
M_θ	bending moment resultant in the circumferential direction.
$M_{x\theta}$, $M_{\theta x}$	twisting moment resultants.
n	even integer.
N_x	direct stress resultant along a generator.
N_θ	direct stress resultant in the circumferential direction.

$N_{x\theta}$, $N_{\theta x}$ shear stress resultants.
P concentrated radial load applied at $x = 0$; $\theta = 0, \pi$.
q distributed radial load.
Q_x, Q_θ shear stress resultants acting normal to the surface.
u', v', w' displacements respectively along a generator, a circumference, and a radius.
u, v, w non-dimensional displacements defined by $u = u'/a$, $v = v'/a$, $w = w'/a$.
x' distance measured along a generator.
x non-dimensional distance defined by $x = x'/a$.
δ_n $(2n^2-1)/4K^2$.
κ_n $1+K^4/n^4$.
λ introduced by equation (1).
λ_{1n}, λ_{2n} roots of the auxiliary equation

$$(\lambda^2+n^2)^2(\lambda^2+n^2-1)^2+4K^4\lambda^4 = 0.$$

ν Poisson's ratio.
θ angular coordinate.

Subscripts following a comma indicate differentiation, e.g.

$$w_{,xx\theta\theta} \equiv \partial^4 w/\partial x^2\partial\theta^2.$$

Laplace's operator is denoted by ∇^2 $(\equiv \partial^2/\partial x^2+\partial^2/\partial\theta^2)$.

3. The radial displacement

The thin-walled circular cylinder subjected to equal and opposite radial loads is shown in Fig. 1 and the positive directions of the displacements and resultants are given in this figure and Fig. 2.

The method of analysis follows that employed by Yuan (6) who began by replacing the concentrated radial load P by a distributed load q expressed as a function of the coordinates along a generator and a circumference. Thus,

$$q(x,\theta) = \frac{P}{\pi^2 a^2}\lim_{\delta\to 0}\int_0^\infty \left\{\frac{\sin(\lambda\delta/a)}{(\lambda\delta/a)} + 2\sum_{n=2,4,\ldots}^{\infty}\frac{\sin(n\delta/a)\sin(\lambda\delta/a)}{(n\delta/a)(\lambda\delta/a)}\cos n\theta\right\}\cos\lambda x\, d\lambda. \tag{1}$$

Now, unlike Yuan who used first Donnell's and then Flügge's equation to govern the behaviour of the non-dimensional radial displacement w, the new equation (8)

$$\nabla^4(\nabla^2+1)^2 w+4K^4 w_{,xxxx} = \frac{a^3}{D}\nabla^4 q \tag{2}$$

is used. Substituting equation (1) into (2) and taking the limit as δ

approaches zero yields

$$w(x,\theta)=\frac{2aP}{\pi^2 D}\left\{\frac{1}{2}\int_0^\infty \frac{\cos(\lambda x)}{(\lambda^2-1)^2+4K^4}\,d\lambda+\right.$$

$$\left.+\sum_{n=2,4,\ldots}^{\infty}\cos n\theta\int_0^\infty \frac{(\lambda^2+n^2)^2\cos(\lambda x)}{(\lambda^2+n^2)^2(\lambda^2+n^2-1)^2+4K^4\lambda^4}\right\}d\lambda. \quad (3)$$

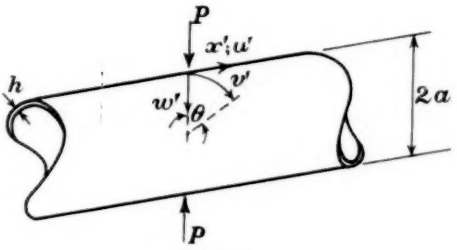

FIG. 1

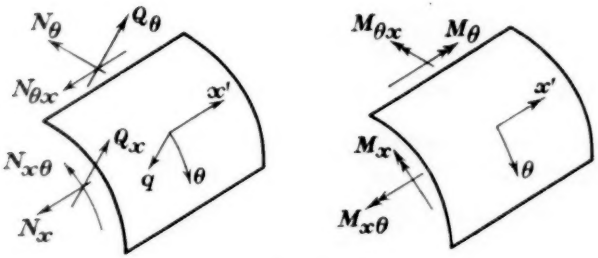

FIG. 2

The integrals in this equation are readily evaluated with the aid of the calculus of residues and it is found that

$$w(x,\theta)=\frac{aP}{2\pi D}\left[\frac{1}{4K^4}\exp\{-x(K^2-\tfrac{1}{2})^{\frac{1}{2}}\}\{(K^2+\tfrac{1}{2})^{\frac{1}{2}}\cos[x(K^2+\tfrac{1}{2})^{\frac{1}{2}}]+\right.$$

$$+(K^2-\tfrac{1}{2})^{\frac{1}{2}}\sin[x(K^2+\tfrac{1}{2})^{\frac{1}{2}}]\}-$$

$$\left.-2\sum_{n=2,4,\ldots}^{\infty}\mathrm{im}\left\{\frac{\lambda_{1n}(\lambda_{1n}^2+n^2)e^{ix\lambda_{1n}}}{(\lambda_{1n}^2+n^2-1)(\lambda_{1n}^4-n^4+n^2)}+\frac{\lambda_{2n}(\lambda_{2n}^2+n^2)e^{ix\lambda_{2n}}}{(\lambda_{2n}^2+n^2-1)(\lambda_{2n}^4-n^4+n^2)}\right\}\cos n\theta\right] \quad (4)$$

where the λ_{1n} and λ_{2n} are the roots of the auxiliary equation

$$(\lambda^2+n^2)^2(\lambda^2+n^2-1)^2+4K^4\lambda^4 = 0. \tag{5}$$

Referring to the previous paper (**8**), the roots of equation (5) are given by

$$\left.\begin{aligned}\lambda_{1n}^2 &= -n^2+\tfrac{1}{2}-iK^2\left[1-\left\{1-\frac{i(2n^2-1)}{K^2}\right\}^{\frac{1}{2}}\right]\\ \lambda_{2n}^2 &= -n^2+\tfrac{1}{2}+iK^2\left[1+\left\{1+\frac{i(2n^2-1)}{K^2}\right\}^{\frac{1}{2}}\right]\end{aligned}\right\}. \tag{6}$$

The above equations are noticeably simpler than the corresponding ones derived by Yuan (**7**) in his second and more accurate analysis employing Flügge's equation. Nevertheless, a close inspection reveals the possibility of further simplification which enables the numerical calculations to be carried out with satisfying rapidity and accuracy.

4. A method of numerical approximation

As noted by Hoff (**4**), the non-dimensional structural parameter K must have a numerical value greater than 5 because for lower values the assumptions of thin shell theory are invalid. On the other hand, K must be less than 50 otherwise the shell is so thin-walled that it can hardly fulfil structural requirements.

Bearing these values in mind and making the substitution

$$\delta_n = \frac{2n^2-1}{4K^2}, \tag{7}$$

then the first of equations (6) can be rewritten as

$$\begin{aligned}\lambda_{1n}^2 &= K^2[-2\delta_n-i\{1-(1-4i\delta_n)^{\frac{1}{2}}\}]\\ &= K^2[-2\delta_n-i\{1-(1-2i\delta_n+2\delta_n^2+4i\delta_n^3-10\delta_n^4+\ldots)\}]\\ &\doteq 2iK^2\delta_n^2(1+2i\delta_n), \quad \text{when } 5\delta_n^2 \text{ is neglected in comparison with unity.}\end{aligned}$$

In fact, the roots λ_{1n} and λ_{2n} of equation (6) can be approximated by

$$\lambda_{1n} \doteq \delta_n\lambda_{2n}, \qquad \lambda_{2n} \doteq (1+i)K(1+i\delta_n), \tag{8}$$

provided that it is agreed to neglect $5\delta_n^2$ in comparison with unity.†

† With regard to the accuracy, it is interesting to note the following. Flügge's auxiliary equation is

$$(\lambda_F^2+n^2)^2(\lambda_F^2+n^2-1)^2+4K^4\lambda_F^4+2(1-\nu)(\lambda_F^4-n^4+n^2) = 0,$$

so that if λ is a root of the present auxiliary equation (5) then

$$\lambda_F = (1+\epsilon)\lambda,$$

where the error ϵ is approximately

$$\epsilon \doteq \frac{-(1-\nu)(\lambda^4-n^4+n^2)}{2[2(\lambda^2+n^2-\frac{1}{2})(\lambda^2+n^2-1)(\lambda^2+n^2)+4K^4\lambda^2+(1-\nu)(3\lambda^4-n^4+n^2)]}$$

from Newton's approximation. If now the rough approximation is made of neglecting $4\delta_n$ in comparison with unity, it is found on employing equations (8) to (10) that the error ϵ

Furthermore, within the same approximation,

$$\left.\begin{aligned}\lambda_{1n}^4-n^4+n^2 &\doteq -n^2(n^2-1)\\ \lambda_{2n}^4-n^4+n^2 &\doteq \lambda_{2n}^4\end{aligned}\right\}. \tag{9}$$

The accuracy of equations (8) and (9) is at its best for the terms containing the smaller values of n and these terms are usually the most important constituents of the final solution.

Employing the approximations (8) and (9) together with the identities

$$\left.\begin{aligned}(\lambda_{1n}^2+n^2)(\lambda_{1n}^2+n^2-1) &\equiv -2iK^2\lambda_{1n}^2\\ (\lambda_{2n}^2+n^2)(\lambda_{2n}^2+n^2-1) &\equiv 2iK^2\lambda_{2n}^2\end{aligned}\right\}, \tag{10}$$

which are valid for all values of n, the relevant terms of equation (4) simplify to

$$\left.\begin{aligned}\frac{\lambda_{1n}(\lambda_{1n}^2+n^2)}{(\lambda_{1n}^2+n^2-1)(\lambda_{1n}^4-n^4+n^2)} &\doteq -\frac{(1+i)}{K(2n^2-1)}\left\{\frac{n^2}{n^2-1}+i\left(\frac{2n^2-1}{4K^2}\right)\right\}\\ \frac{\lambda_{2n}(\lambda_{2n}^2+n^2)}{(\lambda_{2n}^2+n^2-1)(\lambda_{2n}^4-n^4+n^2)} &\doteq -\frac{(1+i)}{4K^3}\end{aligned}\right\}. \tag{11}$$

The above approximation is not sufficiently accurate for the larger values of the even integer n, but it is then permissible to neglect unity in comparison with n^2. If, furthermore, it is assumed that

$$\lambda^2+n^2-1 \doteq \lambda^2+n^2$$

then the roots λ_{1n} and λ_{2n} of equation (6) can be approximated by

$$\left.\begin{aligned}2\lambda_{1n} &\doteq K-n\sqrt{2}(\kappa_n-1)^{\frac{1}{2}}+i\{n\sqrt{2}(\kappa_n+1)^{\frac{1}{2}}-K\}\\ 2\lambda_{2n} &\doteq K+n\sqrt{2}(\kappa_n-1)^{\frac{1}{2}}+i\{n\sqrt{2}(\kappa_n+1)^{\frac{1}{2}}+K\}\end{aligned}\right\}, \tag{12}$$

where

$$\kappa_n^2 = 1+\frac{K^4}{4n^4}, \tag{13}$$

is nearly independent of n and

$$|\epsilon| \doteq \frac{1-\nu}{4K^2}.$$

Therefore, consistently with this value of ϵ, it is sometimes permissible to neglect quantities greater than $5\delta_n^2$ in comparison with unity. On such occasions, $C(n, K)\delta_n^2$ can be neglected in comparison with unity, where

$$C(n, K) = \frac{1}{\delta_n^2}\left(\frac{1-\nu}{4K^2}\right).$$

Some typical values of $C(n, K)$ are tabulated below for Poisson's ratio $\nu = 0{\cdot}3$:

n	2	2	4	2	4	6
K	5	10	10	50	50	50
$C(n, K)$	< 5	5·7	< 5	143	7·3	< 5

Finally, since $\delta_n \geqslant 10\epsilon$ there is justification in retaining the term δ_n in the expression

$$\lambda_{2n} \doteq (1+i)K(1+i\delta_n).$$

and the identities of equation (10) can be replaced by

$$\left.\begin{aligned}\lambda_{1n}^2+n^2 &\doteq (1-i)K\lambda_{1n}\\ \lambda_{2n}^2+n^2 &\doteq (1+i)K\lambda_{2n}\end{aligned}\right\}. \tag{14}$$

Equations (12) to (14) are identical with those obtained directly from Donnell's equation and their accuracy improves as the value of n increases.

Using equations (12) to (14) the approximation corresponding to equation (11) above is

$$\left.\begin{aligned}\frac{\lambda_{1n}(\lambda_{1n}^2+n^2)}{(\lambda_{1n}^2+n^2-1)(\lambda_{1n}^4-n^4+n^2)} &\doteq \frac{i}{2K\{K\lambda_{1n}-(1+i)n^2\}}\\ \frac{\lambda_{2n}(\lambda_{2n}^2+n^2)}{(\lambda_{2n}^2+n^2-1)(\lambda_{2n}^4-n^4+n^2)} &\doteq \frac{-i}{2K\{K\lambda_{2n}-(1-i)n^2\}}\end{aligned}\right\}, \tag{15}$$

where the roots λ_{1n} and λ_{2n} are obtained from equation (12).

In a numerical application this second approximation is superior to the first one given in equations (8), (9), and (11) whenever

$$5n^2\delta_n^2 > 1,$$

or, on substituting from equation (7), whenever

$$5n^2(2n^2-1)^2 > 16K^4. \tag{16}$$

In the special case when x is zero, equation (4) for the non-dimensional radial displacement simplifies to

$$\left(\frac{a}{h}\right)\left(\frac{Eh^2}{P}\right)w(0,\theta) \doteq \frac{K}{2\pi}+\frac{2K}{\pi}\sum_{n=2,4,\ldots}^{m-2}\left\{1+\frac{2K^2n^2}{(n^2-1)(2n^2-1)}\right\}\cos n\theta+$$

$$+\frac{K^4\sqrt{2}}{\pi}\sum_{n=m,m+2,\ldots}^{\infty}\frac{(\kappa_n+1)^{\frac{1}{2}}}{n^3\kappa_n}\cos n\theta, \tag{17}$$

where m is the first even integer satisfying

$$5m^2(2m^2-1)^2 > 16K^4. \tag{18}$$

The second summation in equation (17) was first derived by Yuan (6).

The errors in the physical quantities, such as the displacements and the resultants, are of the order $(h/a)\times 100$ per cent and, consistently with this, it is assumed in the sequel that

$$h/a \text{ is negligible compared with unity} \tag{19}$$

for the first term and for those containing the smaller values of n. This has already been done in equation (17).

5. Numerical results

The maximum radial displacement occurs underneath the point of application of the concentrated radial load and Yuan (7) has calculated the values of the displacement quantity $(a/h)(Eh^2/P)w(0,0)$ using both Flügge's and Donnell's equations. His results are reproduced in Table 1 below along with those obtained from the present equation (17). The calculations are appropriate to a thin-walled cylinder with $(a/h) = 100$ and a Poisson's ratio $\nu = 0{\cdot}3$, which gives a value for the non-dimensional structural parameter of $K = 12{\cdot}85$. The value of the even integer m is soon found from equation (18) to be $m = 6$.

TABLE 1

Comparison of the Fourier coefficients for the displacement quantity $(a/h)(Eh^2/P)w(0,0)$

n	0	2	4	6	8	10
Present equation (17)	2	523	101	43	24	14
Flügge . . .	—	521	99	44	24	14
Donnell . . .	—	348	91	43	24	14

It is seen from Table 1 that there is little difference between the results obtained from the present simple calculation and those obtained at length by Yuan using the more accurate but very complex Flügge equation. Furthermore, whereas Donnell's equation yields a value for the displacement w, underneath the load, which is 25 per cent in error, the present accuracy is to within 0·5 per cent.†

6. The resultants in terms of the displacements

Attention is confined to the bending moment resultants M_θ, M_x and the direct stress resultants N_θ, N_x because it seems that these are the quantities most commonly required in practice. If needed, however, the twisting moments $M_{x\theta}$, $M_{\theta x}$ and the shear stress resultants $N_{x\theta}$, $N_{\theta x}$, Q_x, and Q_θ can be dealt with in the same way.

It is customary and concise to express the resultants in terms of the three displacements u, v, and w, but, for their calculation, it is usually more convenient for them to be expressed in terms only of the radial displacement w.

Now, when u and v are eliminated from Flügge's resultants (which are listed in the previous paper (8), they become

$$M_\theta = -\frac{D}{a}\{w_{,\theta\theta}+w+\nu w_{,xx}\}, \tag{20}$$

† See Appendix.

$$\nabla^4 M_x = -\frac{D}{a}\Big[\nabla^4\{w_{,xx}+\nu(w_{,\theta\theta}+w)\}-(1-\nu^2)w_{,xx\theta\theta}+$$
$$+\frac{1}{12}\Big(\frac{h}{a}\Big)^2\Big\{(1-2\nu)\nabla^2 w_{,xx\theta\theta}-\nabla^2 w_{,xxxx}+\frac{3(1-\nu)}{2}\,\frac{1}{12}\Big(\frac{h}{a}\Big)^2 w_{,xxxx\theta\theta}\Big\}\Big], \quad (21)$$

$$\left.\begin{aligned}\nabla^4 N_\theta &= -\frac{D}{a^2}\Big\{4K^4 w_{,xxxx}+\nabla^4(\nabla^2+1)w+(1-\nu)(w_{,\theta\theta\theta\theta}-w_{,rxxx})_{,xx}-\\ &\qquad -\frac{3\nu(1-\nu)}{2}\,\frac{1}{12}\Big(\frac{h}{a}\Big)^2 w_{,xxxx\theta\theta}\Big\}\\ &= -a\nabla^4 q+\frac{D}{a^2}\Big\{\nabla^6(\nabla^2+1)w-(1-\nu)(w_{,\theta\theta\theta\theta}-w_{,xxxx}+2w_{,\theta\theta})_{,xx}+\\ &\qquad +\frac{3\nu(1-\nu)}{2}\,\frac{1}{12}\Big(\frac{h}{a}\Big)^2 w_{,xxxx\theta\theta}\Big\}\end{aligned}\right\}, \quad (22)$$

$$\nabla^4 N_x = -\frac{D}{a^2}\Big\{4K^4 w_{,xx\theta\theta}-2(1-\nu)\nabla^2 w_{,xx\theta\theta}-\frac{3(1-\nu)}{2}\,\frac{1}{12}\Big(\frac{h}{a}\Big)^2 w_{,xxxx\theta\theta}\Big\}. \quad (23)$$

These equations contain many terms which are so small that their retention is not justified by the initial assumptions. When the substitution is made for w from equation (4), and the numerical approximations described in section 4 are applied, these small terms are revealed and can then be discarded. However, before writing down these final equations it is interesting to make a premature application of the approximations and so rewrite the above equations retaining only the significant terms. They are

$$M_\theta = -\frac{D}{a}\{w_{,\theta\theta}+w+\nu w_{,xx}\}, \quad (24)$$

$$M_x = -\frac{D}{a}\{w_{,xx}+\nu(w_{,\theta\theta}+w)\}, \quad (25)$$

$$\nabla^4 N_\theta = -\frac{4DK^4}{a^2}w_{,xxxx} \quad \text{or} \quad N_\theta = -aq+\frac{D}{a^2}\nabla^2(\nabla^2+1)w, \quad (26)$$

$$\nabla^4 N_x = -\frac{4DK^4}{a^2}w_{,xx\theta\theta}. \quad (27)$$

In arriving at equations (24) to (27)† it is necessary to neglect some terms

† The corresponding equations obtained from Donnell's approximation are

$$M_\theta = -\frac{D}{a}(w_{,\theta\theta}+\nu w_{,xx}), \qquad M_x = -\frac{D}{a}(w_{,xx}+\nu w_{,\theta\theta}),$$
$$\nabla^4 N_\theta = -\frac{4DK^4}{a^2}w_{,xxxx} \quad \text{or} \quad N_\theta = -aq+\frac{D}{a^2}\nabla^4 w,$$
$$\nabla^4 N_x = -\frac{4DK^4}{a^2}w_{,xx\theta\theta}.$$

When q and w are independent of x then the equations should satisfy those defining the behaviour of a circular ring, i.e.

$$N_\theta+\frac{1}{a}M_{\theta,\theta\theta} = N_{\theta,\theta\theta}+N_\theta = -aq \quad \text{and} \quad \Big(\frac{d^2}{d\theta^2}+1\Big)^2 w = \frac{a^3 q}{D}.$$

Equations (24) to (27) satisfy these, but Donnell's equations do not.

which are only noticeable when the wavelength of distortion is so short that the assumptions of thin shell theory are invalid. The second of equations (26) reveals the expected direct relationship between circumferential stress resultant and applied radial loading.

7. Calculation of the stress resultants

Starting with the circumferential bending moment M_θ and substituting for w from equation (4) into equation (24) there results

$$M_\theta(x,\theta) = -\frac{P}{2\pi}\left[\frac{\nu e^{-xK}}{2K}(\sin xK - \cos xK) + \right.$$
$$+2\sum_{n=2,4,\ldots}^{\infty} \mathrm{im}\left\{\frac{\lambda_{1n}(\nu\lambda_{1n}^2+n^2-1)(\lambda_{1n}^2+n^2)e^{ix\lambda_{1n}}}{(\lambda_{1n}^2+n^2-1)(\lambda_{1n}^4-n^4+n^2)} + \right.$$
$$\left.\left. + \frac{\lambda_{2n}(\nu\lambda_{2n}^2+n^2-1)(\lambda_{2n}^2+n^2)e^{ix\lambda_{2n}}}{(\lambda_{2n}^2+n^2-1)(\lambda_{2n}^4-n^4+n^2)}\right\}\cos n\theta\right], \quad (28)$$

where equation (19) is used to simplify the first term. Now, before applying the numerical approximation described in section 4, it is advantageous to take note of the consequences of equation (19) for the smaller values of the even integer n. The consequences are, for Poisson's ratio $\nu = 0{\cdot}3$, that

$$\left.\begin{array}{c} \dfrac{1}{2K^2} \text{ is negligible compared with } 0{\cdot}3 \\ |\lambda_{1n}^2| \text{ is negligible compared with } 0{\cdot}3n^4 \\ 1 \text{ is negligible compared with } 0{\cdot}3|\lambda_{2n}^2| \end{array}\right\}. \quad (29)$$

Using these, together with equations (7) to (10), the relevant terms in equation (28) simplify for the smaller values of n to

$$\left.\begin{array}{l} \dfrac{\lambda_{1n}(\nu\lambda_{1n}^2+n^2-1)(\lambda_{1n}^2+n^2)}{(\lambda_{1n}^2+n^2-1)(\lambda_{1n}^4-n^4+n^2)} \doteqdot -\dfrac{(1+i)n^2}{K(2n^2-1)} + \dfrac{(1-i)(1+\nu)n^2}{4K^3} \\ \dfrac{\lambda_{2n}(\nu\lambda_{2n}^2+n^2-1)(\lambda_{2n}^2+n^2)}{(\lambda_{2n}^2+n^2-1)(\lambda_{2n}^4-n^4+n^2)} \doteqdot \dfrac{\nu(1-i)}{2K} - \dfrac{(1+i)(1+\nu)n^2}{4K^3} \end{array}\right\}. \quad (30)$$

This approximation is insufficiently accurate for the larger values of n, but it is then possible to neglect unity in comparison with n^2. Using equations (10) and (12) to (15), equation (30) becomes

$$\left.\begin{array}{l} \dfrac{\lambda_{1n}(\nu\lambda_{1n}^2+n^2-1)(\lambda_{1n}^2+n^2)}{(\lambda_{1n}^2+n^2-1)(\lambda_{1n}^4-n^4+n^2)} \doteqdot \dfrac{\nu(1+i)}{2K} + \dfrac{i(1+\nu)n^2}{2K\{K\lambda_{1n}-(1+i)n^2\}} \\ \dfrac{\lambda_{2n}(\nu\lambda_{2n}^2+n^2-1)(\lambda_{2n}^2+n^2)}{(\lambda_{2n}^2+n^2-1)(\lambda_{2n}^4-n^4+n^2)} \doteqdot \dfrac{\nu(1-i)}{2K} - \dfrac{i(1+\nu)n^2}{2K\{K\lambda_{2n}-(1-i)n^2\}} \end{array}\right\}, \quad (31)$$

where the roots λ_{1n} and λ_{2n} are given by equation (12). Equations (28), (30), and (31) combine to give a particularly simple expression for M_θ when

x is zero, i.e.

$$M_\theta(0,\theta) \doteq \frac{P}{2\pi}\left[\frac{\nu}{2K} + \sum_{n=2,4,\ldots}^{m-2}\left\{\frac{2n^2}{K(2n^2-1)} + \frac{\nu}{K} + \frac{n^2(1+\nu)}{K^3}\right\}\cos n\theta + \right.$$
$$\left. + \frac{\sqrt{2}(1+\nu)}{2}\sum_{n=m,m+2,\ldots}^{\infty}\frac{(\kappa_n+1)^{\frac{1}{2}}}{n\kappa_n}\cos n\theta\right], \quad (32)$$

where κ_n is given by equation (13) and the value of the even integer m is inferred from equation (18). The infinite series converges as $\cos n\theta/n$ which is too slow for practical computation, but advantage can be taken of the known summation

$$\sum_{n=2,4,\ldots}^{\infty}\frac{\cos n\theta}{n} = -\tfrac{1}{2}\log(2\sin\theta). \quad (33)$$

Underneath the point of application of the concentrated radial load, where both x and θ are zero, it is seen from equation (32) that the bending moment is infinite and this is in agreement with the results of the elementary theory of bending of flat plates.

The explicit equations are not given for the bending moment resultant M_x along a generator because, from equations (24) and (25), it is readily seen that

$$\left(\frac{M_x+M_\theta}{D}\right) = (1+\nu)\left[\frac{M_\theta(x,\theta)}{D}\right]_{\nu=1}. \quad (34)$$

The stress resultant N_θ in the circumferential direction is given by equation (26) and on substitution for w from equation (4) it is found that

$$N_\theta(x,\theta) = -aq - \frac{P}{2\pi a}\left[Ke^{-xK}(\cos xK + \sin xK) + \right.$$
$$\left. + 2\sum_{n=2,3,\ldots}^{\infty}\operatorname{im}\left\{\frac{\lambda_{1n}(\lambda_{1n}^2+n^2)^2 e^{ix\lambda_{1n}}}{(\lambda_{1n}^4-n^4+n^2)} + \frac{\lambda_{2n}(\lambda_{2n}^2+n^2)^2 e^{ix\lambda_{2n}}}{(\lambda_{2n}^4-n^4+n^2)}\right\}\cos n\theta\right]. \quad (35)$$

The relevant terms in this equation can be approximated by, for the smaller values of n,

$$\left.\begin{aligned}\frac{\lambda_{1n}(\lambda_{1n}^2+n^2)^2}{(\lambda_{1n}^4-n^4+n^2)} &\doteq -\frac{(1+i)n^2}{2K}\\ \frac{\lambda_{2n}(\lambda_{2n}^2+n^2)^2}{(\lambda_{2n}^4-n^4+n^2)} &\doteq (1+i)K + \frac{(1-i)n^2}{2K}\end{aligned}\right\}, \quad (36)$$

where equations (7) to (9) and (29) have been used. For the larger values of n, where it is possible to neglect unity in comparison with n^2, equations

(36) become

$$\left.\begin{aligned}\frac{\lambda_{1n}(\lambda_{1n}^2+n^2)^2}{(\lambda_{1n}^4-n^4+n^2)} &\doteq (1-i)K+\frac{n^2K}{K\lambda_{1n}-(1+i)n^2}\\ \frac{\lambda_{2n}(\lambda_{2n}^2+n^2)^2}{(\lambda_{2n}^4-n^4+n^2)} &\doteq (1+i)K+\frac{n^2K}{K\lambda_{2n}-(1-i)n^2}\end{aligned}\right\}, \tag{37}$$

where the roots λ_{1n} and λ_{2n} are given by equation (12). When x is zero, equations (35) to (37) combine to give

$$N_\theta(0,\theta) \doteq -aq-\frac{P}{2\pi a}\Big\{K+\frac{2}{K}\sum_{n=2,4,\ldots}^{m-2}(K^2-n^2)\cos n\theta+ \\ +K^2\sqrt{2}\sum_{n=m,m+2,\ldots}^{\infty}\frac{(\kappa_n-1)^{\frac{1}{2}}}{n\kappa_n}\cos n\theta\Big\}, \tag{38}$$

where κ_n is given by equation (13) and the value of the even integer m is inferred from equation (18). The infinite series converges quite rapidly.

Finally, the stress resultant N_x along a generator is given by equation (27) which, on substitution for w from equation (4), becomes

$$N_x(x,\theta)=\frac{P}{\pi a}\sum_{n=2,4,\ldots}^{\infty}\operatorname{im}\Big\{\frac{4K^4n^2\lambda_{1n}^3e^{i.x\lambda_{1n}}}{(\lambda_{1n}^2+n^2-1)(\lambda_{1n}^2+n^2)(\lambda_{1n}^4-n^4+n^2)}+ \\ +\frac{4K^4n^2\lambda_{2n}^3e^{i.x\lambda_{2n}}}{(\lambda_{2n}^2+n^2-1)(\lambda_{2n}^2+n^2)(\lambda_{2n}^4-n^4+n^2)}\Big\}\cos n\theta. \tag{39}$$

For the smaller values of n, the relevant terms in this equation can be simplified to

$$\left.\begin{aligned}\frac{4K^4n^2\lambda_{1n}^3}{(\lambda_{1n}^2+n^2)(\lambda_{1n}^2+n^2-1)(\lambda_{1n}^4-n^4+n^2)} &\doteq \frac{K(2n^2-1)(1-i)}{2(n^2-1)}\Big(1+\frac{in^2}{2K^2}\Big)\\ \frac{4K^4n^2\lambda_{2n}^3}{(\lambda_{2n}^2+n^2)(\lambda_{2n}^2+n^2-1)(\lambda_{2n}^4-n^4+n^2)} &\doteq -\frac{n^2(1-i)}{2K}\end{aligned}\right\}, \tag{40}$$

where equations (7) to (10) and (29) have been used. For large values of n, where it is possible to neglect unity in comparison with n^2, equation (40) becomes

$$\left.\begin{aligned}\frac{4K^4n^2\lambda_{1n}^3}{(\lambda_{1n}^2+n^2)(\lambda_{1n}^2+n^2-1)(\lambda_{1n}^4-n^4+n^2)} &\doteq -\frac{n^2K}{K\lambda_{1n}-(1+i)n^2}\\ \frac{4K^4n^2\lambda_{1n}^3}{(\lambda_{2n}^2+n^2)(\lambda_{2n}^2+n^2-1)(\lambda_{2n}^4-n^4+n^2)} &\doteq -\frac{n^2K}{K\lambda_{2n}-(1-i)n^2}\end{aligned}\right\}, \tag{41}$$

where the roots λ_{1n} and λ_{2n} are given in equation (12). When x is zero,

equations (39) to (41) combine to give

$$N_x(0,\theta) \doteq -\frac{P}{2\pi a}\left[\frac{1}{K}\sum_{n=2,4,\ldots}^{m-2}\left\{\left(\frac{2n^2-1}{n^2-1}\right)K^2-\frac{(4n^2+1)}{2}\right\}\cos n\theta+\right.$$

$$\left.+K^2\sqrt{2}\sum_{n=m,m+2,\ldots}^{\infty}\frac{(\kappa_n-1)^{\frac{1}{2}}}{n\kappa_n}\cos n\theta\right], \quad (42)$$

where κ_n is given by equation (13) and the value of the even integer m is inferred from equation (18). The infinite series in this last equation is identical to that in equation (38) for the stress resultant $N_\theta(0,\theta)$ in the circumferential direction.

No numerical values are given for the resultants because it seems that there are no values determined experimentally or calculated from Flügge's equations with which to obtain a comparison. It has, however, been demonstrated how to obtain expressions for the resultants which are simple and which have an accuracy of the order of $(h/a)\times 100$ per cent.

APPENDIX

In a further and recent paper, which came to the author's notice after completion of the present paper, Ting and Yuan (**10**) have again re-examined the problem but this time using the 'complete Donnell equation'

$$\nabla^8 w + 2w_{,\theta\theta\theta\theta\theta\theta} + w_{,\theta\theta\theta\theta} + 4K^4 w_{,xxxx} = \frac{a^3}{D}\nabla^4 q,$$

which was introduced by Donnell in 1938 (**11**). This equation, which contains all the vital constituents present in Flügge's equation, seems to have remained unknown and unused until now.

Corresponding to equation (17), Ting and Yuan obtain

$$\left(\frac{a}{h}\right)\left(\frac{Eh^2}{P}\right)w(0,\theta) \doteq \frac{2K}{\pi}\sum_{n=2,4,\ldots}^{m-2}\frac{K^2}{n^2(1-n^{-2})^{\frac{1}{2}}}\cos n\theta+\frac{K^4\sqrt{2}}{\pi}\sum_{n=m,m+2,\ldots}^{\infty}\frac{(\kappa_n+1)^{\frac{1}{2}}}{n^3\kappa_n}\cos n\theta,$$

where m is now, presumably, the first even integer satisfying $m^2 > K$.

For $a/h = 100$, this leads to a value of $m = 4$ and the following supplement to Table 1 above.

Supplement to Table 1

Fourier coefficients for the displacement quantity

$(a/h)(Eh^2/P)w(0,0)$

n	0	2	4	6	8	10
'complete Donnell equation'	—	520	91	43	24	14

REFERENCES

1. N. J. Hoff, Joseph Kempner, and Frederick V. Pohle, 'Line load applied along generators of thin-walled circular cylindrical shells of finite length', *Quart. App. Math.* **11** (1953) 411.

2. N. J. Hoff, 'Boundary-value problems of the thin-walled circular cylinder', *J. App. Mech.* **21** (1954) 343.
3. L. H. Donnell, *Stability of Thin-walled Tubes under Torsion*, N.A.C.A. Report No. 479 (1933).
4. N. J. Hoff, 'The accuracy of Donnell's equations', *J. App. Mech.* **22** (1955) 329.
5. W. Flügge, *Statik und Dynamik der Schalen* (Berlin, 1934), pp. 110 et seq.
6. Shao Wen Yuan, 'Thin cylindrical shells subjected to concentrated loads', *Quart. App. Math.* **4** (1946) 13.
7. S. W. Yuan and L. Ting, 'On radial deflections of a cylinder subjected to equal and opposite concentrated radial loads', *J. App. Mech.* **24** (1957) 278.
8. L. S. D. Morley, 'An improvement on Donnell's approximation for thin-walled circular cylinders', *Quart. J. Mech. App. Math.* **12** (1959) 89.
9. F. B. Hildebrand, E. Reissner, and G. B. Thomas, *Notes on the Foundations of the Theory of Small Displacements of Orthotropic Shells*, N.A.C.A. Technical Note No. 1833 (1949).
10. L. Ting and S. W. Yuan, 'On radial deflection of a cylinder of finite length with various end conditions', *Jour. Aero. Sci.* **25** (1958) 230.
11. L. H. Donnell, 'A discussion of thin-shell theory', *Proceedings of the Fifth International Congress of Applied Mechanics, Cambridge, Mass.* (1938) 66.

NOTE ON A PAPER BY G. M. L. GLADWELL 'SOME MIXED BOUNDARY VALUE PROBLEMS OF AEOLOTROPIC THIN PLATE THEORY'

By F. J. HAWLEY

(*City of Portsmouth College of Technology*)

[Received 4 June 1959]

SUMMARY

In section 5 of Gladwell's paper (**1**) it is stated: 'The author believes, but has been unable to prove, that κ_1, κ_2 are positive in the general case.' This note proves that κ_1, κ_2 are positive for the general case of digonal symmetry.

1. Introduction

Gladwell (**1**) in his discussion of the mixed boundary-value problem for the half-plane introduces a parameter κ satisfying the equation

$$\left.\begin{aligned}&(A\bar{A}-BC)\kappa^2+(B^2+C^2-2A\bar{A})\kappa+(A\bar{A}-BC)=0\\ \text{where}\quad &A=a_3\left(\frac{\gamma_1+\gamma_2}{\gamma_1\gamma_2}\right)+a_2\\ &B=a_1-\frac{a_3}{\gamma_1\gamma_2}\\ &C=a_3\bar{\gamma}_1\bar{\gamma}_2-a_1\end{aligned}\right\},\tag{1.1}$$

and γ_1, γ_2 are the two roots of

$$a_3+2a_2\gamma+(2a_1+a_4)\gamma^2+2\bar{a}_2\gamma^3+\bar{a}_3\gamma^4=0\tag{1.2}$$

satisfying $|\gamma_1|<1$, $|\gamma_2|<1$. Gladwell proves that the roots κ_1, κ_2 are always real and that they are positive when the material is orthotropic. It will now be proved that κ_1, κ_2 are positive in the general case of digonal symmetry; this completes Gladwell's solution of the mixed boundary-value problem for the half-plane.

2. Method

If we put $\gamma_1=r_1e^{i\theta_1}$, $\gamma_2=r_2e^{i\theta_2}$ where $r_1<1$, $r_2<1$ and write

$$\theta_1-\theta_2=\phi,\quad s_1=r_1+1/r_1,\quad s_2=r_2+1/r_2$$

then it may be shown by using the relationships between the roots and coefficients of (1.2) that

$$\begin{aligned}a_3&=Re^{i(\theta_1+\theta_2)},\\ a_2&=-\tfrac{1}{2}Re^{i\theta_2}(s_1+s_2e^{i\phi}),\\ 2a_1+a_4&=R(s_1s_2+2\cos\phi)\end{aligned}$$

so that

$$BC-A\bar{A} = a_1 R\left(r_1 r_2+\frac{1}{r_1 r_2}\right)-a_1^2-\frac{R^2}{4}\left[(1+r_1^2 r_2^2)\left(\frac{1}{r_1^2}+\frac{1}{r_2^2}\right)+\right.$$
$$\left.+2\cos\phi\left(r_1-\frac{1}{r_1}\right)\left(r_2-\frac{1}{r_2}\right)\right]. \quad (2.1)$$

The positive-definiteness of the elastic energy function demands, in the general case of digonal symmetry, that the determinant

$$G \equiv \begin{vmatrix} a_1 & \bar{a}_2 & \bar{a}_3 \\ a_2 & a_4 & \bar{a}_2 \\ a_3 & a_2 & a_1 \end{vmatrix}$$

and all its principal minors shall be positive. The conditions $a_1 > 0$, $a_1^2 > a_3\bar{a}_3$, and $G > 0$ yield

$$\tfrac{1}{2}R^2(1+r_1^2 r_2^2)(1/r_1^2+1/r_2^2) < a_1 R s_1 s_2 - 2a_1^2 \quad (2.2)$$

and

$$a_1 > R\cos\phi. \quad (2.3)$$

If (2.2) is substituted into (2.1) it is found that

$$BC-A\bar{A} > \tfrac{1}{2}R(a_1-R\cos\phi)(r_1-1/r_1)(r_2-1/r_2)$$
$$> 0$$

and this is the condition for κ_1, κ_2 to be positive.

REFERENCES

1. G. M. L. Gladwell, *Quart. J. Mech. App. Math.* **12** (1959) 72.
2. —— *Studies in Complex Variable treatment of Isotropic and Anisotropic thin plates*, Ph.D. Thesis, London, 1957.

THE DAMPING EFFECT OF DISTRIBUTED AND CONCENTRATED RESISTANCES ON SMALL PERTURBATIONS IN A UNIFORM FLOW

By A. P. BURGER† *and* T. W. VAN DER LINGEN‡

[Received 5 February 1959]

SUMMARY

The damping effect of a distributed resistance on small stationary harmonic perturbations in a uniform incompressible flow is theoretically analysed for the two-dimensional case. A quadratic friction law is assumed.

A solution is obtained for the damping factor and simplified versions are found for the cases of widely distributed resistances and concentrated resistances. These solutions have applications to the damping effect of flat plate heaters used in blow-down tunnels and gauze wire screens respectively. It is shown that there is good agreement between the theoretical result for a concentrated resistance and experimental results achieved on gauze screens by previous investigators.

Notation

a	half-length of resistance plates.
h	friction factor.
k	drag coefficient.
l	perturbation wavelength in y-direction.
p	wave number $= 2\pi/l$.
u, v	perturbation velocity components.
x, y	space coordinates.
A	non-dimensional half-length of resistance plates.
L, M, N	flow regions as indicated in Fig. 1.
P	non-dimensional wave number.
U	constant speed of basic current.
V	total flow speed.
X, Y	non-dimensional space coordinates.
$\alpha_s, \beta_s, \gamma_s$	integration constants.
γ_2/γ_1	damping factor.
ζ	vorticity.
λ_s	solutions of equation (6).
Π	(perturbation) pressure.
ρ	fluid density.
ψ	perturbation stream function.
Ψ	x-dependent part of ψ.
ϕ	non-dimensional form of Ψ.

† National Physical Research Laboratory, South African C.S.I.R., Pretoria.

‡ National Mechanical Engineering Research Institute, South African C.S.I.R., Pretoria.

1. Introduction

The damping effect of concentrated resistances, such as gauze screens, on small perturbations in a uniform flow has been analysed by Prandtl (**1**), Collar (**2**), and Taylor and Batchelor (**3**). The results of the first two authors were embodied by Taylor and Batchelor in a relation for damping in which they used a factor α determined by the directions of the perturbations when entering and leaving the screen. They established the value of α by means of experiments on an undisturbed flow and found good correlation with the experimental results of Collar and MacPhail (**3**) for gauze screens.

Recent advances in the technique of pressure driven intermittent wind-tunnels have, however, brought forward the need for an analytical method of determining the damping effect of a distributed resistance in a uniform stream. A flat plate temperature stabilizer of the type conceived by van Spiegel (**4**) may be used to damp out perturbations in the tunnel flow, if it is placed behind the blow-down valve. The temperature stabilizer consists of flat plates set parallel to each other and to the air stream which, by virtue of their heat capacity, limit the drop in temperature of the air stream during the blow-down period.

With such an arrangement two possibilities, which may be treated two-dimensionally, arise. The first is that of perturbations distributed in a plane at right angles to the plates. If incompressible flow is assumed, the velocity between a pair of plates will be constant and the flow at the exit will be parallel to the plates. In (**3**) it is shown that in this case the original solution due to Prandtl will apply.

The second possibility is that there are perturbations in a plane parallel to the plates, so that the flow between a pair of plates is to be considered and the plates themselves do not constrain the flow. This case is treated in the present analysis. If the static pressure at normal sections of the flow is then assumed constant, a useful approximation to the damping effect may be found in a simple manner. In section 5 it is derived in the form $u_2/u_1 = e^{-2ha}$, where u_2/u_1 is the ratio of the amplitude of perturbations before and after damping and $2ha$ is the total resistance coefficient of the plates.

From physical considerations it may be deduced that the condition of constant static pressure at normal sections will apply when the length of the element forming the distributed resistance is large compared with the scale of the perturbations. In this case sharp curvature of the streamlines with the attendant normal pressure gradients will not be required to redistribute the flow.

However, it is not clear from this result how long a resistance element should in fact be, before the above damping equation will apply. On the other hand, the solution for gauze screens is applicable when the length of resistance element is very short compared with the scale of the perturbations that are being damped.

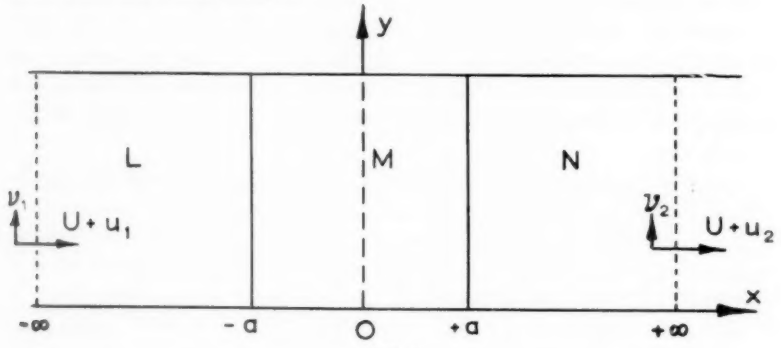

FIG. 1

In order to determine the damping effect of distributed resistances, a solution must therefore be found in terms of the length of the resistance element and the wavelength of the perturbation. This solution may be expected to yield the results for a very long resistance element and for a gauze screen when the ratio of wavelength to length of resistance element tends to zero and to infinity respectively. The solution derived below yields the above-mentioned constant static pressure result, and a useful approximation to the behaviour of gauze screens, in the respective limiting cases.

2. Idealized arrangement

The idealized two-dimensional arrangement, in which a solution for the damping is sought, is shown in Fig. 1. We consider a uniform two-dimensional incompressible flow of velocity U in the X-direction, with small stationary perturbations u and v in the X- and Y-directions respectively. The perturbation passes over a region L from $x = -\infty$ to $x = -a$ in which there is no resistance, followed by a region M from $x = -a$ to $x = +a$ in which resistance is proportional to the square of speed, and by a final region N from $x = +a$ to $x = +\infty$ in which there is again no resistance.

This corresponds to the set-up of Taylor and Batchelor (**3**), with the gauze screen replaced by a third flow region subject to distributed resistance.

3. Flow equations

As the third dimension, normal to the resistance plates, has been omitted, the resistance is taken to act uniformly on the flow in the middle region M. We assume a quadratic law, so that the magnitude of the resistance force per unit mass is

$$\tfrac{1}{2}hV^2$$

where V is the speed and h is a proportionality factor. Denoting the pressure by Π, the equations of motion are then

$$\dot{u}' = -\frac{\Pi'_x}{\rho} - \tfrac{1}{2}hVu' \tag{1}$$

$$\dot{v} = -\frac{\Pi_y}{\rho} - \tfrac{1}{2}hVv, \tag{2}$$

in which dots denote time derivatives, subscripts x and y denote partial differentiation, while u and Π_x with primes indicate values pertaining to the total field of flow, i.e. basic current plus perturbation.

Forming the curl of these equations, and denoting vorticity by ζ, yields

$$\dot{\zeta} = -\tfrac{1}{2}h\{V\zeta + vV_x - (U+u)V_y\}$$

which, on linearization with respect to the uniform basic current, becomes

$$U\zeta_x = -\tfrac{1}{2}h(U\zeta - UV_y) = -\tfrac{1}{2}hU(v_x - u_y - u_y)$$

i.e.

$$\zeta_x = h(u_y - \tfrac{1}{2}v_x).$$

In the regions L and N of free flow, h vanishes, so that we have in the three regions

$$\zeta_x = \begin{cases} h(u_y - \tfrac{1}{2}v_x) & (|x| < a) \\ 0 & (|x| > a). \end{cases}$$

Since the flow is assumed incompressible, a perturbation stream function ψ exists such that $u = -\psi_y$ and $v = \psi_x$, and the equations become

$$\nabla^2\psi_x = \begin{cases} h(-\psi_{yy} - \tfrac{1}{2}\psi_{xx}) & (|x| < a) \\ 0 & (|x| > a). \end{cases}$$

If the problem is further simplified by making the variation of the perturbation sinusoidal in y, so that

$$\psi = \Psi(x)\sin py$$

we get $$\Psi'''' - p^2\Psi'' = \begin{cases} h(p^2\Psi - \tfrac{1}{2}\Psi'') & (|x| < a) \\ 0 & (|x| > a) \end{cases}$$

where accents denote derivatives with respect to x. Finally, non-dimensional quantities are introduced by taking l/h as unit of length and U as unit of speed, viz.

$$X, Y, A = hx, hy, ha,$$

$$\phi(X) = \frac{h}{U}\Psi(x),$$

$$P = \frac{p}{h}.$$

The equations then become

$$\phi''' + \tfrac{1}{2}\phi'' - P^2(\phi' + \phi) = 0 \quad (|X| < A), \tag{3}$$

$$\phi''' - P^2\phi' = 0 \quad (|X| > A). \tag{4}$$

4. Boundary conditions

If the lateral walls are parallel to the basic current, their positions may be assumed to be situated at the zeros of $\sin py$; the boundary condition $v = 0$ at the wall is then automatically satisfied.

If it is assumed that the plates are infinitely thin, no concentrated forces act on the flow at their edges $x = \pm a$, and we therefore require the stream-function and its derivatives of first and second order to be continuous.

On the other hand, the blockage effect may be taken into account by following Prandtl's discussion on vortices entering a contraction, as given by Uberoi (**5**). If the contracted section is designated by suffix c and the open section by suffix 0, and if the blockage factor is defined by $U_c = cU_0$, the relations $u_c = (1/c)u_0$, $v_c = v_0$, and $\zeta_c = (1/c)\zeta_0$ are obtained for the two-dimensional case, i.e. $\phi_c = c\phi_0$, $\phi_c' = \phi_0'$, $\phi_c'' = c\phi_0''$. If these conditions are used instead of the above-mentioned continuity conditions, the damping factor obtained is not influenced, to first-order approximation, in the two limiting cases investigated.

As the solution must be finite everywhere, we therefore have eight boundary conditions, namely, six continuity (or jump) conditions at the two edges of the plates, and two boundedness conditions at the extreme ends of the x-axis. The third-order differential equations applying in the

three regions L, M, and N, supply nine integration constants. The damping factor, or amplitude ratio, is therefore uniquely determined.

5. Solution for zero perturbation pressure

As was mentioned in the introduction, some indication of the behaviour of the system can be obtained simply by assuming zero perturbation pressure. This would seem to correspond to the case of closely distributed waves passing over a relatively long resistance.

The equation of motion for the uniform basic flow is

$$0 = -\frac{\overline{\Pi}_x}{\rho} - \tfrac{1}{2}hU^2, \tag{5}$$

the bar over the Π_x indicating that the basic flow is to be taken. Linearization of the first equation of motion for the perturbed flow gives

$$Uu_x = -\frac{\overline{\Pi}_x + \Pi_x}{\rho} - \tfrac{1}{2}h(U^2 + 2Uu)$$

and therefore

$$Uu_x = -\frac{\Pi_x}{\rho} - hUu.$$

If we now assume Π_x to be of higher order than the first this equation simplifies to

$$u_x = -hu.$$

Therefore the damping factor over the length of the plates is e^{-2ha}.

6. Damping factor in the general case

The general solution of equation (3), valid for $|X| < A$, is

$$\phi = \sum_{s=1}^{3} \alpha_s e^{\lambda_s X}$$

where the λ's are the three solutions of

$$\lambda^3 + \tfrac{1}{2}\lambda^2 - P^2(\lambda + 1) = 0, \tag{6}$$

while the α's are constants.

For the two outside regions we get, after application of the boundedness conditions,

$$\phi = \begin{cases} \beta_1 e^{PX} + \gamma_1 & (X < -A) \\ \beta_2 e^{-PX} + \gamma_2 & (X > A) \end{cases}$$

in which the β's and γ's are constants.

Substituting these expressions in the continuity conditions at $X = \pm A$ yields a set of six equations, from which the damping factor γ_2/γ_1 can immediately be obtained in determinantal form, as

$$\frac{\gamma_2}{\gamma_1} = \frac{\begin{vmatrix} e^{-PA} & 0 & -1 & -e^{-\lambda_1 A} & -e^{-\lambda_2 A} & -e^{-\lambda_3 A} \\ Pe^{-PA} & 0 & 0 & -\lambda_1 e^{-\lambda_1 A} & & \\ P^2e^{-PA} & 0 & 0 & -\lambda_1^2 e^{-\lambda_1 A} & & \\ 0 & e^{-PA} & 0 & -e^{\lambda_1 A} & & \\ 0 & -Pe^{-PA} & 0 & -\lambda_1 e^{\lambda_1 A} & & \\ 0 & P^2e^{-PA} & 0 & -\lambda_1^2 e^{\lambda_1 A} & & \end{vmatrix}}{\begin{vmatrix} e^{-PA} & 0 & 0 & -e^{-\lambda_1 A} & -e^{-\lambda_2 A} & -e^{-\lambda_3 A} \\ Pe^{-PA} & 0 & 0 & -\lambda_1 e^{-\lambda_1 A} & & \\ P^2e^{-PA} & 0 & 0 & -\lambda_1^2 e^{-\lambda_1 A} & & \\ 0 & e^{-PA} & 1 & -e^{\lambda_1 A} & & \\ 0 & -Pe^{-PA} & 0 & -\lambda_1 e^{\lambda_1 A} & & \\ 0 & P^2e^{-PA} & 0 & -\lambda_1^2 e^{\lambda_1 A} & & \end{vmatrix}}$$

in which the blank spaces are filled by cyclic permutation of the index of λ in the last three columns. After simplification this becomes

$$e^{2(\lambda_1+\lambda_2+\lambda_3)A} \frac{\begin{vmatrix} \lambda_1(P-\lambda_1)e^{-2\lambda_1 A} & \lambda_2(P-\lambda_2)e^{-2\lambda_2 A} & \lambda_3(P-\lambda_3)e^{-2\lambda_3 A} \\ -(P+\lambda_1) & & \\ P^2-\lambda_1^2 & & \end{vmatrix}}{\begin{vmatrix} P-\lambda_1 & P-\lambda_2 & P-\lambda_3 \\ P^2-\lambda_1^2 & & \\ -\lambda_1(P+\lambda_1)e^{2\lambda_1 A} & & \end{vmatrix}}$$

and since, by (6), $\lambda_1+\lambda_2+\lambda_3 = -\frac{1}{2}$, the factor outside the determinants is clearly e^{-A}. Therefore

$$\frac{\gamma_2}{\gamma_1} = e^{-A} \frac{\lambda_1(P-\lambda_1)(P+\lambda_2)(P+\lambda_3)(\lambda_3-\lambda_2)e^{-2\lambda_1 A}+\ldots}{-\lambda_1(P+\lambda_1)(P-\lambda_2)(P-\lambda_3)(\lambda_3-\lambda_2)e^{+2\lambda_1 A}-\ldots}.$$

A form which, for some purposes, is slightly more convenient, is obtained by noting that the left-hand side of (6) may be written as

$$(\lambda-\lambda_1)(\lambda-\lambda_2)(\lambda-\lambda_3) = \lambda^3+\tfrac{1}{2}\lambda^2-P^2(\lambda+1)$$

so that

$$(P-\lambda_1)(P-\lambda_2)(P-\lambda_3) = -\tfrac{1}{2}P^2 = -(P+\lambda_1)(P+\lambda_2)(P+\lambda_3)$$

and therefore, finally

$$\frac{\gamma_2}{\gamma_1} = e^{-A} \frac{\lambda_1\{(\lambda_1-P)/(\lambda_1+P)\}(\lambda_3-\lambda_2)e^{-2\lambda_1 A}+\ldots}{\lambda_1\{(\lambda_1+P)/(\lambda_1-P)\}(\lambda_3-\lambda_2)e^{2\lambda_1 A}+\ldots}. \tag{7}$$

7. Asymptotic solution for small-scale perturbations

For perturbation wavelengths small compared with the characteristic value $1/h$ (corresponding to the length of the plates for unit resistance coefficient), the frequency parameter P is large, and we obtain the following asymptotic values for the solutions of (6)

$$\lambda_1 = -1-\frac{1}{2P^2}+\dots$$

$$\lambda_2 = P+\tfrac{1}{4}-\frac{7}{32P}-\dots$$

$$\lambda_3 = -P+\tfrac{1}{4}+\frac{7}{32P}-\dots.$$

Substitution into our basic formula (7) gives

$$\frac{\gamma_2}{\gamma_1} \sim e^{-A}\frac{\lambda_3\{(\lambda_3-P)/(\lambda_3+P)\}(\lambda_2-\lambda_1)e^{-2\lambda_3 A}}{\lambda_2\{(\lambda_2+P)/(\lambda_2-P)\}(\lambda_1-\lambda_3)e^{2\lambda_3 A}} = e^{-2A}[1+O(P^{-2})]. \quad (8)$$

8. Solution for large-scale perturbations

For small P, i.e. for long perturbation wavelengths, the solutions of (6) become

$$\lambda_1 = -\tfrac{1}{2}+2P^2+\dots,$$
$$\lambda_2 = \sqrt{2}P-P^2+\dots,$$
$$\lambda_3 = -\sqrt{2}P-P^2+\dots$$

and substitution in (7) now yields

$$\frac{\gamma_2}{\gamma_1} \sim e^{-A}\frac{\sqrt{2}P[e^A-\frac{1}{2}\{(\sqrt{2}-1)/(\sqrt{2}+1)\}-\frac{1}{2}\{(\sqrt{2}+1)/(\sqrt{2}-1)\}]}{\sqrt{2}P[e^{-A}-\frac{1}{2}\{(\sqrt{2}+1)/(\sqrt{2}-1)\}-\frac{1}{2}\{(\sqrt{2}-1)/(\sqrt{2}+1)\}]} \sim \frac{1-3e^{-A}}{e^{-A}-3}. \quad (9)$$

This expression decreases from 1 to $-\frac{1}{3}$ as A increases, and vanishes when $A = \ln 3 = 1{\cdot}1$. It is valid if A is of lower order than P^{-1}.

9. Application to distributed resistances and gauzes

For the interpretation of the results we return to physical variables. Integrating (5) over the length of the plates from $-a$ to a gives

$$2ah = \frac{\Pi_1-\Pi_2}{\frac{1}{2}\rho U^2},$$

which is the drag coefficient k defined by Taylor and Batchelor (**3**), and therefore

$$2A = 2ah = k.$$

If l is the wavelength (in the y-direction) of the perturbation,

$$P = \frac{2\pi}{lh} = \frac{4\pi a}{lk}.$$

This means that large values of P correspond to a/k large compared with l, representing a widely distributed resistance. The limiting result (8) agrees with that obtained by assuming zero perturbation pressure (section 5).

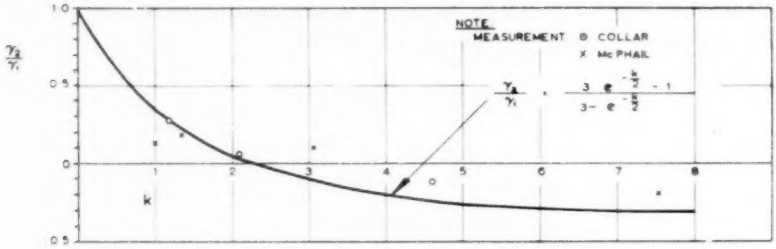

FIG. 2

If k is kept fixed it is seen that for small P, a is small compared with l, which represents a concentrated resistance. The solution (9) for small P therefore approximates to the case of a gauze with wires running in one direction only. It seems unlikely, when the flow is nearly normal to the gauze, that wires running across the flow would have a constraining effect apart from that due to their resistance. The above results for a 'one-dimensional' gauze may therefore be compared with the results for 'two-dimensional' gauzes obtained in (3). The resistance coefficient giving perfect damping in the present case is $k = 2A = 2{\cdot}2$.

The value obtained by Taylor and Batchelor using empirical relations, is $k = 2{\cdot}76$. In Fig. 2 the present result is plotted with the experimental results of Collar and McPhail (recorded in 3). Over the available range of values of k the agreement seems good. It therefore appears that the damping effect of gauzes is theoretically explained by the present analysis, and that the formulae may with confidence be applied in practice.

10. Acknowledgement

This paper is published with the permission of the South African Council for Scientific and Industrial Research.

REFERENCES

1. L. PRANDTL, *The Attainment of a Steady Air Stream in Wind Tunnels*, translated as N.A.C.A. (U.S.A.) Tech. Mem. 726 (1933).
2. A. R. COLLAR, *The Effect of a Gauze on the Velocity Distribution in a Uniform Duct*, British A.R.C., R and M 1867 (1939).
3. G. I. TAYLOR and G. K. BATCHELOR, 'The effect of wire gauze on small disturbances in a uniform stream', *Quart. J. Mech. App. Math.* **11** (1949) 1.
4. E. VAN SPIEGEL, *Method of Calculation for Heat-generators of Blowdown Wind Tunnels*, Report NLL–TM F. 190 (1956), National Luchtvaart-laboratorium, Amsterdam, Netherlands.
5. M. S. UBEROI, 'Effect of wind-tunnel contraction on free stream turbulence', *J. Aero. Sci.* **23** (1956) 754.

A NOTE ON LIFTING LINE THEORY

By K. STEWARTSON (*The University, Durham*)

[Received 2 April 1959]

SUMMARY

The distribution of circulation round a semi-infinite plane wing of constant chord is calculated using the lifting line approximation. The results are used to determine the lift and induced drag of a rectangular plane wing of large aspect ratio.

1. Introduction

PRANDTL's concept of the lifting line has proved of immense value to the theory of lift on three-dimensional quasi-planar wings placed at a small angle of incidence in a stream of incompressible fluid. In his theory the wing is replaced by a straight line l, parallel to its leading edge, around which the circulation $\Gamma(y)$ is assumed to be a function of the distance y along l from some convenient datum point. Since the circulation is varying there will be in addition a trailing vortex sheet, lying behind l and approximately in the plane of flow of the undisturbed stream, whose strength can be determined in terms of $\Gamma(y)$. This trailing vortex sheet deflects the main stream in the neighbourhood of the wing, altering its effective angle of incidence. On equating this effective angle of incidence to the circulation round l by means of the Joukowski hypothesis an integro-differential equation for $\Gamma(y)$ is obtained. Once $\Gamma(y)$ is known it is a comparatively simple matter to infer the lift and induced drag of the wing.

The methods proposed for solving the equation for $\Gamma(y)$ depend either on replacing $\Gamma(y)$ by a Fourier series with period equal to the span of the wing or on taking a particular form for $\Gamma(y)$ and determining the corresponding shape of the wing. The reader is referred to Glauert (**1**) and to Robinson and Laurmann (**2**) for a full discussion of these methods. The disadvantage of the methods using Fourier series is that they inevitably become less accurate as the aspect ratio of the wing increases while the alternative methods have led to solutions relevant to wings with rounded tips only. Accordingly it is of interest to determine the form of the circulation function for a rectangular wing of very large aspect ratio as an example of a wing for which neither of the general methods mentioned above is strictly applicable.

In this note we shall first determine the exact solution for a semi-infinite wing of constant chord and then use it to find the leading terms

of the expansion of the lift and drag on a rectangular wing, in descending powers of the aspect ratio.

2. The semi-infinite wing of constant chord

According to Robinson and Laurmann (**2**), the integro-differential equation for the circulation $\Gamma(y)$ around the y-axis is

$$\Gamma(y) = \tfrac{1}{2}a_0 c\left(U\alpha_0 + \frac{1}{4\pi}\int_0^s \frac{\Gamma'(y_1)\,dy_1}{y_1 - y}\right). \tag{2.1}$$

In this equation the y-axis is in the plane of the wing and parallel to the leading edge, the wing extends from $y = 0$ to $y = s$, $c(y)$ is the chord of the wing, α_0 is the geometrical angle of attack of the wing, U is the velocity of main stream, and a_0 is a constant equal to 2π for a flat plate. Further, the circulation must be zero at the wing tips and so

$$\Gamma(0) = \Gamma(s) = 0. \tag{2.2}$$

In this section we shall obtain a complete formal solution of (2.1) in the particular case of a semi-infinite wing of constant chord so that $s = \infty$ and c is a constant.

At points distant from the tip the circulation must tend to its two-dimensional value and accordingly the appropriate boundary conditions on Γ in our particular problem are

$$\Gamma(0) = 0, \qquad \Gamma(\infty) = \tfrac{1}{2}a_0 c\alpha U. \tag{2.3}$$

Write $$\Gamma(y) = \tfrac{1}{2}a_0 cU\alpha_0\{1 - f(x)\}, \quad \text{where } y = a_0 cx/8; \tag{2.4}$$

then $$f(x) = \frac{1}{\pi}\int_0^\infty \frac{f'(x_1)\,dx_1}{x_1 - x} \quad (x > 0), \tag{2.5}$$

subject to $f(0) = 1$, $f(\infty) = 0$. In order to solve this equation we shall first solve formally the slightly more complicated integral equation

$$f(\alpha, x) = -\frac{\alpha}{\pi}\int_0^\infty dx_1 f(\alpha, x_1) K_1(\alpha|x_1 - x|)\operatorname{sgn}(x_1 - x) \quad (x > 0), \tag{2.6}$$

subject to $f(\alpha, 0) = 1$ and $f(\alpha, \infty) = 0$, where α is real and positive, and K_1 is the Bessel function of order one, of the second kind and with imaginary argument. Having solved (2.6) formally the solution of (2.5) follows on letting $\alpha \to 0+$ and writing

$$f(x) = f(0, x). \tag{2.7}$$

If we set $f(\alpha, x) = 0$ for all $x < 0$ it follows that

$$F_+(\omega) = \int_{-\infty}^{\infty} f(\alpha, x) e^{i\omega x}\, dx \tag{2.8}$$

is a regular function of ω in the upper half plane, $\operatorname{im}\omega > 0$. This is expressed notationally by the suffix $+$. In a similar way a suffix $-$ will be used below to signify that a function is regular in the lower half plane, $\operatorname{im}\omega < 0$. Inverting the Fourier transform (2.8)

$$f(\alpha, x) = \frac{1}{2\pi} \int_{-\infty}^{\infty} F_+(\omega) e^{-i\omega x}\, d\omega; \tag{2.9}$$

since $F_+(\omega)$ is regular in the upper half plane of ω, the integral vanishes if $x < 0$. Substituting (2.9) into (2.6) we get

$$F_+(\omega) + M_-(\omega) = \frac{1}{\pi}\{-1 - i\omega F_+(\omega)\} \int_{-\infty}^{\infty} dx\, e^{-i\omega x} K_1(\alpha|x|)\operatorname{sgn} x \tag{2.10}$$

$$= \frac{\omega}{(\omega^2+\alpha^2)^{\frac{1}{2}}}\{i - \omega F_+(\omega)\} \tag{2.11}$$

where $M_-(\omega)$, like $F_+(\omega)$, is at present unknown, and $(\omega^2+\alpha^2)^{\frac{1}{2}}$ is regular in the ω plane cut along the imaginary axis from $i\alpha$ to $i\infty$ and from $-i\infty$ to $-i\alpha$. Equation (2.11) may now be rewritten as

$$F_+(\omega)\left\{1 + \frac{\omega^2}{(\omega^2+\alpha^2)^{\frac{1}{2}}}\right\} = \frac{i\omega}{(\omega^2+\alpha^2)^{\frac{1}{2}}} - M_-(\omega). \tag{2.12}$$

Following the Wiener–Hopf technique, the coefficient of $F_+(\omega)$ in (2.12) will now be written as the ratio of two functions, one regular and non-zero in the upper half plane $\operatorname{im}\omega > -\alpha$, the other regular and non-zero in the lower half plane $\operatorname{im}\omega < \alpha$. Thus

$$\frac{L_+(\alpha, \omega)}{L_-(\alpha, \omega)} = 1 + \frac{\omega^2}{(\omega^2+\alpha^2)^{\frac{1}{2}}}. \tag{2.13}$$

These functions may be found by taking a contour C in the ζ-plane consisting of the two infinite straight lines C_+, C_- parallel to the real axis, of which one is just above and one just below the real axis, both lying inside $|\operatorname{im}\zeta| = \alpha$. Then if ω is a point inside C,

$$\log L_+(\alpha, \omega) - \log L_-(\alpha, \omega) = \frac{1}{2\pi i} \int_C \log \frac{1 + \zeta^2(\zeta^2+\alpha^2)^{-\frac{1}{2}}}{\zeta - \omega}\, d\zeta. \tag{2.14}$$

Hence

$$\log L_+(\alpha, \omega) = \frac{1}{2\pi i} \int_{C_-} \log \frac{1 + \zeta^2(\zeta^2+\alpha^2)^{-\frac{1}{2}}}{\zeta - \omega}\, d\zeta \tag{2.15}$$

since this integral still defines a regular function if the range of ω is extended over the upper half plane. Differentiating (2.15) and integrating by parts we find

$$\frac{(\partial/\partial\omega)L_+(\alpha,\omega)}{L_+(\alpha,\omega)} = \frac{1}{2\pi i}\int_{C_-} \frac{\zeta(\zeta^2+2\alpha^2)\,d\zeta}{(\zeta-\omega)(\zeta^2+\alpha^2)^{\frac{1}{2}}\{\zeta^2+(\zeta^2+\alpha^2)^{\frac{1}{2}}\}} \tag{2.16}$$

whence $L_+(\alpha,\omega)$ may be obtained formally and shown to satisfy the conditions required of it. However, in the present instance we are most interested in the particular case $\alpha = 0$ when the integral reduces to

$$\frac{1}{\pi i}\int_0^\infty \frac{\zeta\,d\zeta}{(\zeta^2-\omega^2)(\zeta+1)}. \tag{2.17}$$

The two integrals by which $L_+(0,\omega)$ may be found are most easily evaluated when $\omega = it$, t real and positive, and we then find that

$$L_+(0,it) = (1+t^2)^{\frac{1}{4}}\exp\left\{-\frac{1}{\pi}\int_0^t \frac{\log\theta\,d\theta}{1+\theta^2}\right\}, \tag{2.18}$$

taking $L_+(0,0) = L_+(\alpha,0) = 1$. Having obtained $L_+(0,\omega)$ on the positive imaginary axis it can easily be evaluated elsewhere. It is only necessary to cut the ω plane along the negative imaginary axis. If, for example, ω is real,

$$L_+(0,\omega) = (1+|\omega|)^{\frac{1}{4}}\exp\left\{\frac{i}{\pi}\int_0^{|\omega|} \frac{\log\theta\,d\theta}{1-\theta^2}\right\}. \tag{2.19}$$

Similarly, it may be shown that if $\omega = -iu$, u real and positive,

$$L_-(0,\omega) = (1+u^2)^{-\frac{1}{4}}\exp\left\{-\frac{1}{\pi}\int_0^u \frac{\log\theta\,d\theta}{1+\theta^2}\right\}. \tag{2.20}$$

Having formally determined $L_+(\alpha,\omega)$, $L_-(\alpha,\omega)$ let us now reconsider (2.12), which may be rewritten as

$$F_+(\omega)L_+(\alpha,\omega) = \frac{i\omega}{(\omega^2+\alpha^2)^{\frac{1}{2}}}L_-(\alpha,\omega) - M_-(\omega)L_-(\alpha,\omega),$$

and hence, using (2.13) to eliminate $(\omega^2+\alpha^2)^{-\frac{1}{2}}$, as

$$F_+(\omega)L_+(\alpha,\omega) - \frac{i}{\omega}\{L_+(\alpha,\omega)-1\} = -L_-(\alpha,\omega)M_-(\omega) - \frac{i}{\omega}\{L_-(\alpha,\omega)-1\}. \tag{2.21}$$

If now we assume that $F_+(\omega)$ is regular in $\operatorname{im}\omega > -\alpha$ and $M_-(\omega)$ is regular in $\operatorname{im}\omega < +\alpha$ it follows that both sides must be equal to a function H of ω which is regular everywhere. The form of H can be determined by

considering the behaviour of F_+ and L_+ as $\omega \to \infty$. Since $f(\alpha, x) \to 1$ as $x \to 0$, $\omega F_+ \to i$ as $\omega \to \infty$. Again from the symmetry in the definitions of $L_+(\alpha, \omega)$ and $L_-(\alpha, \omega)$ in (2.13), $L_+(\alpha, \omega)/\omega^{\frac{1}{2}}$ must tend to a finite limit as $\omega \to \infty$. Hence as $\omega \to \infty$ the right hand side of (2.21) must tend to zero, so that $H(\omega) \equiv 0$. The verification of the assumptions stated at the beginning of this paragraph now follow *a posteriori* and we have

$$F_+(\omega) = \frac{i}{\omega}\left(1 - \frac{1}{L_+(\alpha, \omega)}\right), \qquad M_-(\omega) = -\frac{i}{\omega}\left(1 - \frac{1}{L_-(\alpha, \omega)}\right). \quad (2.22)$$

The formal solution of (2.6) is now completed by using (2.9). Of particular interest is the special case $\alpha = 0$ for which L_+ and L_- have been found as (2.19), (2.20). In this case

$$f(x) = f(0, x) = \frac{1}{2\pi}\int_{-\infty}^{\infty} \frac{i}{\omega}\left(1 - \frac{1}{L_+(0, \omega)}\right) e^{-i\omega x}\, d\omega$$

$$= \frac{1}{\pi}\int_0^{\infty} \frac{e^{-tx}}{(1+t^2)^{\frac{1}{4}}} \exp\left[-\left\{\frac{1}{\pi}\int_0^t \frac{\log\theta\, d\theta}{1+\theta^2}\right\}\right] dt, \quad (2.23)$$

on deforming the contour into the two sides of the negative imaginary axis of ω and using (2.13), (2.20) to find the values of $L_+(0, \omega)$ on either side of the cut along this line. From (2.23) it is a comparatively simple matter to compute the values of $f(x)$ displayed in the table below:

x	0	0·2	0·4	0·6	0·8	1·0	1·2	1·4	1·6	1·8	2·0	3·0	4·0
$f(x)$	1	0·564	0·438	0·361	0·308	0·267	0·237	0·212	0·192	0·175	0·161	0·113	0·086

If x is large, $f(x)$ can be found by expanding the integrand of (2.23) in ascending powers of t and $\log t$ and integrating term by term. It is found that

$$f(x) = \frac{1}{\pi x} + \frac{1}{\pi^2 x^2}(\gamma + \log x) + \frac{1}{(\pi x)^3}[2(\log x)^2 + 4\gamma \log x - 1 - \tfrac{4}{3}\pi^2] + \ldots \quad (2.24)$$

as $x \to \infty$, where γ is Euler's constant 0·5772.... On the other hand, if x is small, $f(x)$ is found by expanding $L_+(0, \omega)$ in descending powers of ω and interpreting each term separately although some care is needed. We obtain

$$f(x) = 1 - 2\left(\frac{x}{\pi}\right)^{\frac{1}{2}} - \frac{4}{3}\left(\frac{x}{\pi}\right)^{\frac{3}{2}}(\log 4x + \gamma - \tfrac{11}{3}) + O_l\left(\frac{x}{\pi}\right)^{\frac{5}{2}}, \quad (2.25)$$

where O_l means that the order includes an unspecified power of $\log x$.

Perhaps the most useful property of f is the value of

$$\int_0^x f(x_1)\,dx_1 \tag{2.26}$$

when x is large. From (2.9), (2.22)

$$\frac{1}{t}\left(1-\frac{1}{L_+(0,it)}\right)=\int_0^\infty f(x)e^{-xt}\,dt \tag{2.27}$$

if t is real and positive. Now

$$\int_0^\infty \frac{1}{\pi(x+1)}e^{-xt}\,dx = -\frac{1}{\pi}(\gamma+\log t)+O(t\log t) \quad (t \text{ small}), \tag{2.28}$$

and therefore

$$\int_0^\infty \left[f(x)-\frac{1}{\pi(x+1)}\right]dx = \lim_{t\to 0}\left[\frac{1}{t}-\frac{1}{tL_+(0,it)}+\frac{1}{\pi}(\gamma+\log t)\right]=\frac{\gamma+1}{\pi}. \tag{2.29}$$

Accordingly, when x is large,

$$\int_0^x f(x_1)\,dx_1 = \frac{1}{\pi}(\log x+\gamma+1)+o(1). \tag{2.30}$$

Finally, using numerical methods, it was found that

$$\int_0^\infty |f(x)|^2\,dx \doteq 0{\cdot}32. \tag{2.31}$$

3. The lift and drag on a rectangular wing of large aspect ratio

Here we consider a wing of constant chord c and span s such that $A = s/c \gg 1$. For this wing write

$$\Gamma(y) = \frac{a_0 c\alpha_0 U}{2\{1+f(r)\}}\,|1+f(r)-f(x)-f(r-x)+g(x)|, \tag{3.1}$$

where $8s = a_0 cr$. Then

$$g(x) = \frac{1}{\pi}\int_0^r \frac{g'(x_1)\,dx_1}{x_1-x}-\frac{1}{\pi}\int_r^\infty f'(x_1)\,dx_1\left[\frac{1}{x_1-x}+\frac{1}{x_1+x-r}\right] \tag{3.2}$$

and $g(0) = g(r) = 0$. However, if r is large, $f(x) = O(x^{-1})$ $(x > r)$, and

hence the last integral is $O_l(r^{-2})$. It follows that $g(x) = O_l(r^{-2})$. The lift on the wing is

$$L = \rho U \int_0^s \Gamma(y)\, dy = \tfrac{1}{2}\rho U^2 csC_L \tag{3.3}$$

$$= \frac{a_0^2 c^2 \alpha_0 \rho U^2}{16\{1+f(r)\}} \int_0^r [1+f(r)-f(x)-f(r-x)+g(x)]\, dx$$

$$= \frac{a_0^2 c^2 \alpha_0 \rho U^2}{16\{1+f(r)\}} [\{1+f(r)\}r - 2(\log r + 1 + \gamma) + O_l(r^{-1})]. \tag{3.4}$$

Hence
$$C_L = a_0 \alpha_0 \left\{1 - \frac{a_0}{4\pi A}\left[\log \frac{8A}{a_0} + 1 + \gamma\right] + O_l(A^{-2})\right. \tag{3.5}$$

when A is large. Taking $a_0 = 2\pi$, (3.5) gives a value of 4·99 for the slope of the lift coefficient at $A = 10$ which may be compared with a value 5·04 quoted by Glauert (**1**). Equation (3.5) should also be compared with

$$C_L = a_0 \alpha_0 \left[1 - \frac{a_0}{\pi A} + O(A^{-2})\right] \tag{3.6}$$

which is the equation for lift coefficient of an elliptically loaded wing of large aspect ratio. This means that the effect on the lift of having rectangular instead of rounded tips to a wing of large aspect ratio is manifested by the presence of the logarithmic terms in (3.5).

The induced drag of a three-dimensional wing is

$$D_i = \int_0^s \rho w \Gamma(y)\, dy = \tfrac{1}{2}\rho U^2 csC_{D_i} \tag{3.7}$$

(**1**, 140), where w is the downwash and is connected with the circulation through the equation
$$2\Gamma = a_0 c(U\alpha - w). \tag{3.8}$$

Substituting (3.1), (3.8) into (3.7) and using (2.30), (2.31) it is found that

$$C_{D_i} = \frac{a_0^2 \alpha^2}{4A\pi}\left(\log \frac{8A}{a_0} + \gamma + 0{\cdot}0\right) + O_1(A^{-2}) \tag{3.9}$$

when A is large. Expressing this result in the manner conventional to aerofoil theory,

$$C_{D_i} = \frac{C_L^2}{\pi A}\left[\frac{1}{4}\left(\log \frac{8A}{a_0} + \gamma\right) + O_l(A^{-1})\right] \tag{3.10}$$

when A is large, which may be compared with the formula

$$C_{D_i} = \frac{C_L^2}{\pi A} \tag{3.11}$$

for an elliptically loaded wing.

REFERENCES

1. H. Glauert, *The Elements of Aerofoil and Airscrew Theory*, 2nd ed. (Cambridge, 1948).
2. A. Robinson and J. A. Laurmann, *Wing Theory* (Cambridge, 1956).

A SOLUTION OF THE COMPRESSIBLE LAMINAR BOUNDARY LAYER EQUATIONS WITH HEAT TRANSFER AND ADVERSE PRESSURE GRADIENT

By G. POOTS

(*Department of Theoretical Mechanics, Bristol University*)

[Received 12 August 1958; revise received 19 December 1958]

SUMMARY

A solution of the two-dimensional compressible laminar boundary layer equations with heat transfer and adverse pressure gradient is given. The problem arises from the application of Stewartson's transformation to the compressible laminar boundary layer equations. In the transformed incompressible-plane the main stream velocity and dimensionless temperature at the surface have been chosen to be $U_e = u_0(1-\frac{1}{8}X)$ and $S_w = 1$ respectively, where X is the longitudinal coordinate in the incompressible plane. These forms have been chosen so as to simplify the numerical work involved in solving the coupled partial differential equations which occur. A solution for the coupled partial differential equations is obtained, for small X, by means of a power series in terms of X, where the coefficients in the expansion are obtained on integrating a series of ordinary differential equations; for values of X approaching the separation point the partial differential equations are integrated using standard relaxation methods in conjunction with the Hartree–Womersley method.

In the incompressible-plane boundary layer characteristics such as displacement thickness, etc., are evaluated from the numerical solution and compared with those obtained by considering an approximate solution of the transformed momentum, energy, and thermal-integral equations. On transformation of these results to the compressible-plane information is obtained for the compressible laminar boundary layer on a flat plate with heat addition and in the presence of a retarded main stream velocity distribution. In particular dimensionless quantities related to the shear stress and heat transfer at the wall are evaluated at various stations along the plate from the leading edge to the point of separation.

1. Introduction

THE solution of the compressible laminar boundary layer equations depends on the pressure gradient in the main stream, Mach number, and heat transfer over the solid boundary, together with the properties of the fluid under consideration. As shown by Cope and Hartree (**1**) the numerical work involved in a complete study of these equations is prohibitive when allowance is made for the empirical variation of viscosity with temperature. However, Howarth (**2**) and Stewartson (**3**) gave a transformation such that the boundary layer equations of the compressible fluid may be

transformed into a form identical with those of the incompressible case. In Howarth's analysis the following assumptions are made:

(a) the surface of the body is insulated,
(b) the viscosity (μ) varies as the absolute temperature T,
(c) the Prandtl number (σ) of the fluid is unity.

Stewartson (**3**) further simplified Howarth's analysis and extended it to include the case of arbitrary surface temperature. It is the purpose of the present paper to give a numerical solution of the compressible laminar boundary layer equations for the flow along a flat plate, maintained at a certain surface temperature, and in the presence of an adverse pressure gradient. In the following we adhere to Stewartson's analysis.

The equations of the steady, two-dimensional compressible laminar boundary layer for perfect fluids are, in the usual notation,

$$\rho u\frac{\partial u}{\partial x}+\rho v\frac{\partial u}{\partial y}=-\frac{\partial p}{\partial x}+\frac{\partial}{\partial y}\left(\mu\frac{\partial u}{\partial y}\right), \tag{1.1}$$

$$0=-\frac{\partial p}{\partial y}, \tag{1.2}$$

$$\frac{\partial}{\partial x}(\rho u)+\frac{\partial}{\partial y}(\rho v)=0, \tag{1.3}$$

and

$$Jc_p\left(\rho u\frac{\partial T}{\partial x}+\rho v\frac{\partial T}{\partial y}\right)-u\frac{\partial p}{\partial x}=\frac{\partial}{\partial y}\left(Jc_p\mu\frac{\partial T}{\partial y}\right)+\mu\left(\frac{\partial u}{\partial y}\right)^2. \tag{1.4}$$

These equations may now be transformed into equations similar to those for the two-dimensional incompressible laminar boundary layer by means of Stewartson's transformation. Stewartson introduced the following variables

$$dX=dx\left(\frac{a_e}{a_0}\right)^{(3\gamma-1)/(\gamma-1)}, \tag{1.5}$$

$$dY=dy\frac{a_e}{a_0\sqrt{\nu_0}}\left(\frac{\rho}{\rho_0}\right), \tag{1.6}$$

and the stream function defined by

$$\psi_y=\frac{\rho}{\rho_0\sqrt{\nu_0}}u, \qquad \psi_x=-\frac{\rho}{\rho_0\sqrt{\nu_0}}v, \tag{1.7}$$

where the suffix 0 refers to some standard state, taken to be the main stream at $x=0$. The suffix e refers to local conditions at the outer edge of the boundary layer. Applying equations (1.5) to (1.7) to the boundary layer equations (1.1) to (1.4) and assuming that $\sigma=1$, we obtain the following equations in the incompressible-plane

$$\frac{\partial U}{\partial X}+\frac{\partial V}{\partial Y}=0, \tag{1.8}$$

$$U\frac{\partial U}{\partial X}+V\frac{\partial U}{\partial Y}=U_e\frac{dU_e}{dX}(1+S)+\frac{\partial^2 U}{\partial Y^2}, \tag{1.9}$$

$$U\frac{\partial S}{\partial X}+V\frac{\partial S}{\partial Y}=\frac{\partial^2 S}{\partial Y^2}, \tag{1.10}$$

where S is the dimensionless temperature defined by

$$\frac{T}{T_e}=1+\frac{T_0}{T_e}\left(1+\frac{(\gamma-1)}{2}M_0^2\right)S+\frac{(\gamma-1)}{2a_e^2}(u_e^2-u^2), \tag{1.11}$$

and where the stream function has been replaced by the transformed velocities (U, V) defined by

$$U=\psi_y, \qquad V=-\psi_x. \tag{1.12}$$

The resulting relationship between the transformed and physical velocities is $U=(a_0/a_e)u$. In the main stream we have also that

$$a_e^2+\frac{(\gamma-1)}{2}u_e^2=a_0^2+\frac{(\gamma-1)}{2}u_0^2=\text{constant} \tag{1.13}$$

and

$$\frac{p}{p_0}=\left(\frac{a_e}{a_0}\right)^{2\gamma/(\gamma-1)}. \tag{1.14}$$

The relationship between U_e and u_e is [1, 1], so that for every problem in the incompressible-plane there is an associated problem in the compressible-plane. Thus we have two alternatives: either we can take an assumed form for the retarded main stream velocity u_e in the compressible-plane and determine U_e in the incompressible-plane by equations (1.5) and (1.13) or vice versa. Since the assumed form could never be obtained physically, it is advantageous from the viewpoint of the numerical work to assume a simple form for the retarded main stream velocity in the incompressible-plane. Hence we shall consider a transformed main stream velocity distribution given by

$$U_e=u_0(1-\tfrac{1}{8}X). \tag{1.15}$$

Furthermore we shall assume the dimensionless temperature at the wall in the incompressible-plane to be given by $S_w=1$. The main stream velocity and temperature distribution, together with the wall temperature distribution in the compressible-plane may now be obtained. Substituting equation (1.15) in (1.13) we find that

$$\left(\frac{a_e}{a_0}\right)^2=\frac{1+\frac{1}{2}(\gamma-1)M_0^2}{1+\frac{1}{2}(\gamma-1)M_e^2} \tag{1.16}$$

where $M_e=M_0(1-\frac{1}{8}X)$. Therefore

$$\frac{u_e}{u_0}=\frac{a_e}{a_0}(1-\tfrac{1}{8}X) \tag{1.17}$$

and
$$x = \int_0^X \left\{\frac{1+\frac{1}{2}(\gamma-1)M_e^2}{1+\frac{1}{2}(\gamma-1)M_0^2}\right\}^{(3\gamma-1)/2(\gamma-1)} dX. \tag{1.18}$$

If $\gamma = 1{\cdot}4$, the integral (1.18) reduces to

$$x = (1+\tfrac{1}{5}M_0^2)^{-4}[X+\tfrac{32}{15}M_0^2\{1-(1-\tfrac{1}{8}X)^3\}+\tfrac{48}{125}M_0^4\{1-(1-\tfrac{1}{8}X)^5\}+ \\ +\tfrac{32}{875}M_0^6\{1-(1-\tfrac{1}{8}X)^7\}+\tfrac{8}{5625}M_0^8\{1-(1-\tfrac{1}{8}X)^9\}]. \tag{1.19}$$

In the main stream $S = 0$; hence

$$\frac{T_0}{T_e} = 1+\frac{(\gamma-1)}{2a_e^2}(u_e^2-u_0^2),$$

giving, on using equation (1.16),

$$T_e = T_0\frac{1+\frac{1}{2}(\gamma-1)M_0^2}{1+\frac{1}{2}(\gamma-1)M_e^2}. \tag{1.20}$$

The dimensionless temperature distribution S evaluated at the wall determines the wall temperature. Thus

$$\frac{T_w}{T_e} = 1+\frac{T_0}{T_e}\{1+\tfrac{1}{2}(\gamma-1)M_0^2\}S_w+\tfrac{1}{2}(\gamma-1)M_e^2,$$

and on using equation (1.20) the result is

$$T_w = T_0(1+S_w)\{1+\tfrac{1}{2}(\gamma-1)M_0^2\}. \tag{1.21}$$

Hence the case for which $M_0 = 1$, $\gamma = 1{\cdot}4$, $S_w = 1$ corresponds to a wall temperature 2·4 times the free stream temperature T_0 at $x = 0$.

The boundary conditions to be imposed on equations (1.8), (1.9), and (1.10) are

$$U(X,0) = V(X,0) = 0,$$
$$S_w = S(X,0) = 1,$$
$$\lim_{Y\to\infty} U = U_e(X) = u_0(1-\tfrac{1}{8}X), \tag{1.22}$$

and
$$\lim_{Y\to\infty} S = 0.$$

Thus by solving equations (1.8), (1.9), (1.10) subject to (1.22) information on shear stress, heat transfer, etc., may be obtained for the compressible boundary layer on a flat plate maintained at wall temperature

$$T_w = 2T_0\{1+\tfrac{1}{2}(\gamma-1)M_0^2\}$$

and in the presence of a retarded main stream velocity $u_e = u_0(1-\frac{1}{8}X)a_e/a_0$ and main stream temperature distribution $T_e = T_0(a_e/a_0)^2$. In particular, separation will occur in the compressible-plane when $(\partial u/\partial y)_{y=0} = 0$, i.e. in the incompressible-plane, when $(\partial U/\partial Y)_{Y=0} = 0$, since the shear stress evaluated at the wall

$$\tau_w = \left(\mu\frac{\partial u}{\partial y}\right)_{y=0} = \rho_0\sqrt{\nu_0}\left(\frac{a_e}{a_0}\right)^{(4\gamma-2)/(\gamma-1)}\left(\frac{\partial U}{\partial Y}\right)_{Y=0}. \tag{1.23}$$

In section 2 of this paper a series solution in powers of X for the coupled partial differential equations (1.8) to (1.10), subject to the boundary conditions (1.22), is obtained following the method used by Howarth (**4**) in his discussion of the problem of the incompressible flow over a flat plate in the presence of a linear retarded main stream velocity. The coefficients in the expansion are obtained on the numerical solution of a linear set of ordinary differential equations. The amount of numerical work involved is large and the expansions have only been evaluated up to and including the term X^4. This is insufficient to obtain precise information near the separation point. In section 3 details are given on the determination of velocity and thermal profiles at various values of X, up to the separation point, by solving the basic equations using a numerical method developed by Hartree and Womersley (see Hartree (**5**)). Section 4 deals with the approximate solution of the momentum, energy, and thermal integral equations in the incompressible-plane by means of a modified Polhausen method. The boundary layer characteristics, such as displacement thickness, etc., so obtained are then compared with those evaluated using the more precise results obtained in sections 2 and 3. In section 5 the dimensionless quantities u/u_e, T_e/T_0, T_w/T_0, and those related to the local skin friction $C_f = \tau_w/\frac{1}{2}\rho_w u_e^2$ and the wall Nusselt number

$$\mathrm{Nu} = x\left(\frac{\partial T}{\partial y}\right)_{y=0}(T_0 - T_w)^{-1}$$

are calculated for the compressible-plane for a range of free stream Mach numbers ($M_0 = 1$, 2, 3, 4, and 6) as functions of x/x_s, where x_s is the distance of the point of separation from the leading edge. Finally in section 6 conclusions are given.

2. Series solution

We consider here the solution in series for the boundary layer equations in the incompressible-plane. Following Howarth (**4**) we introduce the variables

$$\xi = X, \qquad \eta = \tfrac{1}{2}u_0^{\frac{1}{2}} Y X^{-\frac{1}{2}}. \tag{2.1}$$

The stream function is defined as

$$\psi = u_0^{\frac{1}{2}} \xi^{\frac{1}{2}} \phi(\xi, \eta), \tag{2.2}$$

where the function $\phi(\xi, \eta)$ must satisfy the equation

$$\frac{\partial^3 \phi}{\partial \eta^3} + \phi \frac{\partial^2 \phi}{\partial \eta^2} + 2\xi\left(\frac{\partial \phi}{\partial \xi}\frac{\partial^2 \phi}{\partial \eta^2} - \frac{\partial \phi}{\partial \eta}\frac{\partial^2 \phi}{\partial \xi \partial \eta}\right) - \xi(1 - \tfrac{1}{8}\xi)(1 + S) = 0, \tag{2.3}$$

and the dimensionless temperature S must satisfy

$$\frac{\partial^2 S}{\partial \eta^2} + \phi \frac{\partial S}{\partial \eta} + 2\xi\left(\frac{\partial \phi}{\partial \xi}\frac{\partial S}{\partial \eta} - \frac{\partial \phi}{\partial \eta}\frac{\partial S}{\partial \xi}\right) = 0. \tag{2.4}$$

The boundary conditions are

$$\phi = \frac{\partial \phi}{\partial \eta} = 0, \qquad S = 1 \text{ at } \eta = 0 \text{ for } \xi \geqslant 0;$$

$$\lim_{\eta \to \infty} \frac{\partial \phi}{\partial \eta} = 2 - \tfrac{1}{4}\xi, \qquad \lim_{\eta \to \infty} S = 0 \text{ for } \xi \geqslant 0. \tag{2.5}$$

We now assume expansions of the type

$$\phi(\xi, \eta) = \sum_{r=0}^{\infty} (-1)^r \xi^r \phi_r(\eta) \tag{2.6}$$

and

$$S(\xi, \eta) = \sum_{r=0}^{\infty} (-1)^r \xi^r S_r(\eta). \tag{2.7}$$

When equations (2.6) and (2.7) are substituted into equations (2.3) and (2.4) and like powers of ξ are equated, the following differential equations result:

$$\phi_0''' + \phi_0 \phi_0'' = 0, \tag{2.8}$$

$$\phi_1''' + \phi_0 \phi_1'' - 2\phi_0' \phi_1' + 3\phi_0'' \phi_1 = -(1 + S_0), \tag{2.9}$$

$$\phi_2''' + \phi_0 \phi_2'' - 4\phi_0' \phi_2' + 5\phi_0'' \phi_2 = -\tfrac{1}{8}(1 + S_0) - S_1 + 2(\phi_1')^2 - 3\phi_1 \phi_1'', \tag{2.10}$$

and for $r \geqslant 3$

$$\phi_r''' + \phi_0 \phi_r'' - 2r\phi_0' \phi_r' + (2r+1)\phi_0'' \phi_r = -\tfrac{1}{8} S_{r-2} - S_{r-1} + \sum_{p=1}^{\alpha} \sum_{q=1}^{\beta} \{2q\phi_q' \phi_p' - (2p+1)\phi_p \phi_q''\}, \tag{2.11}$$

where the prime denotes differentiation with respect to η and the summation is restricted by the selection rule $\alpha + \beta = r$ and $\alpha, \beta = 1, 2, 3, \ldots, r$. Equation (2.4) for S reduces to

$$S_r'' + (2r+1)\phi_0 S_r' - 2r\phi_0' S_r = \sum_{p=1}^{\alpha} \sum_{q=1}^{\beta} \{2q\phi_q' S_p - (2p+1)\phi_p S_q'\} \tag{2.12}$$

for $r = 0, 1, 2, \ldots$, where the double summation is restricted by the same selection rule as its counterpart in equation (2.11). The boundary conditions are

$$\begin{aligned} &\phi_r = \phi_r' = 0 && \text{for } r = 0, 1, 2, \ldots \text{ at } \eta = 0, \\ &S_0 = 1, S_r = 0 && \text{for } r = 1, 2, 3, \ldots \text{ at } \eta = 0, \\ &\phi_0' = 2, \phi_1' = \tfrac{1}{4}, \phi_r' = 0 && \text{for } r = 2, 3, 4, \ldots \text{ at } \eta = \infty, \\ \text{and} \quad &S_r = 0 && \text{for } r = 0, 1, 2, \ldots \text{ at } \eta = \infty. \end{aligned} \tag{2.13}$$

The differential equations for ϕ_1, ϕ_2, ϕ_3, etc., and S_0, S_1, S_2, etc., are ordinary linear non-homogeneous differential equations with variable coefficients. Since the coefficients on the left-hand side of each equation are not known analytically, the equations must be integrated numerically. The functions ϕ_1, ϕ_2, ϕ_3, ϕ_4, S_1, S_2, S_3, and S_4 and their derivatives have

been obtained using the Adams–Bashforth method, and the Blasius function ϕ_0 and its derivatives are as tabulated by Howarth (**4**). The calculations were performed to seven decimals and the resulting functions quoted to four decimals are given in Tables 1 and 2. The function S_0 is not tabulated as it may readily be obtained from Howarth's table of ϕ_0', since $S_0 = \frac{1}{2}(2-\phi_0')$.

In the incompressible plane separation will occur at $X = X_s$ when

$$\left(\frac{\partial U}{\partial Y}\right)_{Y=0} = 0 \quad \text{or} \quad \left(\frac{\partial^2 \phi}{\partial \eta^2}\right)_{\eta=0} = 0.$$

Although all the $\phi_r''(0)$ increase with r in absolute magnitude, some indication of the value of X_s may be obtained from the existing numerical work. Separation occurs when

$$\sum_{r=0}^{\infty} (-1)^r X^r \phi_r''(0) = 0. \tag{2.14}$$

Noting that the ratios $|\phi_3''(0)|/|\phi_2''(0)|$ and $|\phi_4''(0)|/|\phi_3''(0)|$ are approximately equal to 1·02, let us suppose that $|\phi_r''(0)| \doteq 1{\cdot}02|\phi_{r-1}''(0)|$ for $r \geqslant 4$. On using Table 1 a suitable approximation to equation (2.14) is then

$$1{\cdot}32824 - 1{\cdot}5939X - 0{\cdot}2608X - 0{\cdot}2644X^2 - 0{\cdot}2780\frac{X^4}{1-1{\cdot}02X} = 0, \tag{2.15}$$

giving an estimate of $X_s = 0{\cdot}64$. The above approximation to equation (2.14) presupposes from the slender evidence already obtained that the $|\phi_r''(0)|$ do in fact increase as r increases. It is interesting to note that more detailed numerical work, as carried out in section 3, gave $X_s = 0{\cdot}60$. This indicates that the $|\phi_r''(0)|$ may increase more rapidly for large r than estimated above.

Although the above series expansions (2.6) and (2.7) could, with some labour, be extended beyond the term X^4, it was found that considerable accuracy was lost in proceeding to the calculation of the higher functions. This was mainly due to the numerical magnitude of the variable coefficients on the left-hand side and to cancellation within the summation on the right-hand side of equations (2.11) and (2.12). Nevertheless the finite forms

$$\phi = \sum_{r=0}^{4} (-1)^r \xi^r \phi_r, \tag{2.16}$$

and

$$S = \sum_{r=0}^{4} (-1)^r \xi^r S_r \tag{2.17}$$

were found extremely useful in checking at $\xi = 0{\cdot}2$ the velocity and thermal profiles obtained by the Hartree–Womersley method, as described in section 3.

3. The application of the Hartree-Womersley method to the basic equations (2.3) and (2.4)

The essential idea of the application of the Hartree–Womersley method (see Hartree (**5**)) to the basic equations (2.3) and (2.4) is that at any two stations $\xi = \xi_A$ and $\xi = \xi_B$ we replace derivatives in the ξ-direction by finite differences (without truncation error) and all other quantities by averages. Thus we obtain

$$(\phi_A'''+\phi_B''')+\tfrac{1}{2}\alpha\{(\phi_A')^2-(\phi_B')^2\}+\tfrac{1}{2}(\phi_A''+\phi_B'')\{\phi_A+\phi_B+\alpha(\phi_B-\phi_A)\}+ \\ +\alpha(2+S_A+S_B)(U_B^2 e-U_A^2 e)=0 \quad (3.1)$$

and

$$(S_A''+S_B'')+\tfrac{1}{2}\alpha(S_A-S_B)(\phi_A'+\phi_B')+\tfrac{1}{2}\alpha(S_A'+S_B')(\phi_B-\phi_A)+ \\ +\tfrac{1}{2}(S_A'+S_B')(\phi_A+\phi_B)=0, \quad (3.2)$$

where $\alpha = 2(\xi_B+\xi_A)/(\xi_B-\xi_A)$ and the primes denote η-derivatives at the stations $\xi = \xi_A$ and $\xi = \xi_B$. The boundary conditions for ϕ_A, ϕ_B, S_A, and S_B are

$$\phi_A = \phi_B = \phi_A' = \phi_B' = 0, \qquad S_A = S_B = 1 \quad \text{at } \eta = 0 \text{ for } \xi \geqslant 0, \\ \phi_A' = 2-\tfrac{1}{4}\xi_A, \qquad \phi_B' = 2-\tfrac{1}{4}\xi_B, \qquad S_A = S_B = 0 \quad \text{at } \eta = \infty \text{ for } \xi \geqslant 0. \quad (3.3)$$

If we now introduce

$$\Phi = \phi_A+\phi_B, \qquad \Psi = \Phi', \qquad \theta = S_A+S_B \quad (3.4)$$

then equations (3.1), (3.2), and (3.3) simplify as follows:

$$\Psi''+\{\tfrac{1}{2}(1+\alpha)\Phi-\alpha\phi_A\}\Psi'+\alpha(\phi_A'-\tfrac{1}{2}\Psi)\Psi+\alpha(U_B^2 e-U_A^2 e)(2+\theta)=0, \quad (3.5)$$

$$\theta''+\{\tfrac{1}{2}(1+\alpha)\Phi-\alpha\phi_A\}\theta'-\tfrac{1}{2}\alpha\Psi\theta+\alpha S_A\Psi=0, \quad (3.6)$$

together with the boundary conditions

$$\Psi = 0, \qquad \theta = 2, \quad \text{at } \eta = 0, \\ \Psi = 2(U_B e-U_A e) = 4-\tfrac{1}{4}(\xi_A+\xi_B), \quad \theta = 0 \quad \text{at } \eta = \infty. \quad (3.7)$$

Equations (3.5) and (3.6) represent a pair of coupled ordinary differential equations in Ψ and θ, the equation in Ψ being non-linear. If we know ϕ_A, ϕ_A', and S_A the boundary value problem is then completely defined.

The integration procedure is started at $\xi_A = 0$ since ϕ_A, ϕ_A', and S_A are known from Howarth's table (**4**). Taking $\xi_B = 0{\cdot}2$, and thus $\alpha = 2$, the required functions Ψ and θ may be found by standard relaxation methods. These functions Ψ and θ will only be approximate due to the use of simple truncated finite-difference formulae in the ξ-direction. An improvement in accuracy is then obtained using Richardson's process of h^2-extrapolation. We calculate Ψ and θ at $\xi_B = 0{\cdot}2$ in one and two steps $\xi = 0$ to $0{\cdot}1$ and $\xi = 0{\cdot}1$ and $0{\cdot}2$. If $\Psi^{(1)}$ and $\theta^{(1)}$ are the results for the one-step

calculation, and if $\Psi^{(2)}$ and $\theta^{(2)}$ are the results of the two-step calculation, then by h^2-extrapolation the 'final' results are

$$\Psi = \Psi^{(2)} + \tfrac{1}{3}(\Psi^{(2)} - \Psi^{(1)})$$

and

$$\theta = \theta^{(2)} + \tfrac{1}{3}(\theta^{(2)} - \theta^{(1)}) \tag{3.8}$$

with error $O(h^4)$, where h is the mesh length in the ξ-direction (see Fox (**6**)). That h^2-extrapolation is the correct extrapolation for the above equations has been verified numerically by comparing at $\xi = 0{\cdot}2$ the functions ϕ, ϕ', and S (obtained from the final h^2-extrapolated functions Φ, Ψ, and θ) with the series solution given by equations (2.16) and (2.17). The difference was found to be not more than one unit in the fourth decimal, which is in good agreement with the allowed possible error $O(h^4)$, since $h = 0{\cdot}2$. Further details on the relaxation solution of equations (3.5) and (3.6) for $\xi \leqslant 0{\cdot}2$ and $0{\cdot}2 \leqslant \xi \leqslant \xi_{\text{sep}}$ is described in an appendix.

In Table 3 the velocity $U = \frac{1}{2}u_0 \partial\phi/\partial\eta$, and thermal profiles S are tabulated at intervals of $\eta = 0{\cdot}1$ for the stations $\xi = 0{\cdot}2$, $0{\cdot}4$, and $0{\cdot}6$. At stations $\xi = 0{\cdot}2$ and $0{\cdot}4$ the functions U/u_0 and S are rounded off to four decimals since the difference between the one- and two-step calculations was less than ten units in the fourth decimal, the maximum difference occurring at $\eta = 1{\cdot}4$. It is believed that the fourth decimal in the 'final' h^2-extrapolated values of U/u_0 and S, at $\xi = 0{\cdot}2$ and $0{\cdot}4$, is reliable. However, in the calculation of U/u_0 and S at $\xi = 0{\cdot}6$, in one and two steps from $\xi = 0{\cdot}4$, the difference in the one- and two-step calculation was less than forty units in the fourth decimal, the maximum again occurring at about $\eta = 1{\cdot}4$. Final h^2-extrapolated functions at $\xi = 0{\cdot}6$ are thus rounded off to three decimals and it is believed that the third decimal is reliable.

At $\xi = 0{\cdot}6$ the shear stress, $(\partial U/\partial Y)_{Y=0}$, in the incompressible plane was found to be of the order 10^{-4}. Hence separation will occur very near to $X_s = 0{\cdot}60$. Since the calculations at $\xi = 0{\cdot}6$ become rather unstable, it is possible that the numerical process may break down if an attempt is made to pass the point of separation. Indeed, for the incompressible flow over a flat plate in the presence of a linear retarded main stream velocity, Hartree (**5**) found, on reinvestigation of Howarth's problem (**4**), a strong suggestion of the existence of an algebraic singularity in the neighbourhood of separation. This conclusion was later confirmed by Leigh (**7**) in repeating Hartree's calculations using much finer steps in the ξ-direction (in the neighbourhood of the separation point) and working to a greater number of decimals using automatic computing machinery. The question as to whether or not an algebraic singularity in $(\partial U/\partial Y)_{Y=0}$ exists for the present problem remains unanswered due to the prohibitive amount of necessary numerical work. It has been the intention in this section to

obtain over-all trends and gross effects rather than precise results. However, the velocity and thermal profiles obtained are sufficiently accurate to examine the exactness of various approximate methods which may be developed and which proved so fruitful in the study of the incompressible boundary layer.

4. The momentum, energy, and thermal-integral equations in the incompressible-plane

In the previous two sections details have been given on the numerical solution of the transformed boundary layer equations (1.8), (1.9), (1.10), and (1.20). It is desirable to compare with these solutions the accuracy of approximate methods. Since any approximate method applied in the incompressible-plane can be taken over directly to the compressible-plane (see Stewartson (**3**)) we shall develop, for the sake of simplicity, an approximate method in the incompressible-plane. For the laminar incompressible boundary layer the skin friction and dissipation of energy are connected with the boundary layer thickness by the momentum and energy-integral equations, which represent the balance of momentum and energy within a small section of the boundary layer. These equations are due to von Kármán (**8**) and Wieghardt (**9**). In the following we shall derive the momentum, energy, and thermal-integral equations in the incompressible-plane and proceed to obtain an approximate solution of the transformed boundary layer equations (1.8), (1.9), (1.10), and (1.20).

We make the assumption that, in the incompressible-plane, the hydrodynamic and thermal boundary layer thicknesses are identical and equal to Δ. Integrating equations (1.9) and (1.10) with respect to Y between the limits $Y = 0$ and $Y = \Delta$, and taking account of equations (1.8) and (1.20), we obtain the momentum and thermal-integral equations

$$U_e\frac{d\Theta^2}{dX}+2\frac{dU_e}{dX}\Theta^2\left(2+\frac{(\Delta^*+E)}{\Theta}\right)=\frac{2\Theta}{U_e}\left(\frac{\partial U}{\partial Y}\right)_{Y=0}, \tag{4.1}$$

$$U_e\frac{dE^{*2}}{dX}+2\frac{dU_e}{dX}E^{*2}=-2E^*\left(\frac{\partial S}{\partial Y}\right)_{Y=0}. \tag{4.2}$$

Multiplying equation (1.9) by U and integrating with respect to Y between the limits $Y = 0$ and Δ, we have the energy-integral equation

$$U_e\frac{d\Theta^{*2}}{dX}+2\frac{dU_e}{dX}\Theta^{*2}\left(3+\frac{2E^*}{\Theta^*}\right)=\frac{4\Theta^*}{U_e^2}\int_0^\Delta\left(\frac{\partial U}{\partial Y}\right)^2dY. \tag{4.3}$$

Here the boundary layer characteristics in the incompressible-plane, i.e. the displacement thickness Δ^*, momentum thickness Θ, energy thickness

Θ^*, thermal thickness E, and thermal flux thickness E^*, are defined as

$$\Delta^* = \int_0^\Delta \left(1 - \frac{U}{U_e}\right) dY, \tag{4.4}$$

$$\Theta = \int_0^\Delta \left(1 - \frac{U}{U_e}\right)\frac{U}{U_e}\, dY, \tag{4.5}$$

$$\Theta^* = \int_0^\Delta \left(1 - \frac{U^2}{U_e^2}\right)\frac{U}{U_e}\, dY, \tag{4.6}$$

$$E = \int_0^\Delta S\, dY, \tag{4.7}$$

$$E^* = \int_0^\Delta \frac{U}{U_e} S\, dY. \tag{4.8}$$

Note that if S is put equal to zero in equations (4.1) and (4.3) we obtain the momentum and energy integral equations derived by von Kármán (**8**) and Wieghardt (**9**) respectively for the incompressible boundary layer.

In the original method of von Kármán and Polhausen (**10**), applied to the incompressible boundary layer, a fourth degree polynomial for the velocity profile was assumed and the coefficients were determined using the boundary conditions at the wall and in the main stream. The momentum-integral equation could then be solved approximately. It was found that the velocity profile could be expressed as a member of a one-parameter family of curves, with $\lambda = \Theta^2(dU_e/dX)$, the so-called Polhausen parameter. On examination of the various exact solutions known for incompressible boundary layer theory, it was found that the above procedure was adequate for favourable pressure gradients but for adverse pressure gradients it is evident that the Polhausen parameter is not sufficient to determine the velocity profile. Wieghardt (**9**) suggested using a two-parameter velocity profile, one parameter being the Polhausen parameter, to be found in the usual manner from the momentum-integral equations, and a second new parameter which was to be found by using the energy-integral equation. In Wieghardt's method an eleventh-degree polynomial for the velocity profile was assumed. This procedure, although it gives satisfactory results, has been further simplified by Tani (**11**) with considerable improvement in accuracy. Tani assumes a fourth-degree polynomial in which four of the coefficients are determined using the conditions at the wall and in the main stream and the remaining coefficient is determined by satisfying the energy-integral equation. In what follows,

Tani's method is modified to deal with problems in the incompressible-plane.

We assume velocity and thermal profiles of the type

$$\frac{U}{U_e} = \sum_{n=0}^{4} a_n(X)\left(\frac{Y}{\Delta}\right)^4, \qquad S = \sum_{n=0}^{4} b_n(X)\left(\frac{Y}{\Delta}\right)^n \tag{4.9}$$

and determine the coefficients a_n and b_n from the conditions

$$U = 0, \qquad S = 1 \quad \text{at} \quad Y = 0,$$

$$U = U_e, \qquad S = 0, \qquad \frac{\partial U}{\partial Y} = \frac{\partial^2 U}{\partial Y^2} = \frac{\partial S}{\partial Y} = \frac{\partial^2 S}{\partial Y^2} = 0 \quad \text{at } Y = \Delta. \tag{4.10}$$

The usual conditions

$$\left(\frac{\partial^2 U}{\partial Y^2}\right)_{Y=0} = -U_e\frac{dU_e}{dX}(1+S(0)) = -2U_e\frac{dU_e}{dX}, \qquad \left(\frac{\partial^2 S}{\partial Y^2}\right)_{Y=0} = 0,$$

which imply that equations (1.9) and (1.10) are satisfied at the wall, are not used so that in each case one of the coefficients denoted by a and b respectively may be left undetermined. We thus obtain

$$\frac{U}{U_e} = \frac{Y^2}{\Delta^2}\left(6-8\frac{Y}{\Delta}+3\frac{Y^2}{\Delta^2}\right)+a\frac{Y}{\Delta}\left(1-\frac{Y}{\Delta}\right)^3 \tag{4.11}$$

and

$$S = 1-\frac{Y^2}{\Delta^2}\left(6-8\frac{Y}{\Delta}+3\frac{Y^2}{\Delta^2}\right)-b\frac{Y}{\Delta}\left(1-\frac{Y}{\Delta}\right)^3. \tag{4.12}$$

The 'new' coefficients a and b are then adopted as parameters for the velocity and thermal profiles, and are to be identified with the velocity and thermal gradients at the wall since

$$\frac{1}{U_e}\left(\frac{\partial U}{\partial Y}\right)_{Y=0} = \frac{a}{\Delta}, \qquad \left(\frac{\partial S}{\partial Y}\right)_{Y=0} = -\frac{b}{\Delta}. \tag{4.13}$$

Introducing the dimensionless quantities

$$d = \frac{\Delta^*}{\Delta}, \qquad e = \frac{\Theta}{\Delta}, \qquad f = \frac{\Theta^*}{\Delta}, \qquad g = \frac{E}{\Delta},$$

$$h = \frac{E^*}{\Delta}, \qquad k = \frac{2\Delta}{U_e^2}\int_0^{\Delta}\left(\frac{\partial U}{\partial Y}\right)^2 dY, \qquad \alpha = \frac{\Theta^*}{\Theta},$$

and

$$\beta = \frac{E^*}{\Theta}, \tag{4.14}$$

we can write equations (4.1), (4.2), and (4.3) in the forms

$$U_e\frac{d\Theta^2}{dX}+2\Theta^2\frac{dU_e}{dX}\left(2+\frac{d}{e}+\frac{g}{e}\right) = p, \tag{4.15}$$

$$U_e\frac{d(\alpha^2\Theta^2)}{dX}+2\alpha^2\Theta^2\frac{dU_e}{dX}\left(3+2\frac{h}{f}\right) = q, \tag{4.16}$$

and

$$U_e\frac{d(\beta^2\Theta^2)}{dX}+2\beta^2\Theta^2\frac{dU_e}{dX} = r. \tag{4.17}$$

The quantities d, e, f, g, h, k, p, q, and r are functions of a and b only. Substituting equations (4.11) and (4.12) in equations (4.4) to (4.8) and using the definitions given in equation (4.14), there results†

$$d = \frac{2}{5} - \frac{a}{20}, \tag{4.18}$$

$$e = \frac{4}{35} + \frac{a}{105} - \frac{a^2}{252}, \tag{4.19}$$

$$f = \frac{876}{5005} + \frac{73}{5005}a - \frac{23}{5460}a^2 - \frac{1}{2860}a^3, \tag{4.20}$$

$$g = \frac{2}{5} - \frac{b}{20}, \tag{4.21}$$

$$h = \frac{4}{35} + \frac{25}{840}a - \frac{17}{840}b - \frac{1}{252}ab, \tag{4.22}$$

$$k = \frac{2}{35}(48 - 4a + 3a^2), \tag{4.23}$$

$$p = \frac{2}{U_e}\left(\frac{\partial U}{\partial Y}\right)_{Y=0} = 2Ea, \tag{4.24}$$

$$q = \frac{4\Theta^*}{U_e^2}\int_0^\Delta \left(\frac{\partial U}{\partial Y}\right)^2 dY = 2kf, \tag{4.25}$$

and

$$r = -2E^*\left(\frac{\partial S}{\partial Y}\right)_{Y=0} = 2bh. \tag{4.26}$$

The first-order differential equations (4.15), (4.16), and (4.17) are to be solved subject to the boundary conditions $\Theta = 0$ at $X = 0$. They represent, together with equations (4.18) to (4.26), three coupled first-order differential equations in a, b, and Δ. A more suitable form of these equations for numerical integration is obtained on introducing the Pohlhausen type parameter

$$\Lambda = \alpha^2\lambda = \alpha^2\Theta^2\frac{dU_e}{dX}. \tag{4.27}$$

Then for the main stream velocity $U_e = u_0(1 - \frac{1}{8}X)$, the approximate energy-integral equation (4.16) becomes

$$(X - 8)\frac{d\Lambda}{dX} + \Lambda\left(6 + 4\frac{h}{f}\right) = q, \tag{4.28}$$

† Formulae (4.18) to (4.20), (4.23) to (4.25) have already been given by Tani (11).

and on using equation (4.16) we can eliminate $d\Theta^2/dX$ from the equations (4.15) and (4.16), giving

$$a = \frac{ke}{f} - \Lambda\frac{e}{f}\left\{1 + 2\frac{h}{f} - \frac{(d+g)}{e}\right\} + \Lambda(8-X)\frac{e}{f^2}\frac{d}{dX}\left(\log\frac{f}{e}\right) \tag{4.29}$$

and

$$b = \frac{kh}{f} - \Lambda\frac{2h}{f^2}\left(1 + \frac{h}{f}\right) + \Lambda(8-X)\frac{d}{dX}\left(\log\frac{f}{h}\right). \tag{4.30}$$

Since $\alpha = \Theta^*/\Theta$ is finite at $X = 0$, the boundary condition to be imposed on equations (4.28), (4.29), and (4.30) is

$$\Lambda = 0 \quad \text{at} \quad X = 0. \tag{4.31}$$

The integration of equations (4.28), (4.29), and (4.30) subject to equation (4.31) has been carried out using the Milne–Simpson step-by-step integration procedure for first-order differential equations (see Milne (**12**)). The interval was taken to be $X = 0{\cdot}02$ and the iterative procedure for calculating a, b, and Λ was carried out using four significant figures. Although it is difficult to extend the calculation right up to the separation point (i.e. when $(\partial U/\partial Y)_{Y=0} = a/\Delta = 0$), due to the rapid growth of the derivatives $d(\log f/e)/dX$ and $d(\log f/h)/dX$ in this region, it is possible to arrive at a point so near separation that the latter point may be extrapolated with confidence. It was found on extrapolation that

$$\left(\frac{\partial U}{\partial Y}\right)_{Y=0} = \frac{a}{\Delta} = 0{\cdot}000 \quad \text{at} \quad X = 0{\cdot}60,$$

i.e. $a = O(10^{-3})$.

Using the tabulated values of a, b, and Λ at $X = 0(0{\cdot}02)0{\cdot}58$ and the extrapolated values at $X = 0{\cdot}60$ we can calculate, for the incompressible-plane, the boundary layer characteristics

$$\Delta^*, \quad \Theta, \quad \Theta^*, \quad E, \quad E^*, \quad \left(\frac{\partial S}{\partial Y}\right)_{Y=0} \quad \text{and} \quad \frac{1}{u_0}\left(\frac{\partial U}{\partial Y}\right)_{Y=0}.$$

In Table 4 these approximate results are tabulated for the stations $X = 0{\cdot}2$, $0{\cdot}4$, and $0{\cdot}6$ together with the more precise values evaluated from Tables 1, 2, and 3. We note that the agreement is excellent at $X = 0{\cdot}2$ and $0{\cdot}4$ and the discrepancies at $X = 0{\cdot}6$ are not serious. Results for the approximate solution are given graphically in Figs. 1 and 2, and those obtained using the series solution and the Hartree–Womersley method are the indicated points in these figures.

5. Boundary layer characteristics in the compressible-plane

In sections 2, 3, and 4 the boundary-layer characteristics in the incompressible-plane have been calculated for the main stream velocity $U_e = u_0(1 - \frac{1}{8}X)$ and dimensionless wall temperature $S_w = 1$. It is the

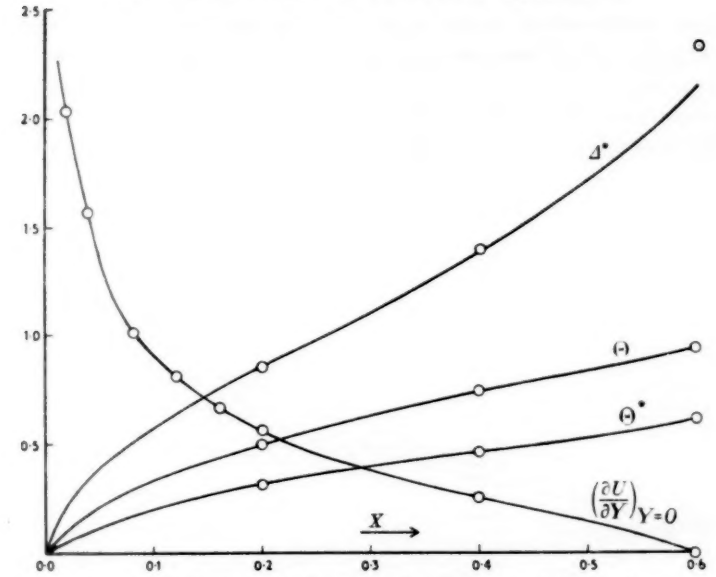

FIG. 1. Hydrodynamic boundary layer characteristics in the incompressible-plane.

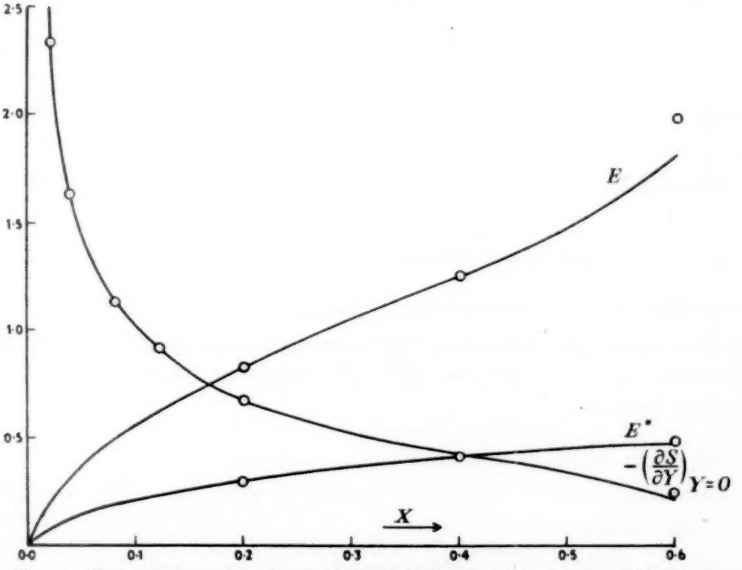

FIG. 2. Thermal boundary layer characteristics in the incompressible-plane.

purpose of this section to give in tabular and graphical form some of the essential boundary layer characteristics in the compressible-plane for a range of free stream Mach numbers $M_0 = 0, 1, 2, 3, 4$, and 6. The argument of tabulation is taken for convenience to be x/x_s, where x_s is the distance of the separation point from the leading edge. In the following we take $\gamma = 1{\cdot}4$.

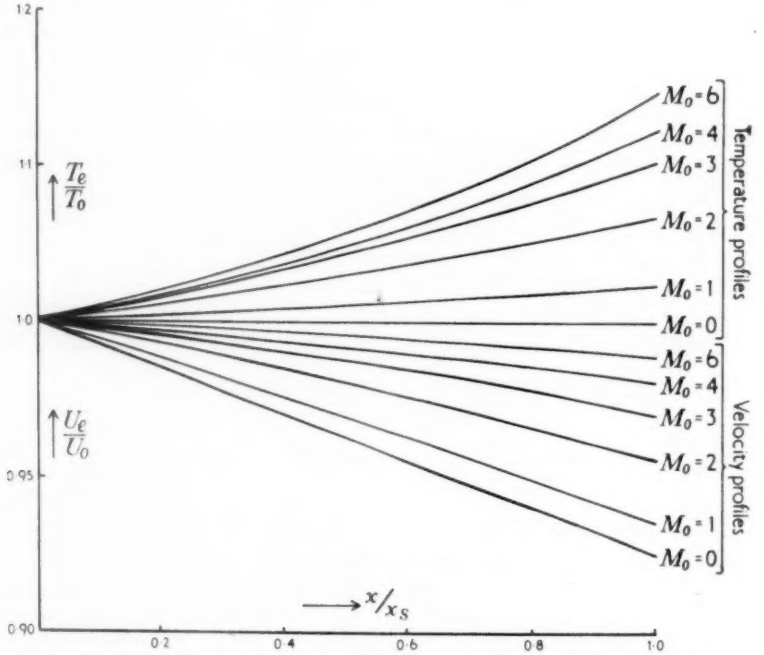

FIG. 3. Main stream velocity distributions and the associated main stream temperature distributions for $M_0 = 0, 1, 2, 3, 4$, and 6.

(i) *Velocity and thermal profiles in the main stream*

These have already been defined by equations (1.17) and (1.20). The quantities u_e/u_0 and T_e/T_0 are given graphically in Fig. 3 and in tabular form in Table 6.

(ii) *Shear stress and local skin friction coefficient*

The shear stress at the wall is defined by equation (1.23). On using (2.1) and (2.2) we obtain

$$\tau_w = \rho_0 \sqrt{\nu_0} \frac{u_0^{\frac{1}{2}}}{4X^{\frac{1}{4}}} \left(\frac{\partial^2 \phi}{\partial \eta^2}\right)_{\eta=0}. \tag{5.1}$$

This can be made dimensionless on introducing the local skin friction coefficient $C_f = \tau_w/\frac{1}{2}\rho_w u_e^2$ and the Reynolds number $\mathrm{Re}_w = xu_e/\nu_w$ resulting in the relationship

$$C_f\sqrt{(\mathrm{Re}_w)} = \tfrac{1}{2}x^{\frac{1}{2}}\{X(1-\tfrac{1}{8}X)^3\}^{-\frac{1}{2}}\left(\frac{a_e}{a_0}\right)^{(3\gamma-1)/(2\gamma-1)}\left(\frac{\partial^2\phi}{\partial\eta^2}\right)_{\eta=0}. \qquad (5.2)$$

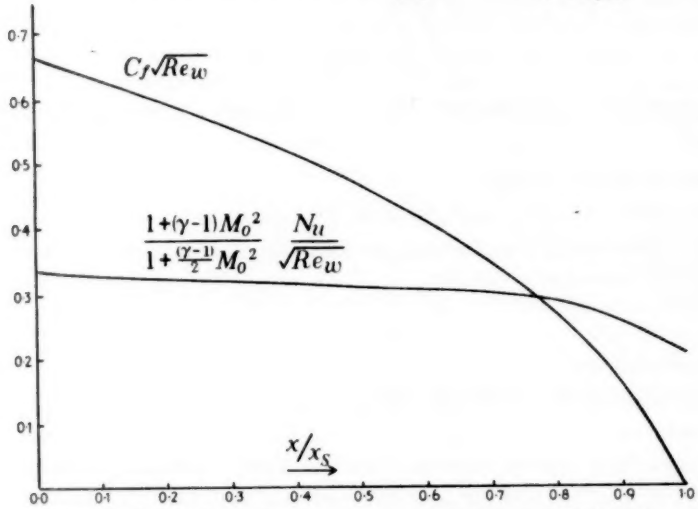

FIG. 4. Effect of an adverse pressure gradient on wall shear and Nusselt number for $0 \leqslant M_0 \leqslant 6$.

The negligible variation of $C_f\sqrt{(\mathrm{Re}_w)}$ with Mach number will be noticed from Table 6. For this reason the single curve of $C_f\sqrt{(\mathrm{Re}_w)}$ against x/x_s in Fig. 4 is sufficient for the range of Mach numbers $0 \leqslant M_0 \leqslant 6$.

(iii) *Nusselt number*

The local heat transfer at the wall is described by means of the dimensionless Nusselt number $\mathrm{Nu} = x\left(\frac{\partial T}{\partial y}\right)_w \Big/ (T_0 - T_w)$. The Nusselt number can thus be explicitly expressed in terms of known results. We have, on using equations (1.6), (1.11), and (2.1), the result

$$\left(\frac{\partial T}{\partial y}\right)_w = T_0\left(1+\frac{\gamma-1}{2}M_0^2\right)\frac{a_e\rho}{a_0\rho_0\sqrt{\nu_0}}\frac{u_0^{\frac{1}{2}}}{2X^{\frac{1}{2}}}\left(\frac{\partial S}{\partial\eta}\right)_{\eta=0}, \qquad (5.3)$$

hence, on using (1.21), we obtain

$$\mathrm{Nu} = -\tfrac{1}{2}\sqrt{(\mathrm{Re}_w)}x^{\frac{1}{2}}\{X(1-\tfrac{1}{8}X)\}^{-\frac{1}{2}}\times$$
$$\times\frac{1+\frac{1}{2}(\gamma-1)M_0^2}{1-(1+S_w)\{1+\frac{1}{2}(\gamma-1)M_0^2\}}\left(\frac{a_e}{a_0}\right)^{(3\gamma-1)/(2\gamma-1)}\left(\frac{\partial S}{\partial\eta}\right)_{\eta=0}. \qquad (5.4)$$

In particular, for the case $S_w = 1$,

$$\frac{\mathrm{Nu}}{\sqrt{(\mathrm{Re}_w)}} = \tfrac{1}{2}x^{\frac{1}{2}}\{X(1-\tfrac{1}{8}X)\}^{-\frac{1}{2}}\frac{1+\frac{1}{2}(\gamma-1)M_0^2}{1+(\gamma-1)M_0^2}\left(\frac{a_e}{a_0}\right)^{(3\gamma-1)/(2\gamma-1)}\left(\frac{\partial S}{\partial \eta}\right)_{\eta=0}. \quad (5.5)$$

The ratio $\mathrm{Nu}/\sqrt{(\mathrm{Re}_w)}$ is tabulated as a function of x/x_s for a range of Mach numbers in Table 6. The quantity

$$\frac{1+(\gamma-1)M_0^2}{1+\frac{1}{2}(\gamma-1)M_0^2}\frac{\mathrm{Nu}}{\sqrt{(\mathrm{Re}_w)}}$$

has negligible variation with Mach number and is given graphically in Fig. 4.

(iv) *Reynolds analogy*

Reynolds analogy is not applicable to flows with separation. However, it is interesting to demonstrate the variation of the inverse of the usual Reynolds analogy parameter, i.e. $C_f\mathrm{Re}_w/\mathrm{Nu}$, given in tabular form in Table 6.

6. Conclusions

The problem of particular interest is the solution of the compressible laminar boundary layer equations for a flat plate in the presence of a retarded main stream velocity when the plate is heated. If we assume that the Prandtl number is unity and a linear viscosity temperature relationship, then using Stewartson's transformation the resulting equations in the incompressible-plane are more amenable to numerical analysis. A retarded main stream velocity in the compressible-plane may then be obtained on assuming a linear retarded main stream velocity in the incompressible-plane. The essential parameter of the problem is now the dimensionless temperature S_w evaluated at the wall. On stipulating a particular value for S_w and solving the basic equations (1.8) to (1.10), a family of solutions for various free stream Mach numbers M_0 may be derived. The present paper deals with the special case $S_w = 1$. To examine the effect of heat addition to the laminar compressible boundary layer when separation occurs it would be desirable to have solutions for further values of S_w. This task would entail a great deal of laborious calculation. However, the modified Polhausen method developed in section 4 should be sufficiently accurate for this purpose. It should be noted that for the approximate method the amount of numerical work involved is trivial in comparison with that required to obtain the more precise results of sections 2 and 3 but that its usefulness is restricted to the case $\sigma = 1$ (when the hydrodynamic and thermal boundary layer thicknesses are equal).

For the boundary condition $S_w = 0$ equation (1.10) is linear and so can

only have as solution $S \equiv 0$. This will correspond in the compressible-plane to a thermally insulated boundary. Equations (1.8), (1.9), and (1.22) taking $S \equiv 0$ have been solved by Howarth (**4**) and Hartree (**5**). Their results will then give data on a family of solutions in the compressible-plane for various free stream Mach numbers. Table 5 gives values of x_s and T_w (for a range of M_0) corresponding to the case of a thermally insulated plate ($S_w = 0$) and to the case of a heated plate with heat transfer ($S_w = 1$). It is apparent from this table that heat transfer to the boundary-layer moves the point of separation upstream. Furthermore, with regard to the family of solutions corresponding to $S_w = 1$ (see Table 5) it follows that an increase in the free stream Mach number leads to an earlier separation. Some further facts are revealed from these solutions:

(*a*) The dimensionless quantities $C_f\sqrt{(\mathrm{Re}_w)}$ and $\dfrac{1+(\gamma-1)M_0^2}{1+\frac{1}{2}(\gamma-1)M_0^2}\dfrac{\mathrm{Nu}}{\sqrt{(\mathrm{Re}_w)}}$ given graphically as functions of x/x_s in Fig. 4 are sufficient to describe the range of Mach numbers $0 \leqslant M_0 \leqslant 6$.

(*b*) The heat transfer parameter $\mathrm{Nu}/\sqrt{(\mathrm{Re}_w)}$ for $0 \leqslant M_0 \leqslant 6$ is virtually constant in the region $0 \leqslant x \leqslant 0{\cdot}8x_s$ and decreases rapidly in the neighbourhood of the separation point.

Acknowledgements

I should like to thank Professor K. Stewartson for suggesting this problem and for his interest and help during its progress. Most of the computations for this paper were carried out by Miss C. R. Faithful and Mrs. E. B. Tilly for whose care and accuracy the author is grateful.

APPENDIX

Relaxation solution of equations (3.5) *and* (3.6)

Equations (3.5) and (3.6) subject to the boundary conditions (3.7) constitute a two-point boundary value problem.

Method I for $0 \leqslant \xi \leqslant 0{\cdot}2$

In the usual central difference notation (see Fox (**6**)), the residual formulae at any typical point O, in the range of integration, are

$$R_0 = \Psi_1(1+\tfrac{1}{2}hf_0)+\Psi_3(1-\tfrac{1}{2}hf_0)+(-2+h^2g_0)\Psi_0+(C_2+hf_0C_1)\Psi_0+h^2H_0 \qquad \text{(A 1)}$$

and $$M_0 = \theta_1(1+\tfrac{1}{2}hf_0)+\theta_3(1-\tfrac{1}{2}hf_0)+(-2+h^2f_0)\theta_0+(C_2+hf_0C_1)\theta_0+h^2L_0, \qquad \text{(A 2)}$$

where

$$f(\eta) = \tfrac{1}{2}(1+\alpha)\Phi-\alpha\phi_A, \qquad \text{(A 3)}$$

$$g(\eta) = \alpha\left(\frac{d\phi_A}{d\eta}-\Psi\right), \qquad \text{(A 4)}$$

$$k(\eta) = -\tfrac{1}{2}\alpha S_A\Psi, \qquad \text{(A 5)}$$

$$L(\eta) = \alpha S_A \Psi, \tag{A 6}$$

$$H(\eta) = -\tfrac{1}{2}\alpha S_A \Psi, \tag{A 7}$$

$$C_1 = -\tfrac{1}{8}\mu\delta^2 + \tfrac{1}{30}\mu\delta^5, \tag{A 8}$$

$$C_2 = -\tfrac{1}{12}\delta^2 + \tfrac{1}{90}\delta^6, \tag{A 9}$$

and μ is the 'averaging-operator' and h is the mesh length. We take as our first approximation

$$\theta = S_A + S_B \doteq 2S_A \tag{A 10}$$

and

$$\psi \doteq \frac{d\phi_A}{d\eta}\left(1 + \frac{1-\frac{1}{8}\xi_B}{1-\frac{1}{8}\xi_A}\right). \tag{A 11}$$

Point and block relaxation patterns are then constructed for equation (3.6) and residuals are calculated at $\eta = 0(0{\cdot}4)5{\cdot}2$ by means of formulae (A 1), neglecting $C\Psi$. A second approximation to ψ is then obtained using standard relaxation techniques and the procedure repeated until the first two decimals of ψ have been obtained. Note that at this stage it is sufficient to find Φ by using the trapezoidal rule. The functions Φ and Ψ are then inserted in equation (3.6) and θ is found by relaxation to three decimals. Using this θ we now calculate new residuals for Ψ by adding in $C\Psi$. The central differences have been obtained near the origin using Fox's procedure (6), and Φ calculated accurately. Equation (3.6) is then relaxed until we are certain of three decimals in Ψ. The function θ is then calculated accurately using the complete residual formulae (A 2). This repeated relaxation of the two equations is carried out until we are sure of three decimals in Ψ, Φ, and θ. The step $h = 0{\cdot}4$ is then halved to $h = 0{\cdot}2$ and the ψ and θ equations are relaxed so that we are sure of four decimals in the wanted functions. To ensure that the fourth decimal is reliable a further run was completed using $h = 0{\cdot}1$ and working to five decimals. The last step is important since we are interested in determining Ψ'' accurately at $\eta = 0$.

The above method was found to be fairly rapid for values of $\xi \leqslant 0{\cdot}2$. However, for $\xi > 0{\cdot}2$, the initial approximations (A 10) and (A 11) are no longer good, and in particular near $\xi = 0{\cdot}6$ the coupling between the equations (3.5) and (3.6) is strong. Furthermore, the treatment of equation (3.6) for Ψ becomes difficult since probably in this region the non-linear terms are more predominant. It was thus found necessary to modify the procedure.

Method II for $0{\cdot}2 \leqslant \xi < \xi_{\text{sep}}$

The aims of this second method are to weaken the coupling between the equations (3.5) and (3.6), and at the same time effectively to linearize equation (3.5). These aims may be achieved by using a perturbation approach. We define

$$\Psi = \Psi_L + Y, \tag{A 12}$$

$$\Phi = \Phi_L + y, \tag{A 13}$$

$$\theta = \theta_L + G, \tag{A 14}$$

where

$$\Phi_L = \int_0^\eta \Psi_L \, d\eta \quad \text{and} \quad y = \int_0^\eta Y \, d\eta.$$

The functions Ψ_L, Φ_L, and θ_L used in the perturbation procedure are defined as follows:

$$\Psi_L = \frac{d}{d\eta}(\phi_A + \phi_B^{(S)}), \tag{A 15}$$

$$\Phi_L = \phi_A + \phi_B^{(S)}, \tag{A 16}$$

and

$$\theta_L = S_A + S_B^{(S)}, \tag{A 17}$$

where ϕ_A, ϕ'_A, and S_A are known functions at the station $\xi = \xi_A$ and $\phi_B^{(S)}$, $d(\phi_B^{(S)})/d\eta$, and $S_B^{(S)}$ can be calculated at $\xi = \xi_B$ from the series solution given by equations (2.16) and (2.17).

Substituting equations (A 12), (A 13), and (A 14) in (3.5) and (3.6), we arrive at the following differential equations in the perturbation functions Y and G:

$$\frac{d^2Y}{d\eta^2}+\{\tfrac{1}{2}(1+\alpha)\Phi_L-\alpha\phi_A\}\frac{dY}{d\eta}+\alpha\Big(\frac{d\phi_A}{d\eta}-\Psi_L\Big)Y+\tfrac{1}{2}(1+\alpha)y\Big(\frac{dY}{d\eta}+\Psi'_L\Big)-$$

$$-\tfrac{1}{2}\alpha Y^2+\alpha(U_B^2e-U_A^2e)G+M_L(\eta)=0, \quad \text{(A 18)}$$

and

$$\frac{d^2G}{d\eta^2}+\{\tfrac{1}{2}(1+\alpha)\Phi_L-\alpha\phi_A\}\frac{dG}{d\eta}-\tfrac{1}{2}\alpha\Psi_L G+\tfrac{1}{2}(1+\alpha)y\frac{dG}{d\eta}-\tfrac{1}{2}\alpha GY+N_L(\eta)=0, \quad \text{(A 19)}$$

where

$$M_L(\eta)=\frac{d^2\Psi_L}{d\eta^2}+\{\tfrac{1}{2}(1+\alpha)\Phi_L-\alpha\phi_A\}\frac{d\Psi_L}{d\eta}+\alpha\Big(\frac{d\phi_A}{d\eta}-\tfrac{1}{2}\Psi_L\Big)\Psi_L+\alpha(U_B^2e-U_A^2e)(2+\theta_L), \quad \text{(A 20)}$$

and

$$N_L(\eta)=\frac{d^2\theta_L}{d\eta^2}+\{\tfrac{1}{2}(1+\alpha)\Phi_L-\alpha\phi_A\}\frac{d\theta_L}{d\eta}-\frac{\alpha}{2}\Psi_L\theta_L+\alpha S_A\Psi_L+$$

$$+\tfrac{1}{2}(1+\alpha)y\frac{d\theta_L}{d\eta}+\alpha S_AY-\tfrac{1}{2}\alpha\theta_LY. \quad \text{(A 21)}$$

The boundary conditions are

$$Y(0)=Y(\infty)=0, \quad \text{(A 22)}$$

$$G(0)=G(\infty)=0. \quad \text{(A 23)}$$

Equation (A 18) is still non-linear, but if Y, y, and G are small, the non-linear terms will be small and furthermore the coupling between equations (A 18) and (A 19) will present little trouble. It was found that the above procedure was extremely rapid. In the actual relaxation of (A 18), G was neglected in the first instance and Y determined accurately to four decimals using mesh $h = 0{\cdot}1$. The function G was then determined accurately and when inserted into equation (A 18) the new Y virtually remained unchanged. Rarely was it found necessary to return to the G equation again. It was also found that the amount of numerical work involved in solving equation (A 18) could be greatly reduced by the following extrapolation process for Y. By basic iterative procedure we determine at each nodal point four successive estimates of Y, i.e. $Y^{(i)}(\eta)$ for $i = 1, 2, 3,$ and 4. These are then differenced at each value of η giving $\delta_{i+\frac{1}{2}} = Y^{(i+1)}-Y^{(i)}$ for $i = 1, 2,$ and 3. Then we define ratios $\lambda_j = \delta_{j+\frac{1}{2}}/\delta_{j-\frac{1}{2}}$ for $j = 2, 3$. Now it was found that λ_2 and λ_3 differed by less than $\frac{1}{2}$ per cent and thus if we define $\bar{\lambda} = \frac{1}{2}(\lambda_2+\lambda_3)$ then the 'final' $Y = Y^{(3)}+\delta_{\frac{7}{2}}/(1-\bar{\lambda})$ provided $\bar{\lambda} < 1$. The 'final' value of Y extrapolated in this way was found to be extremely accurate. Indeed, the fifth decimal was rarely found to be unreliable, when verified by a further run. Note that equations (A 18) and (A 19) have been arranged so that the relaxation patterns and residual formulae remain unchanged, a serious disadvantage of method I.

TABLE 1

η	ϕ_1	ϕ_1'	ϕ_1''	ϕ_2	ϕ_2'	ϕ_2''	ϕ_3	ϕ_3'	ϕ_3''	ϕ_4	ϕ_4'	ϕ_4''
0·0	0·0000	0·0000	1·5939	−0·0000	−0·0000	−0·2608	0·0000	0·0000	0·2644	−0·0000	−0·0000	−0·2780
0·1	0·0076$_5$	0·1495	1·3972	−0·0013$_5$	−0·0272$_5$	−0·2839	0·0013	0·0264	0·2639$_5$	−0·0014	−0·0278	−0·2775
0·2	0·0292$_5$	0·2797	1·2072	−0·0055	−0·0566	−0·3023	0·0053	0·0527$_5$	0·2624	−0·0055$_5$	−0·0554$_5$	−0·2756
0·3	0·0629$_5$	0·3912	1·0238	−0·0127	−0·0875	−0·3142	0·0118$_5$	0·0788$_5$	0·2593	−0·0125	−0·0828$_4$	−0·2718
0·4	0·1069	0·4846	0·8471$_5$	−0·0230$_5$	−0·1192	−0·3184	0·0210	0·1045	0·2540	−0·0221	−0·1097	−0·2656
0·5	0·1593	0·5608	0·6775	−0·0365$_5$	−0·1509	−0·3137	0·0327$_5$	0·1295$_5$	0·2459$_2$	−0·0344	−0·1358$_5$	−0·2653
0·6	0·2185	0·6204	0·5153	−0·0532	−0·1816	−0·2995	0·0469	0·1536	0·2344	−0·0492	−0·1609	−0·2435$_5$
0·7	0·2823$_5$	0·6641$_5$	0·3615	−0·0728	−0·2104$_5$	−0·2754	0·0634	0·1763	0·2187$_5$	−0·0665	−0·1844	−0·2269
0·8	0·3508	0·6930	0·2171	−0·0952	−0·2364	−0·2414	0·0821	0·1972	0·1983$_5$	−0·0860$_5$	−0·2061	−0·2059
0·9	0·4210	0·7079$_5$	0·0838$_5$	−0·1200	−0·2584	−0·1983	0·1028	0·2158	0·1728	−0·1076$_5$	−0·2254$_5$	−0·1804
1·0	0·4920	0·7102	−0·0365	−0·1467	−0·2758	−0·1472	0·1252	0·2316	0·1418	−0·1306	−0·2420	−0·1501
1·1	0·5626$_5$	0·7011$_5$	−0·1420	−0·1749$_5$	−0·2877	−0·0901	0·1490	0·2440	0·1057	−0·1559$_5$	−0·2553	−0·1153$_5$
1·2	0·6319	0·6823$_5$	−0·2307	−0·2040$_5$	−0·2937	−0·0293	0·1738$_5$	0·2525$_5$	0·0650	−0·1820	−0·2699$_5$	−0·0765
1·3	0·6988$_5$	0·6556	−0·3012	−0·2335	−0·2935	0·0322	0·1993$_5$	0·2569	0·0208	−0·2088	−0·2705	−0·0344
1·4	0·7628	0·6228	−0·3525$_5$	−0·2625$_5$	−0·2873	0·0913	0·2251	0·2567	−0·0250$_5$	−0·2360	−0·2717$_5$	0·0098
1·5	0·8233	0·5857	−0·3848	−0·2907$_5$	−0·2754	0·1449	0·2505$_5$	0·2519	−0·0706	−0·2630	−0·2685$_5$	0·0544$_5$
1·6	0·8799	0·5464	−0·3986$_5$	−0·3175	−0·2586	0·1900	0·2753	0·2426	−0·1135$_5$	−0·2895	−0·2609	0·0976$_5$
1·7	0·9325	0·5065$_5$	−0·3960	−0·3423	−0·2378	0·2247	0·2989	0·2293	−0·1515	−0·3150$_5$	−0·2491	0·1372$_5$
1·8	0·9812	0·4677	−0·3793	−0·3649	−0·2140$_5$	0·2475	0·3211	0·2126	−0·1823$_5$	−0·3392	−0·2336$_5$	0·1713
1·9	1·0261$_5$	0·4311	−0·3515$_5$	−0·3851	−0·1887	0·2582	0·3413$_5$	0·1931$_5$	−0·2046	−0·3617	−0·2151	0·1981
2·0	1·0675$_5$	0·3976	−0·3161$_5$	−0·4026$_5$	−0·1628	0·2575$_5$	0·3596	0·1719$_5$	−0·2174	−0·3822	−0·1943	0·2163$_5$
2·1	1·1058	0·3680	−0·2763	−0·4177	−0·1375	0·2469$_5$	0·3757	0·1500	−0·2208	−0·4005	−0·1721$_5$	0·2255
2·2	1·1413	0·3424	−0·2351	−0·4302	−0·1137	0·2285	0·3896	0·1281	−0·2155	−0·4166	−0·1495	0·2258
2·3	1·1744	0·3210	−0·1947	−0·4405	−0·0920	0·2046	0·4014	0·1071	−0·2029	−0·4304	−0·1272$_5$	0·2180
2·4	1·2056	0·3034	−0·1573	−0·4487	−0·0728$_5$	0·1777	0·4111	0·0877	−0·1848	−0·4421	−0·1061	0·2036
2·5	1·2352	0·2894	−0·1239$_5$	−0·4551	−0·0565	0·1498	0·4190	0·0703	−0·1630$_5$	−0·4517	−0·0867	0·1842
2·6	1·2636	0·2785	−0·0953	−0·4601	−0·0428$_5$	0·1228	0·4252	0·0551$_5$	−0·1397	−0·4595	−0·0694	0·1618$_5$
2·7	1·2910	0·2702	−0·0716	−0·4638	−0·0318$_5$	0·0980	0·4309	0·0423$_5$	−0·1163	−0·4656$_5$	−0·0544	0·1382

2·8	1·3177	0·2640	−0·0525	−0·4665	−0·0231$_5$	0·0762	0·4338	0·0318	−0·0942	−0·4704	−0·0417	0·1148
2·9	1·3439	0·2595	−0·0376$_6$	−0·4685	−0·0165	0·0577$_8$	0·4365	0·0234	−0·0743	−0·4741	−0·0314	0·0929
3·0	1·3696	0·2564	−0·0264	−0·4699	−0·0115	0·0427	0·4385	0·0169	−0·0571$_6$	−0·4768	−0·0231	0·0732
3·1	1·3952	0·2542	−0·0181	−0·4708	−0·0078$_6$	0·0308	0·4399	0·0119	−0·0428	−0·4788	−0·0166	0·0563
3·2	1·4205	0·2527	−0·0121	−0·4715	−0·0052$_8$	0·0217	0·4409	0·0082	−0·0313	−0·4802	−0·0117	0·0422
3·3	1·4457	0·2517	−0·0079$_6$	−0·4719	−0·0034	0·0149	0·4416	0·0055$_8$	−0·0223	−0·4811$_6$	−0·0081	0·0309$_8$
3·4	1·4708	0·2510	−0·0051	−0·4722	−0·0022	0·0100	0·4421	0·0037	−0·0155$_8$	−0·4818	−0·0055	0·0221
3·5	1·4959	0·2506	−0·0032	−0·4723$_8$	−0·0014	0·0066	0·4424	0·0024	−0·0105	−0·4822$_8$	−0·0036$_6$	0·0154
3·6	1·5210	0·2503$_8$	−0·0019$_6$	−0·4725	−0·0008$_8$	0·0042	0·4426	0·0015	−0·0070	−0·4825$_8$	−0·0023$_8$	0·0105
3·7	1·5460	0·2502	−0·0012	−0·4725$_8$	−0·0005	0·0026$_6$	0·4427	0·0006	−0·0045$_8$	−0·4827$_8$	−0·0015	0·0070
3·8	1·5710	0·2501	−0·0007	−0·4726	−0·0003	0·0016	0·4428	0·0006	−0·0029	−0·4829	−0·0009	0·0046
3·9	1·5960	0·2500$_8$	−0·0004	−0·4726	−0·0002	0·0010	0·4428	0·0003$_8$	−0·0018	−0·4829$_8$	−0·0005$_8$	0·0029
4·0	1·6210	0·2500	−0·0002		−0·0001	0·0005$_8$	0·4428$_8$	0·0002	−0·0011	−0·4830	−0·0003	0·0018
4·1			−0·0001		−0·0000$_6$	0·0003	0·4428$_8$	0·0001	−0·0006	−0·4830	−0·0002	0·0011
4·2			−0·0000$_8$		−0·0000	0·0002	0·4429	0·0000$_8$	−0·0003$_8$		−0·0001	0·0007
4·3			−0·0000			0·0001	0·4429	0·0000	−0·0002		−0·0000$_8$	0·0004
4·4						0·0000$_8$			−0·0001		−0·0000	0·0003
4·5						0·0000			−0·0000$_8$			0·0002
4·6									−0·0000			0·0001
4·7												0·0000$_8$
4·8												0·0000

TABLE 2

	S_1	S_1'	S_2	S_2'	S_3	S_3'	S_4	S_4'
0·0	−0·0000	−0·2235	0·0000	0·1051$_5$	−0·0000	−0·0979	0·0000	0·1094
0·1	−0·0223$_5$	−0·2232	0·0105	0·1051	−0·0098	−0·0978	0·0109	0·1093
0·2	−0·0445$_5$	−0·2207$_5$	0·0210	0·1048$_5$	−0·0195	−0·0972	0·0218	0·1085
0·3	−0·0663$_5$	−0·2146	0·0315	0·1042	−0·0292	−0·0958$_5$	0·0326	0·1067$_5$
0·4	−0·0873	−0·2035	0·0418	0·1029	−0·0387	−0·0935	0·0431	0·1037
0·5	−0·1069	−0·1866	0·0520	0·1006	−0·0479	−0·0900	0·0533	0·0992$_5$
0·6	−0·1244	−0·1638	0·0619	0·0971	−0·0566	−0·0854	0·0629$_5$	0·0934$_5$
0·7	−0·1394	−0·1352	0·0714	0·0918	−0·0649	−0·0795$_5$	0·0719$_5$	0·0863
0·8	−0·1513	−0·1018	0·0802	0·0842	−0·0725	−0·0724	0·0801$_5$	0·0778
0·9	−0·1597	−0·0648	0·0881	0·0739	−0·0793	−0·0638	0·0846	0·0679$_5$
1·0	−0·1642	−0·0260	0·0949	0·0606	−0·0852	−0·0536	0·0937	0·0567
1·1	−0·1649	0·0126	0·1004	0·0444	−0·0900	−0·0418	0·0987$_5$	0·0441
1·2	−0·1618	0·0491$_5$	0·1036$_5$	0·0256	−0·0935	−0·0283	0·1025	0·0301
1·3	−0·1552	0·0816	0·1052	0·0050	−0·0956	−0·0133	0·1047	0·0149$_5$
1·4	−0·1456	0·1084	0·1046$_5$	−0·0163$_5$	−0·0961	0·0027$_5$	0·1054	−0·0011
1·5	−0·1337	0·1285	0·1019$_5$	−0·0372	−0·0950	0·0193	0·1045	−0·0176$_5$
1·6	−0·1202	0·1413	0·0972$_5$	−0·0562	−0·0923	0·0355	0·1019	−0·0340
1·7	−0·1057	0·1470	0·0908	−0·0721	−0·0880	0·0505	0·0977	−0·0494
1·8	−0·0910	0·1459	0·0830	−0·0840$_5$	−0·0823	0·0633$_5$	0·0921	−0·0630
1·9	−0·0767	0·1393	0·0742	−0·0915	−0·0754	0·0733	0·0852	−0·0742
2·0	−0·0633	0·1284	0·0648	−0·0944	−0·0677	0·0798	0·0774	−0·0822
2·1	−0·0511	0·1145	0·0554	−0·0930	−0·0596	0·0827$_5$	0·0689	−0·0868
2·2	−0·0404	0·0991	0·0463	−0·0881	−0·0513	0·0822	0·0601	−0·0880
2·3	−0·0313	0·0833	0·0379	−0·0805	−0·0432	0·0786	0·0514	−0·0859
2·4	−0·0238	0·0682	0·0303	−0·0711	−0·0356$_5$	0·0725	0·0430	−0·0810
2·5	−0·0176$_5$	0·0543	0·0237	−0·0608	−0·0288	0·0648	0·0355	−0·0739
2·6	−0·0128$_5$	0·0422	0·0181$_5$	−0·0505	−0·0227	0·0561	0·0285	−0·0652$_5$
2·7	−0·0091$_5$	0·0319	0·0136	−0·0408	−0·0176	0·0472	0·0224$_5$	−0·0561
2·8	−0·0064	0·0236	0·0099$_5$	−0·0320$_5$	−0·0133	0·0385	0·0173	−0·0468
2·9	−0·0044	0·0171	0·0071	−0·0245	−0·0098	0·0307	0·0130$_5$	−0·0381
3·0	−0·0029	0·0120	0·0050	−0·0183	−0·0071	0·0237	0·0096$_5$	−0·0302
3·1	−0·0019	0·0083	0·0034	−0·0133	−0·0050$_5$	0·0179	0·0070	−0·0233
3·2	−0·0012	0·0056	0·0023	−0·0094	−0·0035	0·0132	0·0044$_5$	−0·0175$_5$
3·3	−0·0008	0·0037	0·0015	−0·0065	−0·0024	0·0095	0·0034	−0·0129
3·4	−0·0005	0·0023$_5$	0·0010	−0·0044	−0·0016	0·0066	0·0023	−0·0092$_5$
3·5	−0·0003	0·0015	0·0006	−0·0029	−0·0010	0·0045	0·0015$_5$	−0·0065
3·6	−0·0002	0·0009	0·0004	−0·0018	−0·0007	0·0030	0·0010	−0·0045
3·7	−0·0001	0·0005$_5$	0·0002	−0·0012	−0·0004	0·0020	0·0006$_5$	−0·0030
3·8	−0·0000$_5$	0·0003	0·0001$_5$	−0·0007	−0·0002$_5$	0·0013	0·0004	−0·0019$_5$
3·9	−0·0000	0·0002	0·0001	−0·0004	−0·0001$_5$	0·0008	0·0002$_5$	−0·0012$_5$
4·0		0·0001	0·0000$_5$	−0·0002$_5$	−0·0001	0·0005	0·0001$_5$	−0·0007$_5$
4·1		0·0000$_5$	0·0000	−0·0001$_5$	−0·0000$_5$	0·0003	0·0001	−0·0004$_5$
4·2		0·0000		−0·0001	−0·0000	0·0002	0·0000$_5$	−0·0002$_5$
4·3				−0·0000$_5$		0·0001	0·0000	−0·0001$_5$
4·4				−0·0000		0·0000$_5$		−0·0001
4·5						0·0000		−0·0000$_5$
4·6								0·0000

TABLE 3

	$U(\xi,\eta)/u_0$			$S(\xi,\eta)$		
η	$\xi = 0{\cdot}2$	$\xi = 0{\cdot}4$	$\xi = 0{\cdot}6$	$\xi = 0{\cdot}2$	$\xi = 0{\cdot}4$	$\xi = 0{\cdot}6$
0·0	0·0000	0·0000	0·000	1·0000	1·0000	1·000
0·1	0·0508	$0{\cdot}0328_5$	$0{\cdot}002_5$	$0{\cdot}9385_6$	0·9454	0·963
0·2	$0{\cdot}1034_5$	0·0693	0·010	0·8772	0·8908	$0{\cdot}926_8$
0·3	$0{\cdot}1577_5$	0·1092	0·023	0·8158	0·8361	$0{\cdot}889_5$
0·4	0·2134	0·1523	0·041	0·7548	0·7851	0·852
0·5	0·2701	0·1981	$0{\cdot}063_5$	0·6941	0·7270	$0{\cdot}813_5$
0·6	0·3274	0·2463	0·091	0·6341	0·6727	0·774
0·7	0·3848	0·2964	0·123	0·5751	0·6187	0·734
0·8	0·4418	0·3479	0·159	$0{\cdot}5173_5$	0·5653	$0{\cdot}692_8$
0·9	0·4987	$0{\cdot}4000_5$	$0{\cdot}198_5$	0·4614	0·5127	0·650
1·0	0·5521	0·4523	0·241	0·4077	0·4613	0·607
1·1	0·6043	$0{\cdot}5039_5$	0·286	0·3565	0·4114	$0{\cdot}562_5$
1·2	0·6537	$0{\cdot}5543_5$	0·333	0·3084	$0{\cdot}3634_5$	$0{\cdot}517_5$
1·3	0·6998	0·6029	0·381	0·2637	$0{\cdot}3178_5$	$0{\cdot}472_5$
1·4	$0{\cdot}7422_5$	0·6490	0·430	0·2227	0·2750	0·428
1·5	$0{\cdot}7807_5$	0·6921	0·479	0·1857	0·2352	$0{\cdot}384_5$
1·6	0·8151	0·7318	0·527	0·1527	$0{\cdot}1986_5$	0·342
1·7	0·8452	0·7678	0·574	0·1239	0·1657	0·301
1·8	0·8712	$0{\cdot}7999_5$	0·619	0·0990	0·1363	0·262
1·9	0·8933	$0{\cdot}8281_5$	0·661	0·0779	$0{\cdot}1106_5$	0·225
2·0	0·9116	0·8525	0·700	0·0604	0·0885	0·192
2·1	0·9267	0·8731	$0{\cdot}735_5$	0·0461	0·0698	0·161
2·2	0·9387	0·8903	$0{\cdot}767_5$	$0{\cdot}0345_5$	0·0542	0·134
2·3	0·9482	0·9044	0·796	0·0255	0·0414	$0{\cdot}109_5$
2·4	$0{\cdot}9555_5$	0·9157	0·821	0·0185	0·0312	$0{\cdot}088_5$
2·5	0·9611	0·9246	0·842	0·0132	0·0231	0·070
2·6	0·9653	0·9315	0·860	0·0093	0·0168	0·055
2·7	0·9683	0·9368	$0{\cdot}874_5$	0·0064	0·0120	$0{\cdot}042_5$
2·8	$0{\cdot}9704_5$	0·9407	0·886	0·0043	0·0085	$0{\cdot}032_5$
2·9	0·9720	$0{\cdot}9435_5$	0·896	0·0029	0·0059	0·024
3·0	0·9730	0·9456	$0{\cdot}903_5$	0·0019	0·0040	0·018
3·1	0·9737	$0{\cdot}9470_5$	0·909	0·0012	0·0027	0·013
3·2	0·9742	$0{\cdot}9480_5$	$0{\cdot}913_5$	0·0008	0·0018	$0{\cdot}009_5$
3·3	0·9745	$0{\cdot}9487_5$	0·917	0·0005	$0{\cdot}0011_5$	$0{\cdot}006_5$
3·4	0·9747	$0{\cdot}9492_1$	$0{\cdot}919_5$	0·0003	$0{\cdot}0007_5$	$0{\cdot}004_5$
3·5	0·9748	0·9495	0·921	0·0002	$0{\cdot}0004_5$	0·003
3·6	0·9749	0·9497	$0{\cdot}922_5$	0·0001	0·0003	0·002
3·7	$0{\cdot}9749_5$	0·9498	0·923	0·0000$_5$	0·0002	$0{\cdot}001_5$
3·8	0·9750	0·9499	0·924	0·0000	0·0001	0·001
3·9		$0{\cdot}9499_5$	0·924		$0{\cdot}0000_5$	$0{\cdot}000_5$
4·0		0·9500	$0{\cdot}924_5$		0·0000	0·000
4·1			0·925			

TABLE 4

Boundary layer characteristics in the incompressible-plane, for $U_e = u_0(1-\frac{1}{6}X)$ *and* $S(X,0) = 1$

	$X = 0{\cdot}2$		$X = 0{\cdot}4$		$X = 0{\cdot}6$	
	(*a*)	(*b*)	(*a*)	(*b*)	(*a*)	(*b*)
Δ^*	0·8569	0·8529	1·3964	1·4021	2·335	2·159
Θ	0·3148	0·3139	0·4739	0·4825	0·620	0·617
Θ^*	0·4915	0·4888	0·7334	0·7453	0·948	0·945
E	0·8218	0·8185	1·2755	1·2625	1·992	1·816
E^*	0·2973	0·2961	0·4191	0·4145	0·498	0·478
$(\partial U/\partial Y)_{Y=0}$	0·5570	0·5575	0·2450	0·2436	0·0000	0.000
$(\partial S/\partial Y)_{Y=0}$	−0·6868	−0·6720	−0·4322	−0·4288	−0·244	−0·235

(*a*) Hartree–Womersley method.
(*b*) Approximate solution of the momentum, energy, and thermal-integral equations.

TABLE 5

	Thermally insulated plate ($S_w = 0, \gamma = 1{\cdot}4$)		*Heated plate with heat transfer* ($S_w = 1, \gamma = 1{\cdot}4$)	
M_0	x_s	T_w/T_0	x_s	T_w/T_0
0	0·96	1·0	0·60	2·0
1	0·89	1·2	0·57	2·4
2	0·78	1·8	0·53	3·6
3	0·71	2·8	0·50	5·6
4	0·68	4·2	0·48	8·4
6	0·64	8·2	0·46	16·4

TABLE 6

Boundary layer characteristics for a heated flat plate in the presence of an adverse pressure gradient, taking $\sigma = 1$ and $\gamma = 1{\cdot}4$

For the columns $C_f\sqrt{\mathrm{Re}_w}$, $\mathrm{Nu}/\sqrt{\mathrm{Re}_w}$, and $C_f\mathrm{Re}_w/\mathrm{Nu}$ the upper figure is that obtained using the modified Polhausen method; the lower figure (in parenthesis) is that obtained using the Hartree–Womersley method

X	x/x_s	u_e/u_0	T_e/T_0	$C_f\sqrt{(\mathrm{Re}_w)}$	$\mathrm{Nu}/\sqrt{(\mathrm{Re}_w)}$	$C_f\mathrm{Re}_w/\mathrm{Nu}$
	$M_0 = 1$, $x_s = 0{\cdot}57_2$, $M_s = 0{\cdot}92_5$, $T_w = 2{\cdot}4T_0$					
				0·663	0·285	2·33
0·0	0·000	1·000	1·000	(0·664)	(0·285)	(2·33)
				$0{\cdot}604_5$	0·278	2·18
0·1	$0{\cdot}173_5$	0·990	1·011	(0·605)	(0·281)	(2·15)
				0·537	$0{\cdot}270_5$	$1{\cdot}98_5$
0·2	0·344	0·979	1·022	$(0{\cdot}536_8)$	$(0{\cdot}276_8)$	(1·94)
0·3	0·512	$0{\cdot}968_5$	1·034	0·460	$0{\cdot}265_8$	1·73
				0·358	0·256	$1{\cdot}39_8$
0·4	0·677	0·958	1·045	(0·356)	(0·258)	(1·38)
0·5	0·840	0·947	1·057	0·238	0·237	1·00
					0·181	
0·6	1·000	0·936	1·069	0·000	(0·188)	0·000
	$M_0 = 2$, $x_s = 0{\cdot}527$, $M_s = 1{\cdot}95$, $T_w = 3{\cdot}6T_0$					
				0·663	0·230	2·89
0·0	0·000	1·000	1·000	(0·664)	(0·230)	(2·89)
				0·601	0·223	$2{\cdot}69_8$
0·1	0·186	0·993	1·012	(0·602)	(0·226)	(2·66)
				0·532	0·216	2·46
0·2	0·363	0·986	1·024	(0·531)	(0·221)	(2·40)
0·3	0·533	0·979	1·037	0·453	0·211	2·14
				0·351	0·203	1·73
0·4	0·696	0·971	1·050	(0·349)	(0·205)	(1·70)
0·5	0·852	0·964	1·063	$0{\cdot}232_8$	0·187	1·24
					0·143	
0·6	1·000	0·956	1·077	0·000	(0·148)	0·000
	$M_0 = 3$, $x_s = 0{\cdot}497_7$, $M_s = 2{\cdot}77_8$, $T_w = 5{\cdot}6T_0$					
				0·663	0·202	3·29
0·0	0·000	1·000	1·000	(0·664)	(0·202)	(3·29)
				0·603	0·197	3·07
0·1	0·195	$0{\cdot}995_8$	1·016	(0·604)	(0·199)	$(3{\cdot}03_8)$
				0·535	0·191	2·80
0·2	0·377	0·991	1·033	(0·535)	(0·196)	(2·73)
0·3	$0{\cdot}548_8$	0·986	1·050	0·458	0·188	2·44
				0·356	0·181	1·96
0·4	0·709	0·981	1·067	(0·354)	(0·182)	(1·95)
0·5	0·859	0·976	1·084	0·236	0·167	1·41
					$0{\cdot}127_8$	
0·6	1·000	0·971	1·102	0·000	(0·132)	0·000

X	x/x_s	u_e/u_0	T_e/T_0	$C_f\sqrt{(\mathrm{Re}_w)}$	$\mathrm{Nu}/\sqrt{(\mathrm{Re}_w)}$	$C_f\mathrm{Re}_w/\mathrm{Nu}$
	$M_0 = 4,\ x_s = 0{\cdot}48_0,\ M_s = 3{\cdot}7,\ T_w = 8{\cdot}4T_0$					
				0·663	0·189	3·52
0·0	0·000	1·000	1·000	(0·664)	(0·189)	(3·52)
0·1	$0{\cdot}200_5$	0·997	1·019	(0·606)	(0·186)	(3·26)
				$0{\cdot}538_5$	0·180	3·00
0·2	0·386	0·994	1·039	(0·538)	(0·184)	(2·92)
0·3	0·558	0·991	1·059	0·462	0·177	2·62
				0·360	0·171	2·11
0·4	0·717	0·987	1·080	(0·358)	(0·172)	(2·08)
0·5	0·864	0·984	1·102	0·240	0·158	1·52
					0·121	
0·6	1·000	$0{\cdot}980_5$	1·124	0·000	(0·126)	0·000
	$M_0 = 6,\ x_s = 0{\cdot}46_4,\ M_s = 5{\cdot}55,\ T_w = 16{\cdot}4T_0$					
				0·663	0·177	3·76
0·0	0·000	1·000	1·000	(0·664)	(0·177)	(3·76)
				0·607	0·173	$3{\cdot}50_5$
0·1	0·206	$0{\cdot}998_5$	1·022	(0·607)	(0·176)	(3·45)
				0·542	0·170	$3{\cdot}19_5$
0·2	0·395	0·997	1·045	(0·541)	(0·173)	(3·13)
0·3	0·567	0·995	1·069	0·467	0·167	2·79
				0·365	0·163	2·245
0·4	0·725	$0{\cdot}993_5$	1·094	(0·363)	(0·164)	(2.21)
0·5	0·869	0·992	1·119	0·244	0·151	$1{\cdot}61_5$
					0·116	
0·6	1·000	0·990	1·145	0·000	(0·121)	0·000

REFERENCES

1. W. F. Cope and D. R. Hartree, *Phil. Trans.* A, **241** (1948) 1–70.
2. L. Howarth, *Proc. Roy. Soc.* A, **194** (1948) 16–42.
3. K. Stewartson, ibid. **200** (1949) 84–100.
4. L. Howarth, ibid. **164** (1939) 547–79.
5. D. R. Hartree, A.R.C. R. & M. 2426 (1949).
6. L. Fox, *Numerical Solution of Two-point Boundary Problems in Ordinary Differential Equations* (Oxford, 1957).
7. D. C. F. Leigh, *Proc. Camb. Phil. Soc.* **51** (1955) 320–32.
8. Th. v. Kármán, *Z. angew. Math. Mech.* **1** (1921) 233–52.
9. K. Wieghardt, *Ingenieur-Archiv*, **16** (1948) 231–42.
10. K. Polhausen, *Z. angew. Math. Mech.* **1** (1921) 252–68.
11. I. Tani, *J. Aero. Sci.* **21** (1954) 487–95.
12. W. E. Milne, *Numerical Calculus* (Princeton, 1949).

HEAT TRANSFER BY LAMINAR FLOW BETWEEN PARALLEL PLATES UNDER THE ACTION OF TRANSVERSE MAGNETIC FIELD

By S. D. NIGAM† *and* S. N. SINGH‡
(*Indian Institute of Technology, Kharagpur, India*)

[Received 12 August 1958; revise received 20 January 1959]

SUMMARY

Solutions of the energy equation of magnetohydrodynamics are obtained for the heat-transfer problem corresponding to Hartmann's velocity profile for forced flow between two infinite parallel plates. The semi-infinite plates $z = \pm L$, $x < 0$, are kept at a constant temperature T_0 and the plates $z = \pm L$, $x \geqslant 0$, are kept at a different temperature T_s (constant). Solutions are found which are valid for the regions $x \leqslant 0$ and $x \geqslant 0$ respectively. These are joined smoothly at the plane $x = 0$ by imposing certain continuity conditions. Asymptotic solutions for large $M \geqslant 10$ are presented. A simplified case valid for large Peclet numbers is worked out numerically and the mean mixed temperature and local total Nusselt numbers are tabulated and shown graphically. These are compared with the corresponding values for the heat-transfer problem in which the magnetic field is absent and the fluid is electrically non-conducting. It is found that due to ionic-conductivity the mean mixed temperature at any point is decreased and consequently the local total Nusselt number is increased.

1. Introduction

THE problem of heat transfer in an incompressible viscous fluid for fully developed Couette flow has been studied in a variety of ways by many workers, Prins *et al.* (**1**), van der Does de Bye and Schenk (**2**), Schenk and Beckers (**3**), and Dennis and Poots (**4**). These investigations do not strictly apply when the viscous, incompressible, electrically-conducting fluids or liquid metals are used as heat-transfer media in the presence of magnetic fields.

In this paper, we consider the simplest problem of this type in which an electrically conducting, viscous, incompressible fluid flows between two infinite parallel planes under the action of a constant pressure gradient, when an external magnetic field of constant strength acts in a direction perpendicular to the plates and to the direction of flow. The velocity profile for this flow is the fully developed Hartmann's (**5**) velocity profile, provided that the temperature differences are small enough to permit the neglect of convective heat transfer. This is tantamount to the assumption

† Department of Naval Architecture.

‡ Department of Applied Mathematics. The authors thank the referee for making some suggestions for the improvement of the paper.

that even with moderate velocities, the buoyancy forces caused by the temperature differences are small compared with the inertia and friction forces. The infinite parallel plates are kept at a constant temperature up to a certain cross-section and after that the temperature is changed to a different value. The energy equation of magnetohydrodynamics for this problem reduces to a Sturm–Liouville differential equation, Singh (**6**). The mathematical solutions involving two infinite sets of coefficients, valid for the two regions, are obtained and the coefficients are determined by imposing continuity conditions on the temperature and its first derivative at the junction. Asymptotic solutions are given for large values of the Hartmann number M ($\geqslant 10$). A simplified solution for large values of the Peclet number Pe ($\geqslant 100$) is presented in detail. The first three eigenvalues and the associated eigenfunctions are computed for M equal to 2, 4, and 10. The mean mixed temperature and the local Nusselt number are tabulated and shown graphically. It is found that for a constant value of the pressure gradient the local Nusselt number increases with M.

2. Statement of the problem

Consider a viscous, incompressible, electrically-conducting fluid, moving from left to right between two infinite parallel plates under the action of a constant pressure gradient in the direction of motion and a constant transverse magnetic field H_0 (Fig. 1). The two infinite parallel plates ($z = \pm L$, $x \leqslant 0$) are kept at a constant temperature T_0 up to a certain cross-section $x = 0$ and afterwards ($z = \pm L$, $x \geqslant 0$) their temperature is changed to a different value T_s. Taking x and z as the longitudinal and transverse coordinates with respect to the plates $z = \pm L$, the energy equation due to Pai (**7**) simplifies to

$$\rho c J U_x \frac{\partial T_i}{\partial x} = kJ\left(\frac{\partial^2 T_i}{\partial x^2} + \frac{\partial^2 T_i}{\partial z^2}\right) + \frac{\mu M}{L^2 A} U_m^2 \left(\cosh\frac{Mz}{L} - \frac{\sinh M}{M}\right) + \mu\left(\frac{dU_x}{dz}\right)^2 \quad (i = 1, 2), \quad (2.1)$$

$$\text{with} \qquad U_x = \frac{U_m}{A}\left(\cosh M - \cosh\frac{Mz}{L}\right), \qquad A = \cosh M - \frac{\sinh M}{M}, \qquad (2.2)$$

where ρ is the density, c the specific heat, J the mechanical equivalent of heat, U_m the mean velocity, k the coefficient of thermal conductivity, T_i ($i = 1, 2$) the variable fluid temperature in the regions $x \leqslant 0$ and $x \geqslant 0$ respectively, μ the coefficient of viscosity, and M the Hartmann number ($M = \mu_e L H_0 (\sigma/\mu)^{\frac{1}{2}}$), σ and μ_e being the electric conductivity and permeability respectively.

The boundary conditions compatible with the assumption of the steady state are

$$k\frac{\partial T_1}{\partial z}+h_1T_1=0 \quad \text{for } x\leqslant 0; \qquad k\frac{\partial T_2}{\partial z}+h_2T_2=0 \quad \text{for } x\geqslant 0 \text{ at } z=\pm L,$$

where h_1 and h_2 are the thermal transmissivities of the plates. Two particular cases which are often met with in practice are (i) $h_1=h_2=0$ and (ii) $h_1=h_2=\infty$. The former corresponds to thermally insulated plates, the latter to plates maintained at a constant temperature.

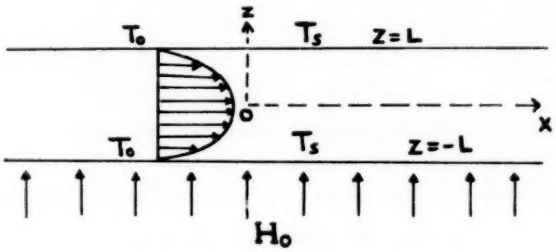

FIG. 1. Flow between two plates.

The boundary conditions for the problem under consideration are

$$T_1=T_0 \quad \text{for } x\leqslant 0,\ z=\pm L, \tag{2.3a}$$

$$T_2=T_s \quad \text{for } x\geqslant 0,\ z=\pm L. \tag{2.3b}$$

The continuity of temperature distribution and its first derivative at the junction $x=0$, gives

$$T_1=T_2 \quad \text{and} \quad \frac{\partial T_1}{\partial x}=\frac{\partial T_2}{\partial x} \quad \text{at } x=0,\ -L<z<L. \tag{2.3c}$$

For infinitely large values of $|x|$, the temperature is the particular solution of

$$kJ\frac{\partial^2 T_i}{\partial z^2}+\frac{\mu M}{L^2A}U_m^2\left(\cosh\frac{Mz}{L}-\frac{\sinh M}{M}\right)+\mu\left(\frac{dU_x}{dz}\right)^2=0. \tag{2.3d}$$

The solution of (2.1) subject to the conditions (2.3) gives the temperature $T=T(x,z)$. The mean mixed temperature and local Nusselt numbers are defined by

$$T_{im}=\int_{-L}^{L}T_i(x,z)U_x\,dz\Big/\int_{-L}^{L}U_x\,dz, \tag{2.4}$$

and

$$\mathrm{Nu}=-L\left(\frac{\partial T_i}{\partial z}\right)_{z=L}\Big/(T_{im}-T_s), \tag{2.5}$$

respectively.

3. Mathematical solution

Introducing the dimensionless variables θ, x', and z' defined by

$$\theta_i = \frac{T_i - T_s}{T_0 - T_s} \quad (i = 1, 2), \qquad x = \tfrac{2}{3}\mathrm{Pe}\, Lx', \qquad z = L\left(\frac{2}{\pi}z' - 1\right), \quad (3.1)$$

equation (2.1) becomes

$$\alpha^2 \frac{\partial^2 \theta_i}{\partial x'^2} + \frac{\partial^2 \theta_i}{\partial z'^2} = \frac{8}{3\pi^2 A}\left(\cosh M - \cosh M\left(\frac{2}{\pi}z' - 1\right)\right)\frac{\partial \theta_i}{\partial x'} +$$

$$+ \frac{QM^2}{A^2}\left[\sinh^2 M\left(\frac{2}{\pi}z' - 1\right) + A\cosh M\left(\frac{2}{\pi}z' - 1\right) - A(\sinh M)/M\right], \quad (3.2)$$

where

$$\mathrm{Pe} = \frac{U_m L\rho c}{k}, \qquad \alpha = \frac{4}{3\pi \mathrm{Pe}}, \quad \text{and} \quad Q = \frac{\mu U_m^2}{4\pi^2 KJ(T_0 - T_s)}, \quad (3.3, 4, 5)$$

θ_1 and θ_2 are the variable temperatures in the regions $x' \leqslant 0$ and $x' \geqslant 0$ respectively. The boundary conditions become

$$\theta_1 = 1, \quad \text{for } x' \leqslant 0,\ z' = 0 \text{ and } \pi, \quad (3.6\,\mathrm{a})$$

$$\theta_2 = 0, \quad \text{for } x' \geqslant 0,\ z' = 0 \text{ and } \pi, \quad (3.6\,\mathrm{b})$$

$$\theta_1 = \theta_2 \quad \text{and} \quad \frac{\partial \theta_1}{\partial x'} = \frac{\partial \theta_2}{\partial x'}, \quad \text{for } x' = 0,\ 0 < z' < \pi, \quad (3.6\,\mathrm{c})$$

$$\theta_1 \to F_1(z', M) + 1 \quad \text{as } x' \to -\infty,\ 0 \leqslant z' \leqslant \pi, \quad (3.6\,\mathrm{d})$$

$$\theta_2 \to F_1(z', M) \quad \text{as } x' \to \infty,\ 0 \leqslant z' \leqslant \pi, \quad (3.6\,\mathrm{e})$$

where

$$F_1(z', M) = \frac{\pi^2}{8}\Big[\cosh 2M\left(\frac{2}{\pi}z' - 1\right) + 8A\cosh M\left(\frac{2}{\pi}z' - 1\right) -$$

$$- (\cosh 2M + 8A\cosh M) + z'M^2(\pi - z')\{1 + (2A\sinh M)/M\}\Big].$$

The solution of (3.2) satisfying the conditions (3.6 a, b) is

$$\theta_1 = \frac{2}{\pi}\sum_{n=1,3}^{\infty} v_{n1}(x')\sin nz' + \frac{Q}{A^2}F_1(z', M) + 1, \quad x' \leqslant 0 \quad (3.7)$$

$$\theta_2 = \frac{2}{\pi}\sum_{n=1,3}^{\infty} v_{n2}(x')\sin nz' + \frac{Q}{A^2}F_1(z', M), \quad x' \geqslant 0 \quad (n = 1, 3, 5, \ldots). \quad (3.8)$$

Multiplying each side of (3.2) by $\sin mz'$, where m need not be the same eigenvalue as n, and integrating with respect to z' from $z' = 0$ to $z' = \pi$, we have

$$\alpha^2 \frac{d^2 v_{ni}}{dx'^2} - n^2 v_{ni} = \frac{8}{3\pi^2 A}\int_0^{\pi}\left(\cosh M - \cosh M\left(\frac{2}{\pi}z' - 1\right)\right)\frac{\partial \theta_i}{\partial x'}\sin mz'\, dz'$$

$$(i = 1, 2), \quad (3.9)$$

with

$$v_{n1}(-\infty) = 0 \quad \text{and} \quad v_{n2}(\infty) = 0. \quad (3.10)$$

In order to evaluate the integral on the right-hand side of (3.9), the expression $\{\cosh M - \cosh M(2z'/\pi - 1)\}$ is expanded in a Fourier cosine series in the interval $(0, \pi)$. The expansion is

$$\left\{\cosh M - \cosh M\left(\frac{2z'}{\pi} - 1\right)\right\} = \tfrac{1}{2}b_0 + \sum_{q=2,4,\ldots}^{\infty} b_q \cos qz' \qquad (3.11)$$

where $$b_0 = 2A, \qquad b_q = -\frac{8M \sinh M}{(4M^2 + \pi^2 q^2)}.$$

Therefore

$$\int_0^{\pi} \left\{\cosh M - \cosh M\left(\frac{2}{\pi}z' - 1\right)\right\} \frac{\partial \theta_i}{\partial x'} \sin mz'\, dz' = \left(A + \frac{M \sinh M}{M^2 + \pi^2 n^2}\right) \frac{dv_{ni}}{dx'} -$$

$$- \sum_{m=1}^{\infty} \frac{16\pi^2 Mmn \sinh M}{[4M^2 + (m-n)^2\pi^2][4M^2 + (m+n)^2\pi^2]} \frac{dv_{mi}}{dx'} \quad (m \neq n), \quad (i = 1, 2), \qquad (3.12)$$

where the summation extends to odd values of m only. Finally equation (3.9) becomes

$$\alpha^2 \frac{d^2 v_{ni}}{dx'^2} - \frac{8}{3\pi^2 A}\left(A + \frac{M \sinh M}{M^2 + \pi^2 n^2}\right) \frac{dv_{ni}}{dx'} - n^2 v_{ni} +$$

$$+ \sum_{m=1,3}^{\infty} \frac{128 mnM \sinh M}{3A[4M^2 + (m-n)^2\pi^2][4M^2 + (m+n)^2\pi^2]} \frac{dv_{mi}}{dx'}$$

$$(m \neq n) = 0. \qquad (3.13)$$

The solution of (3.13) subject to the boundary condition (3.10) is

$$v_{ni}(x') = a_{ni} \exp(\lambda_{ni} x'), \qquad (3.14)$$

provided that

$$a_{ni} f(\lambda, n) + \sum_{m=1}^{\infty} \frac{128 mn\lambda a_{mi} M \sinh M}{3A[4M^2 + (m-n)^2\pi^2][4M^2 + (m+n)^2\pi^2]}$$

$$(m \neq n) = 0, \qquad (3.15)$$

where $$f(\lambda, n) = \alpha^2\lambda^2 - \frac{8\lambda}{3\pi^2 A}\left(A + \frac{M \sinh M}{M^2 + \pi^2 n^2}\right) - n^2.$$

The consistency condition for the set of equations (3.15) is

$$\Delta(\lambda) \equiv \|a_{ij}(\lambda)\| = 0, \qquad (3.16)$$

where $$a_{ij} = \frac{128 ij\lambda M \sinh M}{3A[4M^2 + (i-j)^2\pi^2][4M^2 + (i+j)^2\pi^2]} \quad (i \neq j),$$

and $$a_{ii} = f(\lambda, i).$$

The determinant $\Delta(\lambda)$ is absolutely convergent and all its diagonal elements are quadratics in λ; hence $\Delta(\lambda)$ has an infinity of positive and

negative roots. The positive roots λ_{m1} ($m = 1, 3, 5,...$) are admissible for region $x' \leqslant 0$, while the negative roots λ_{m2} ($m = 1, 3, 5,...$) are to be taken for $x' \geqslant 0$. The two sets of infinite coefficients $a_p^{(mi)}$ ($i = 1, 2$; $p = 1, 3, 5,...$) corresponding to each λ_{m1} and λ_{m2} are determined in the usual way in terms of $a_m^{(m1)}$ and $a_m^{(m2)}$ respectively. Now we write

$$\theta_1 = \frac{2}{\pi} \sum_{m=1}^{\infty} \exp(\lambda_{m1} x') Z_{m1}(z') + \frac{Q}{A^2} F_1(z', M) + 1 \quad (x' \leqslant 0), \tag{3.17}$$

$$\theta_2 = \frac{2}{\pi} \sum_{m=1}^{\infty} \exp(\lambda_{m2} x') Z_{m2}(z') + \frac{Q}{A^2} F_1(z', M) \qquad (x' \geqslant 0), \tag{3.18}$$

where
$$Z_{mi}(z') = \sum_{p=1}^{\infty} a_p^{(mi)} \sin pz' \quad (i = 1, 2). \tag{3.19}$$

The two sets of coefficients $a_m^{(m1)}$ and $a_m^{(m2)}$ are determined by the conditions (3.6 c) at $x' = 0$, namely,

$$\frac{2}{\pi} \sum_{m=1}^{\infty} \sum_{p=1}^{\infty} a_p^{(m1)} \sin pz' + \frac{Q}{A^2} F_1(z', M) + 1$$

$$= \frac{2}{\pi} \sum_{m=1}^{\infty} \sum_{p=1}^{\infty} a_p^{(m2)} \sin pz' + \frac{Q}{A^2} F_1(z', M), \tag{3.20}$$

and
$$\sum_{m=1}^{\infty} \sum_{p=1}^{\infty} \lambda_{m1} a_p^{(m1)} \sin pz' = \sum_{m=1}^{\infty} \sum_{p=1}^{\infty} \lambda_{m2} a_p^{(m2)} \sin pz'. \tag{3.21}$$

Multiplying both sides of (3.20) and (3.21) by $\sin mz'$ and integrating with respect to z' from 0 to π, we obtain

$$\sum_{m=1,3}^{\infty} a_p^{(m1)} + \frac{2}{p} = \sum_{m=1,3}^{\infty} a_p^{(m2)} \quad (p = 1, 3, 5,...), \tag{3.22}$$

$$\sum_{m=1,3}^{\infty} \lambda_{m1} a_p^{(m1)} = \sum_{m=1,3}^{\infty} \lambda_{m2} a_p^{(m2)}. \tag{3.23}$$

The two equations (3.22) and (3.23) determine $a_m^{(m1)}$ and $a_m^{(m2)}$. Because of the slow convergence of the left-hand side of (3.22) we make use of a variational principle. The eigenvalues and the associated eigenfunctions can also be calculated for other forms of the boundary conditions (3.6 a) and (3.6 b).

4. Asymptotic solution for large values of M

For large values of M ($M \geqslant 10$), both $\cosh M$ and $\sinh M$ tend to $\frac{1}{2}e^M$, and hence

$$\frac{8}{3\pi^2 A}\left(A + \frac{M \sinh M}{\pi^2 n^2 + M^2}\right) \simeq \frac{8}{3\pi^2}\left(1 + \frac{M^2}{(M-1)(\pi^2 n^2 + M^2)}\right) \tag{4.1}$$

and the expression under the summation sign of (3.13) becomes

$$\frac{M^2mn}{(M-1)[4M^2+(m-n)^2\pi^2][4M^2+(m+n)^2\pi^2]} \simeq O\left(\frac{1}{M^3}\right)$$

and may be neglected. This corresponds to the case of a magnetic field of high intensity. The equation (3.13) then reduces to

$$\alpha^2\frac{d^2v_{ni}}{dx'^2}-\frac{8}{3\pi^2}\left\{1+\frac{M^2}{(M-1)(\pi^2n^2+M^2)}\right\}\frac{dv_{ni}}{dx'}-n^2v_{ni}=0 \quad (i=1,2). \quad (4.2)$$

The solution of (4.2) subject to the conditions (3.6) is

$$v_{ni}(x')=a_{ni}\exp(\lambda_{ni}x') \quad (i=1,2) \quad (4.3)$$

where

$$\alpha^2\lambda_{ni}^2-\frac{8\lambda_{ni}}{3\pi^2}\left\{1+\frac{M}{(M-1)(\pi^2n^2+M^2)}\right\}-n^2=0. \quad (4.4)$$

Hence the complete solutions for the two regions are

$$\theta_1=\frac{2}{\pi}\sum_{n=1}^{\infty}a_{n1}\exp(\lambda_{n1}x')\sin nz'+\frac{Q}{A^2}F_1(z',M)+1 \quad (n=1,3,\ldots),\ (x'\leqslant 0), \quad (4.5)$$

$$\theta_2=\frac{2}{\pi}\sum_{n=1}^{\infty}a_{n2}\exp(\lambda_{n2}x')\sin nz'+\frac{Q}{A^2}F_1(z',M) \quad (x'\geqslant 0). \quad (4.6)$$

The continuity conditions give

$$a_{n1}+\frac{2}{n}=a_{n2}, \quad (4.7)$$

$$\lambda_{n1}a_{n1}=\lambda_{n2}a_{n2}. \quad (4.8)$$

Hence $a_{n2}=\dfrac{2}{n(1-\lambda_{n2}/\lambda_{n1})}$, and $a_{n1}=\dfrac{2\lambda_{n2}}{n\lambda_{n1}(1-\lambda_{n2}/\lambda_{n1})}$.

Table 1 gives the first three eigenvalues and the coefficients in the case $M=10$, corresponding to Peclet numbers 1, 10, 100, 1,000, and ∞. In Table 2 are given the eigenvalues corresponding to $\mathrm{Pe}=\infty$ when $M=15$, 20, 50, 100, and ∞. The local Nusselt numbers for these values of M at $x'=\infty$ are given below.

M	10	15	20	50	100	∞
[Nu]x	2·275	2·328	2·358	2·420	2·443	2·467

TABLE 1 A

Eigenvalues and coefficients for $x'\leqslant 0$, $M=10$

Pe	1	10	100	1,000	∞
λ_{11}	3·3256	168·46	16,520	16×10^4	∞
λ_{31}	7·9072	185·73	15,914	16×10^4	∞
λ_{51}	12·5800	218·36	15,568	15×10^4	∞
$-a_{11}$	0·6688	0·0384	0·0004	..	0
$-a_{31}$	0·2961	0·0839	0·0013	..	0
$-a_{51}$	0·1869	0·0902	0·0022	0·0002	0

TABLE 1 B

Eigenvalues and coefficients for $x' \geqslant 0$, $M = 10$

Pe	1	10	100	1,000	∞
$-\lambda_{12}$	1·6709	3·2954	3·3588	3·3612	3·3612
$-\lambda_{22}$	6·3189	26·733	31·400	31·460	31·460
$-\lambda_{52}$	11·032	63·550	87·410	89·640	89·650
a_{12}	1·3312	1·9615	1·9996	2·0	2·0
a_{22}	0·3706	0·5828	0·6654	0·6666	0·6667
a_{52}	0·2131	0·3098	0·3978	0·4000	0·4

TABLE 2

$\mathrm{Pe} = \infty$

M	15	20	50	100	∞
$-\lambda_{12}$	3·4641	3·5203	3·6270	3·6641	3·7011
$-\lambda_{22}$	31·69	31·93	32·67	32·89	33·31
$-\lambda_{52}$	89·47	89·61	90·84	92·518	92·527

5. Solution for large values of Peclet number

For large Peclet numbers ($\mathrm{Pe} \geqslant 100$), α^2 in equation (3.13) is of the order 10^{-5} and can be neglected everywhere except in the immediate neighbourhood of the points $x = 0$, $z = \pm L$, where the plate temperatures change abruptly, giving rise to infinite temperature gradients. Near these points it will not be permissible to neglect the derivatives $\partial^2 v_{ni}/\partial x'^2$ in (3.13). The analysis of this section breaks down near $x = 0$, $z = \pm L$. With this proviso, the diagonal elements of the determinant (3.16), instead of being quadratic, are linear factors in λ and hence the infinite determinant has only an infinitude of negative roots valid for the region $x' \geqslant 0$. This excludes the possibility of heat diffusing into the region $x' < 0$. The temperature distribution in the region $x' < 0$ is independent of the x coordinate. This idealization makes the solution valid, to a good approximation, only for high Prandtl number fluids and when the velocity U_m is sufficiently large. The expression for the temperature distribution in the region $x' \leqslant 0$ is

$$\theta_1 = \frac{Q}{A^2} F_1(z', M) + 1. \tag{5.1}$$

The boundary conditions for the region $x' \geqslant 0$ become

$$\theta_2 = 0, \quad \text{for } x' > 0,\ z' = 0 \text{ and } \pi, \tag{5.2a}$$

$$\theta_2 = \frac{Q}{A^2} F_1(z', M) + 1, \quad \text{for } x' = 0 \quad (0 \leqslant z' \leqslant \pi), \tag{5.2b}$$

$$\theta_2 \to \frac{Q}{A^2} F_1(z', M) \quad \text{as } x' \to \infty \quad (0 \leqslant z' \leqslant \pi). \tag{5.2c}$$

The solution of (3.2) satisfying the conditions (5.2 a, c) is

$$\theta_2 = \frac{2}{\pi} \sum_{m=1}^{\infty} \exp(\lambda_m x') \sum_{p=1}^{\infty} a_p^{(m)} \sin pz' + \frac{Q}{A^2} F_1(z', M), \tag{5.3}$$

where λ_m are the roots of the determinant

$$\Delta(\lambda) \equiv \|a_{ij}(\lambda)\| = 0, \tag{5.4}$$

where

$$a_{ij} = \frac{128ij\lambda M \sinh M}{3A[4M^2+(i-j)^2\pi^2][4M^2+(i+j)^2\pi^2]}, \ (i \neq j), \qquad a_{ii} = f(\lambda, i). \tag{5.5}$$

The coefficients $a_p^{(m)}$ can all be expressed in terms of $a_m^{(m)}$ and, using the condition (5.2 b), we obtain

$$\sum_{m=1}^{\infty} a_n^{(m)} = \frac{2}{n}. \tag{5.6}$$

These determine $a_m^{(m)}$ but because of the slow convergence of the right-hand side of (5.6), we make use of the variational principle and get

$$\sum_{p=1}^{\infty} \frac{2}{p} a_p^{(n)} = \sum_{m=1}^{\infty} \sum_{p=1}^{\infty} a_p^{(m)} a_p^{(n)}. \tag{5.7}$$

The mean mixed temperature and the local Nusselt numbers are evaluated from

$$\theta_m = \frac{16M^2 \cosh M}{\pi^2 A} \sum_{m=1}^{\infty} \exp(\lambda_m x') \sum_{p=1}^{\infty} \frac{a_p^{(m)}}{p(\pi^2 p^2 + 4M^2)}, \tag{5.8}$$

and

$$\mathrm{Nu} = \frac{1}{\theta_m} \sum_{m=1}^{\infty} \exp(\lambda_m x') \sum_{p=1}^{\infty} p a_p^{(m)}. \tag{5.9}$$

In order to calculate the eigenvalues approximately we study the determinant formed by retaining the first four columns and the first four rows of (5.4) and evaluate the first three roots λ_m ($m = 1, 3, 5$) for $M = 2$, 4, 10. The corresponding set of coefficients $a_p^{(m)}$ ($p = 1, 3, 5$) are calculated by the use of the variational principle (5.7). Tables 3, 4, and 5 give the first three eigenvalues and the set of constants, the mean mixed temperature and the local Nusselt numbers.

TABLE 3

Eigenvalues and coefficients for $M = 2$, $\alpha = 0$

m	1	3	5
λ_m	−2·9105	−32·420	−86·31
p	$a_p^{(1)}$	$a_p^{(3)}$	$a_p^{(5)}$
1	1·883	0·097	0·022
3	−0·033	0·637	0·072
5	−0·002	−0·088	0·489

Mean mixed temperature and Nusselt number for $M = 2$, $\alpha = 0$

x'	θ_m	Nu
0·01	0·95	4·69
0·02	0·92	3·86
0·05	0·85	2·70
0·1	0·76	2·18
0·15	0·68	2·03
0·2	0·62	1·98
0·25	0·56	1·95
0·5	0·34	1·948
1·0	0·128	1·948
∞	0	1·948

TABLE 4

Eigenvalues and coefficients for $M = 4$, $\alpha = 0$

m	1	3	5
λ_m	−3·0657	−31·504	−90·96
p	$a_p^{(1)}$	$a_p^{(3)}$	$a_p^{(5)}$
1	1·917	0·056	0·021
3	−0·021	0·579	0·109
5	−0·003	−0·054	0·456

Mean mixed temperature and Nusselt number for $M = 4$, $\alpha = 0$

x'	θ_m	Nu
0·01	0·94	4·75
0·02	0·91	3·92
0·05	0·83	2·79
0·1	0·74	2·29
0·15	0·66	2·14
0·2	0·60	2·09
0·25	0·54	2·06
0·5	0·32	2·059
1·0	0·117	2·059
∞	0·0	2·059

TABLE 5

Eigenvalues and coefficients for $M = 10$, $\alpha = 0$

m	1	3	5
λ_m	$-3{\cdot}361$	$-31{\cdot}407$	$-89{\cdot}44$
p	$a_p^{(1)}$	$a_p^{(3)}$	$a_p^{(5)}$
1	1·978	0·014	0·008
3	−0·005	0·638	0·033
5	−0·002	−0·019	0·421

Mean mixed temperature and Nusselt number for $M = 10$, $\alpha = 0$

x'	θ_m	Nu
0·01	0·93	4·96
0·02	0·89	4·20
0·05	0·81	3·09
0·1	0·71	2·54
0·15	0·62	2·37
0·2	0·56	2·29
0·25	0·50	2·254
0·5	0·29	2·251
1·0	0·096	2·251
∞	0·00	2·251

6. Comparison and discussion of the results

The eigenvalues and the coefficients of the cup-mixing mean temperature found for various values of M are given in Table 4. The mean mixed temperature and the local Nusselt numbers are plotted against x' for these values of M in Figs. 2 and 3. It can be seen that the local Nusselt numbers go on increasing with M for the same values of x'. Fig. 4 is the plot of $[\mathrm{Nu}]_\infty$ against M. For M tending to infinity the Nusselt number tends to 2·467. Hence it can be concluded that the heat transfer coefficients of the liquid metals are increased because of the presence of the magnetic field and the thermal entry lengths are considerably decreased.

TABLE 6

Comparison of eigenvalues and mean temperature coefficients for various values of M

	Prins	*Present authors*		
	$M = 0$	$M = 2$	$M = 4$	$M = 10$
$-\frac{8}{3}\lambda_1$	1·885	1·9403	2·0438	2·2407
$-\frac{8}{3}\lambda_3$	21·43	21·6133	21·0	20·938
$-\frac{8}{3}\lambda_5$	62·31	57·54	60·64	59·627
B_1	0·914	0·909	0·893	0·869
B_3	0·053	0·069	0·066	0·078
B_5	0·015	0·016	0·026	0·031

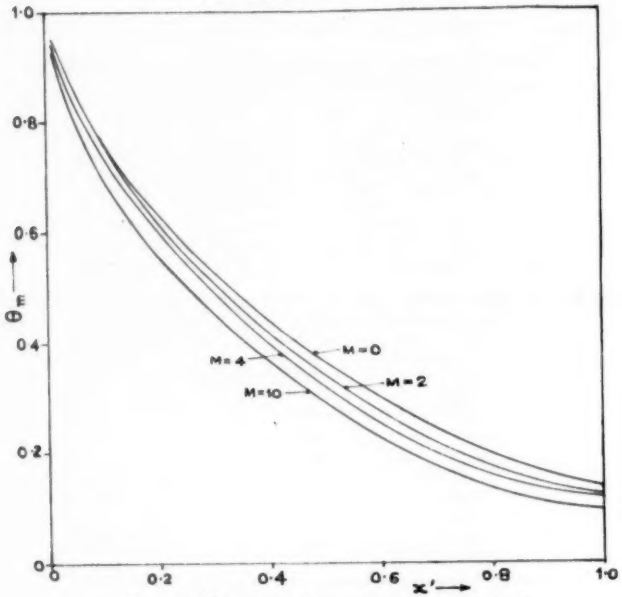

FIG. 2. Mean mixed temperature against x'.

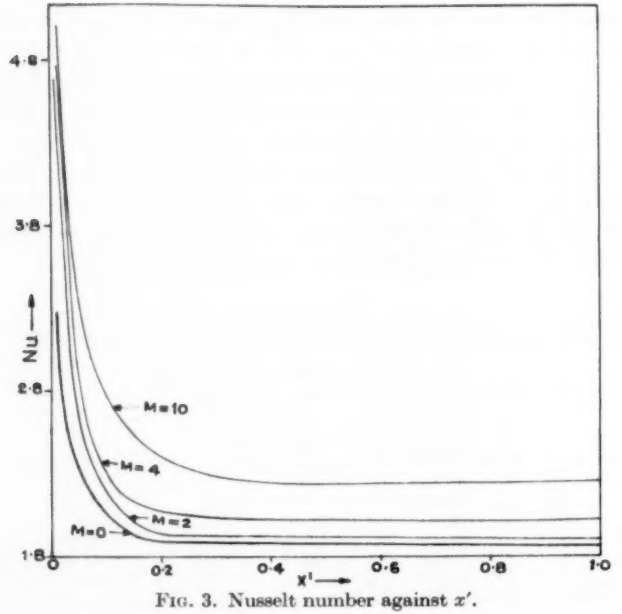

FIG. 3. Nusselt number against x'.

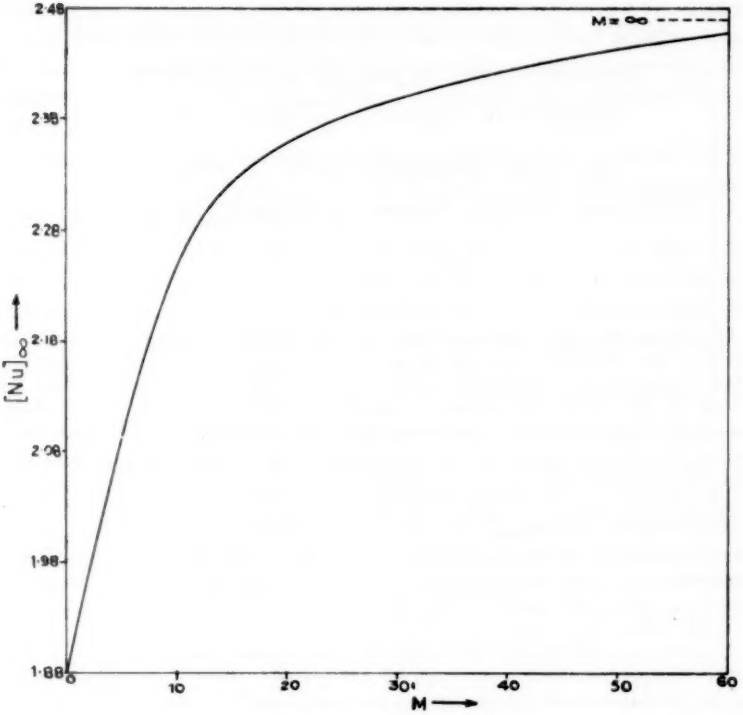

FIG. 4. $[Nu]_\infty$ against M.

REFERENCES

1. J. A. PRINS, J. MULDER, and J. SCHENK, *App. Sci. Res.* A **2** (1951) 431.
2. J. A. W. VAN DER DOES DE BYE and J. SCHENK, ibid. A **3** (1953) 308.
3. J. SCHENK and H. L. BECKERS, ibid. A **4** (1954) 405.
4. S. C. R. DENNIS and G. POOTS, *Quart. App. Math.* **14** (1956) 231.
5. J. HARTMANN, *Math.-fys. Medd.* **15,** No. 6.
6. S. N. SINGH, *App. Sci. Res.* A **7** (1958) 237.
7. S. I. PAI, *Phys. Rev.* **105** (1957) 1424.

DISPLACEMENT FUNCTIONS AND LINEAR TRANSFORMS APPLIED TO DIFFUSION THROUGH POROUS ELASTIC MEDIA

By JOHN McNAMEE *and* R. E. GIBSON

(*University of Alberta, Canada, and Imperial College, London*)

[Received 12 March 1959]

SUMMARY

It is shown that the stresses and the pore pressure in porous elastic media through which a liquid is diffusing can be expressed in terms of two displacement functions. These functions are particularly useful in problems relating to a semi-infinite body or infinite layer when the stresses or displacements are prescribed on the surface. Problems of plane or axially symmetric strain are closely related when expressed in terms of these functions and the introduction of suitable repeated transforms (Fourier or Hankel followed by a Laplace transform) permits a parallel development of solutions for these two types of strain.

The process is time-dependent since it involves diffusion. After an infinite time the pore pressure reduces to zero and the governing equations for the stresses and displacements in the medium reduce to the ordinary equations of infinitesimal elasticity. The limiting forms of the functions used in the paper can then be related to known stress functions.

The Fourier and Hankel transforms can be regarded as specializations of the double Fourier transform, and it is shown in conclusion how the plane strain analysis can be generalized into a three-dimensional treatment.

1. Introduction

THE typical problem with which this paper is concerned can be stated thus: a liquid (usually water) diffuses through the pores of a clay medium under the action of stresses applied at the surface, and we seek to determine the displacements, the stresses, and the pore water pressure in the medium. Problems of this type are embraced in a theory which workers in the field of soil mechanics term 'the theory of consolidation'. We assume at the outset that the medium is elastic but the stresses and the excess pore pressure (i.e. the excess of the pore-water pressure over the hydrostatic pressure at any point—in the text, we often drop the qualification *excess*) are time-dependent since diffusion is a time-dependent process. A peculiar feature of these problems is that we cannot isolate the evaluation of the pore pressure from the evaluation of the elastic deformation: the two must be derived together. It will be seen below that many of our equations are formally identical with the equations for the determination of stress in an elastic solid due to a non-uniform temperature distribution and the

displacement functions which we shall presently introduce can be used in the solution of thermal stress problems. The analogy is not however complete, and, in general, thermal stress problems are much simpler since the temperature distribution is either given or determinable without reference to the stresses.

We shall limit ourselves here to the explanation of methods which facilitate the task of solution (solutions of some outstanding problems in soil mechanics are given elsewhere).

The equations which govern the diffusion of pore water in clay were given earlier by Biot (**1**) and the present work is based on Biot's analysis which we shall quote with a minimum of comment. An adequate explanation of the physical content of the mathematical analysis will be found in most textbooks on soil mechanics, e.g. Terzaghi (**2**).

Problems in soil mechanics frequently relate to the semi-infinite body or the infinite layer, and in succeeding sections of this paper we shall examine separately plane strain and radially symmetric strain. It will be shown at a later stage that the two analyses can be united. An observation of minor interest in the present context is that the time-dependent equations of our analysis reduce to the classical equations of infinitesimal elasticity for $t \to \infty$. It may therefore be anticipated that the displacement functions used in the paper are related to known stress functions of the theory of elasticity and this point is investigated briefly.

Biot (**3**, **4**) has recently recast his earlier work (cited above) in a more general form. Most of these generalizations envisage a more complex physical situation than we shall be concerned with; but one of his conclusions may be quoted here since it is pertinent to our work: he remarks that 'from a mathematical standpoint what distinguishes the consolidation problem from an elasticity problem is the addition of the function ϕ satisfying a heat conduction type equation' (**4**). We have reached a similar conclusion by a different route.

2. The governing equations

2.1. *Notation*

In the main, we have followed standard notation but we have introduced a few changes which conform with present usage in mathematics and soil mechanics. An unusual feature is that soil mechanics workers prefer to regard compressive stresses as positive and we have followed them here. The principal symbols follow.

t	Time coordinate.
x, z, ρ; u, w, u_ρ	Coordinates and displacements in the horizontal, vertical, and radial directions.

e	Volumetric compression per unit volume.
σ_{xx}, σ_{zz}, $\sigma_{\rho\rho}$	Total compressive stresses.
σ	Excess pore-water pressure.
$\sigma'_{xx} = \sigma_{xx} - \sigma$, etc.	Effective stresses acting on the clay skeleton.
σ_{xz}, $\sigma_{\rho z}$	Shearing stresses.
G, ν	Shear modulus and Poisson's ratio for the medium.
$\eta = \dfrac{1-\nu}{1-2\nu}$	An auxiliary elastic constant.
k	Coefficient of permeability in Darcy's law.
$c = 2G\eta k$	The coefficient of consolidation.

$$\nabla^2 \equiv \frac{\partial^2}{\partial x^2} + \frac{\partial^2}{\partial z^2} \equiv \frac{\partial^2}{\partial \rho^2} + \frac{1}{\rho}\frac{\partial}{\partial \rho} + \frac{\partial^2}{\partial z^2}.$$

2.2. *Plane strain in a fully saturated medium*

Biot's equations (1.3) (**1**) written in the above notation are

$$\nabla^2 u - (2\eta - 1)\frac{\partial e}{\partial x} - \frac{1}{G}\frac{\partial \sigma}{\partial x} = 0,$$

$$\nabla^2 w - (2\eta - 1)\frac{\partial e}{\partial z} - \frac{1}{G}\frac{\partial \sigma}{\partial z} = 0, \tag{1}$$

$$c\nabla^2 e = \frac{\partial e}{\partial t},$$

if we take compressive strains as positive and replace $1/(1-2\nu)$ by $(2\eta - 1)$.†

From these we can show by differentiating the first two of equations (1) that

$$\nabla^2(\sigma + 2G\eta e) = 0, \tag{2}$$

and, if S is any harmonic function of x and z, we can write

$$\sigma = 2G\left(\frac{\partial S}{\partial z} - \eta e\right). \tag{3}$$

If we now write

$$u = u_1 + u_2 + u_3,$$

$$w = w_1 + w_2 + w_3,$$

the differential equations (1) are satisfied if the following equations are satisfied:

$$\nabla^2 u_1 + \frac{\partial e}{\partial x} = 0, \qquad \nabla^2 w_1 + \frac{\partial e}{\partial z} = 0, \qquad e = -\left(\frac{\partial u_1}{\partial x} + \frac{\partial w_1}{\partial z}\right); \tag{4 a}$$

† To avoid a possible misunderstanding, we remark that equations (1) to (4) and (7) on pp. 290, 291, of (**2**) do not appear to be consonant with Biot's analysis: we make no use of them in the present paper.

$$\nabla^2 u_2 - 2\frac{\partial^2 S}{\partial x \partial z} = 0, \qquad \nabla^2 w_2 - 2\frac{\partial^2 S}{\partial z^2} = 0, \qquad \frac{\partial u_2}{\partial x} + \frac{\partial w_2}{\partial z} = 0; \tag{4 b}$$

and

$$\nabla^2 u_3 = 0, \qquad \nabla^2 w_3 = 0, \qquad \frac{\partial u_3}{\partial x} + \frac{\partial w_3}{\partial z} = 0. \tag{4 ç}$$

It is readily verified that a solution of equations (4) is

$$\begin{gathered} e = \nabla^2 X, \qquad u_1 = -\frac{\partial X}{\partial x}, \qquad w_1 = -\frac{\partial X}{\partial z}, \\ u_2 = z\frac{\partial S}{\partial x}, \qquad w_2 = z\frac{\partial S}{\partial z} - S, \\ u_3 = -\frac{\partial Y}{\partial x}, \qquad u_3 = -\frac{\partial Y}{\partial z}, \qquad \nabla^2 Y = 0, \end{gathered} \tag{5}$$

where X is an arbitrary differentiable function. If we now write

$$E = X + Y,$$

then

$$\begin{gathered} u = -\frac{\partial E}{\partial x} + z\frac{\partial S}{\partial x}, \\ w = -\frac{\partial E}{\partial z} + z\frac{\partial S}{\partial z} - S, \\ e = \nabla^2 E, \qquad \sigma = 2G\left(\frac{\partial S}{\partial z} - \eta \nabla^2 E\right), \end{gathered} \tag{6}$$

and the governing equations for E and S are (cf. the third of equations (1) and the definition of S)

$$c\nabla^4 E = \nabla^2 \frac{\partial E}{\partial t}, \qquad \nabla^2 S = 0. \tag{7}$$

We can now write down expressions for the stresses in terms of E and S but we defer this for the moment.

2.3. *Axially symmetric strain in a fully saturated medium*

The displacement equations for cylindrical strain are easily derived from Biot's analysis:

$$\begin{gathered} \left(\nabla^2 - \frac{1}{\rho^2}\right) u_e - (2\eta - 1)\frac{\partial e}{\partial \rho} - \frac{1}{G}\frac{\partial \sigma}{\partial \rho} = 0, \\ \nabla^2 w - (2\eta - 1)\frac{\partial e}{\partial z} - \frac{1}{G}\frac{\partial \sigma}{\partial z} = 0, \\ c\nabla^2 e = \frac{\partial e}{\partial t}, \end{gathered} \tag{8}$$

where $$e = -\left(\frac{\partial u_\rho}{\partial \rho}+\frac{u_\rho}{\rho}+\frac{\partial w}{\partial z}\right),$$

and $$\nabla^2 \equiv \frac{\partial^2}{\partial \rho^2}+\frac{1}{\rho}\frac{\partial}{\partial \rho}+\frac{\partial^2}{\partial z^2}.$$

If we make use of the identity

$$\frac{\partial}{\partial \rho}\nabla^2 X \equiv \left(\nabla^2-\frac{1}{\rho^2}\right)\frac{\partial X}{\partial \rho},$$

we can show, as in section 2.2, that

$$\nabla^2(\sigma+2G\eta e) = 0. \tag{9}$$

The functions E and S can be introduced by a procedure similar to that used in section 2.2, and we find that

$$u_\rho = -\frac{\partial E}{\partial \rho}+z\frac{\partial S}{\partial \rho}, \qquad w = -\frac{\partial E}{\partial z}+z\frac{\partial S}{\partial z}-S,$$

$$c\nabla^4 E = \nabla^2\frac{\partial E}{\partial t}, \qquad \nabla^2 S = 0. \tag{10}$$

2.4. *Expressions for the stresses in terms of E and S*

The strain of the medium is related to the *effective* stresses by the ordinary equations of infinitesimal elasticity (the pore pressure causes no strain), e.g.

$$\sigma'_{xx} = 2G\left[-\frac{\partial u}{\partial x}+(\eta-1)e\right],$$

$$\sigma_{xz} = -G\left[\frac{\partial u}{\partial z}+\frac{\partial w}{\partial x}\right].$$

For comparison, we write down in parallel columns the expressions for the displacements and total stresses when the strain is plane or axially symmetric.

Plane strain	*Axially symmetric strain*
$u = -\dfrac{\partial E}{\partial x}+z\dfrac{\partial S}{\partial x},$	$u_\rho = -\dfrac{\partial E}{\partial \rho}+z\dfrac{\partial S}{\partial \rho},$
	$w = -\dfrac{\partial E}{\partial z}+z\dfrac{\partial S}{\partial z}-S,$
$\dfrac{\sigma}{2G} = \dfrac{\partial S}{\partial z}-\eta e,$	
$\dfrac{\sigma_{xx}}{2G} = \left(\dfrac{\partial^2}{\partial x^2}-\nabla^2\right)E-z\dfrac{\partial^2 S}{\partial x^2}+\dfrac{\partial S}{\partial z},$	$\dfrac{\sigma_{\rho\rho}}{2G} = \left(\dfrac{\partial^2}{\partial \rho^2}-\nabla^2\right)E-z\dfrac{\partial^2 S}{\partial \rho^2}+\dfrac{\partial S}{\partial z},$

$$\frac{\sigma_{zz}}{2G} = \left(\frac{\partial^2}{\partial z^2} - \nabla^2\right)E - z\frac{\partial^2 S}{\partial z^2} + \frac{\partial S}{\partial z},$$

$$\frac{\sigma_{\theta\theta}}{2G} = \left(\frac{\partial}{\rho\,\partial\rho} - \nabla^2\right)E - \frac{z}{\rho}\frac{\partial S}{\partial \rho} + \frac{\partial S}{\partial z},$$

$$\frac{\sigma_{xz}}{2G} = \frac{\partial^2 E}{\partial x \partial z} - z\frac{\partial^2 S}{\partial x \partial z}, \qquad \frac{\sigma_{\rho z}}{2G} = \frac{\partial^2 E}{\partial \rho \partial z} - z\frac{\partial^2 S}{\partial \rho \partial z}.$$

It can be seen that the shear modulus G appears in these expressions only as a multiplier and the elastic ratio η appears only in the expression for σ. This is convenient in applications since the elastic constants are introduced at a fairly late stage of the analysis. It can also be seen by inspection that—with the exception of $\sigma_{\theta\theta}$—the expressions for cylindrical strain are immediately obtained from the corresponding expressions for plane strain if x is replaced by ρ everywhere and the appropriate form of ∇^2 is used.

2.5. *The use of non-dimensional quantities*

It is convenient to anticipate here the application we wish to make of the formulae of the preceding section. The typical problem may be stated thus: a uniform pressure f is applied to a strip of width $2b$, or to a circular area whose radius is b, on the boundary of the medium. The complete specification of the problem will then require the intervention of four constants G, f, b, and c (the coefficient of consolidation), together with the dimensionless ratio η. The five constants can be reduced to two if we choose b as unit of length, b^2/c as unit of time, and f as unit of stress. The components of displacements and stress are then replaced by dimensionless quantities, but the expressions tabulated in subsection 2.4 are unchanged in form, save that the coefficient c must be replaced by unity. To demonstrate this point completely would require a complete change of notation and we shall indicate only the first few steps. We write

$$x = bx', \quad \rho = b\rho', \quad z = bz', \quad t = t'b^2/c,$$

using a prime for the new non-dimensional coordinates. Similarly we write

$$E = b^2E', \qquad S = bS'.$$

The differential equations for E and S are transformed to

$$\nabla^4 E' = \nabla^2 \frac{\partial E'}{\partial t}, \qquad \nabla^2 S' = 0.$$

The displacements are replaced by $u' = u/b$, etc., and the stresses by σ_{xx}/f, etc., though it is often convenient to retain the non-dimensional forms $\sigma_{xx}/2G$. We can retain the existing notation and drop the primes provided it is understood that non-dimensional quantities are used. We shall presume this understanding in the following sections.

3. Fourier and Hankel transforms of E and S

The results of the preceding sections enable us to treat the theory of plane and radially symmetric strain in parallel. We remark that the introduction of the functions E and S reduces the number of dependent variables from three (e.g. u, w, σ) to two, but the order of the governing equations has been increased. The reduction may prove to be an illusory advantage unless we can at the same time eliminate one or more of the independent variables by means of suitable transforms. The method is familiar and may be stated briefly. We assume that E and S can be represented by definite integrals and that these integrals exist and can be differentiated the required number of times; in specific problems it is usually possible to verify existence and differentiability *a posteriori* if a solution can be found. The differential equations governing E and S are transformed into simpler equations governing two new functions, say E_c and S_c, the boundary values of E_c and S_c being determined by an inversion. The more common practice of defining transformed functions E_c and S_c and later transforming back to E and S can be justified *a priori* but is less convenient here since it requires the transformation of the displacements and stresses—or at least of those displacements and stresses which appear in the boundary conditions. A minor but not unimportant point is that the introduction of new symbols for the transformed stresses is an additional burden on an already overburdened notation.

The Fourier cosine transform is appropriate to problems of plane strain in which the loading is symmetric about the z-axis. We represent the stress functions E and S by the definite integrals

$$\begin{aligned} E(x,z,t) &= \frac{2}{\pi}\int_0^\infty \cos(x\xi)E_c(\xi,z,t)\,d\xi, \\ S(x,z,t) &= \frac{2}{\pi}\int_0^\infty \cos(x\xi)S_c(\xi,z,t)\,d\xi, \end{aligned} \tag{11}$$

and similar integrals for the displacements and stresses can be obtained by differentiating under the integral sign.

The zero order Hankel transform enables us to eliminate the coordinate ρ in problems of cylindrical strain. We define E and S by

$$\begin{aligned} E(\rho,z,t) &= \int_0^\infty \xi J_0(\rho\xi)E_h(\xi,z,t)\,d\xi, \\ S(\rho,z,t) &= \int_0^\infty \xi J_0(\rho\xi)S_h(\xi,z,t)\,d\xi. \end{aligned} \tag{12}$$

If, for example, we form the derivative $\partial S/\partial\rho$ and assume that we may differentiate under the integral sign, we find that

$$\frac{\partial S}{\partial \rho} = -\int_0^\infty \xi^2 J_1(\rho\xi)\, S_h\, d\xi.$$

If we differentiate again and make use of the differential equation for J_0, we find

$$\nabla^2 S(\rho, z, t) = \int_0^\infty \xi J_0(\rho\xi)\left[\frac{\partial^2}{\partial z^2} - \xi^2\right] S_h\, d\xi$$

$$= 0.$$

This equation is true for $0 \leqslant \rho \leqslant \infty$ and, if we multiply by $\rho J_0(\zeta\rho)\, d\rho$ and integrate from 0 to ∞, we have by Hankel's theorem (see, e.g., (**5**), Theorem 135)

$$\left(\frac{\partial^2}{\partial z^2} - \xi^2\right) S_h(\xi, z, t) = 0 \quad (0 \leqslant \xi \leqslant \infty). \tag{13}$$

The expressions for the stresses and displacements may be tabulated very compactly if we use the notation

$$K\begin{pmatrix} x \\ \rho \end{pmatrix}, \xi\Big) = \frac{2}{\pi}\cos(x\xi) \quad \text{or} \quad \xi J_0(\rho\xi),$$

$$K'\begin{pmatrix} x \\ \rho \end{pmatrix}, \xi\Big) = -\frac{2}{\pi}\xi \sin(x\xi) \quad \text{or} \quad -\xi^2 J_1(\rho\xi)$$

and accept the convention that the first kernel on the right of these equations is to be used in plane strain and the second in axially symmetric problems. We use a single symbol u to signify the horizontal or radial displacement.

$$u = \int_0^\infty K'\begin{pmatrix} x \\ \rho \end{pmatrix}, \xi\Big)\left[-E_{c,h} + zS_{c,h}\right] d\xi,$$

$$w = \int_0^\infty K\begin{pmatrix} x \\ \rho \end{pmatrix}, \xi\Big)\left[-\frac{\partial E}{\partial z} + z\frac{\partial S}{\partial z} - S\right] d\xi,$$

$$e = \int_0^\infty K\begin{pmatrix} x \\ \rho \end{pmatrix}, \xi\Big)\left[\frac{\partial^2}{\partial z^2} - \xi^2\right] E\, d\xi,$$

$$\frac{\sigma}{2G} = -\eta e + \int_0^\infty K\begin{pmatrix} x \\ \rho \end{pmatrix}, \xi\Big)\frac{\partial S}{\partial z}\, d\xi.$$

In problems where surface tractions are specified, expressions for the components of *total* stress are required and these are derivable from the

above formulae for the displacements and the pore water pressure. For example

$$\frac{\sigma_{zz}}{2G} = \int_0^\infty K\left(\frac{x}{\rho}, \xi\right)\left[\xi^2 E + \frac{\partial S}{\partial z} - z\xi^2 S\right] d\xi,$$

$$\frac{\sigma_{xz}}{2G}, \frac{\sigma_{\rho z}}{2G} = \int_0^\infty K'\left(\frac{x}{\rho}, \xi\right)\left[\frac{\partial E}{\partial z} - z\frac{\partial S}{\partial z}\right] d\xi.$$

The differential equations for $E_{c,h}$ and $S_{c,h}$ are

$$\left(\frac{\partial^2}{\partial z^2} - \xi^2\right)\left(\frac{\partial^2}{\partial z^2} - \xi^2 - \frac{\partial}{\partial t}\right) E(\xi, z, t) = 0,$$
$$\left(\frac{\partial^2}{\partial z^2} - \xi^2\right) S(\xi, z, t) = 0. \tag{14}$$

In these equations, and in the table above, the quantities E and S should bear the appropriate suffix c, or h, as we have indicated in the expression for u.

4. Repeated transforms of E and S

The partial differential equations (14) can be transformed into ordinary equations by means of a Laplace transform. Remembering that the initial state of the medium is determined by the consideration that the pore water diffuses with a finite velocity, we know that the volumetric strain is zero initially. Since

$$e = \nabla^2 E,$$

we must have $\nabla^2 E = 0 \quad \text{for } t = 0;$

or, equivalently, $$\left(\frac{\partial^2}{\partial z^2} - \xi^2\right) E_{c,h} = 0 \quad \text{for } t = 0. \tag{15}$$

We now drop the suffix c, h except when necessary to avoid ambiguity.

If we write

$$E(\xi, z, t) = \frac{1}{2\pi i} \int_{\gamma - i\infty}^{\gamma + i\infty} e^{pt} \bar{E}(\xi, z, p)\, dp \quad (\gamma \geqslant 0) \tag{16}$$

then, using (15),

$$\frac{\partial}{\partial t}\left(\frac{\partial^2}{\partial z^2} - \xi^2\right) E = \frac{1}{2\pi i} \int_{\gamma - i\infty}^{\gamma + i\infty} p e^{pt} \left(\frac{d^2}{dz^2} - \xi^2\right) \bar{E}\, dp,$$

and the first of (14) becomes

$$\left(\frac{\partial^2}{\partial z^2} - \xi^2\right)\left(\frac{\partial^2}{\partial z^2} - \xi^2 - \frac{\partial}{\partial t}\right) E(\xi, z, t)$$
$$= \frac{1}{2\pi i} \int_{\gamma - i\infty}^{\gamma + i\infty} e^{pt} \left(\frac{d^2}{dz^2} - \xi^2 - p\right)\left(\frac{d^2}{dz^2} - \xi^2\right) \bar{E}\, dp = 0.$$

This equation is true for all positive values of t and we shall assume

$$E(\xi, z, t) = 0 \quad (t < 0).$$

If we now multiply the equation by $e^{-p't}dt$ and integrate from $-\infty$ to ∞, we have by an obvious modification of Fourier's double integral theorem [see (6) equation 7.1 (2)]

$$\left(\frac{d^2}{dz^2} - \xi^2 - p'\right)\left(\frac{d^2}{dz^2} - \xi^2\right)\bar{E} = 0, \tag{17}$$

the left-hand side being analytic in the half-plane $\mathrm{re}(p') > \gamma$. Similarly, the second of (14) becomes

$$\left(\frac{d^2}{dz^2} - \xi^2\right)\bar{S} = 0, \tag{18}$$

where

$$S(\xi, z, t) = \frac{1}{2\pi i}\int_{\gamma - i\infty}^{\gamma + i\infty} e^{pt}\bar{S}(\xi, z, p)\, dp. \tag{19}$$

It is unnecessary to rewrite the table of section 3 in terms of double integrals since we can in most problems perform the integration with respect to p before using these expressions.

5. Bilateral displacement functions for infinite layers

The functions E and S of section 2 are convenient for the solution of problems relating to the semi-infinite body $z \geqslant 0$ when the loading is applied at $z = 0$. They may also be used in problems of the infinite layer $0 \leqslant z \leqslant h$, but it is sometimes preferable to modify these functions so that the boundary conditions at the upper and lower surfaces may be simply incorporated. Since three conditions must be satisfied at each surface, the boundary conditions form a sixth-order matrix and it is expedient to simplify the algebra as much as possible at the outset of the work (a boundary condition on the pore pressure σ must be satisfied in addition to the usual two boundary conditions of elastic theory).

We shall illustrate the use of bilateral displacement functions by considering briefly their application in plane strain problems. Retaining the notation of section 2.2, we write

$$u = u' + u'', \qquad w = w' + w'',$$
$$E = E' + E'', \qquad S = S' + S''.$$

It is easy to verify that, if $z_1 = h - z$,

$$u' = -\frac{\partial E'}{\partial x} + z\frac{\partial S'}{\partial x}, \qquad w' = -\frac{\partial E'}{\partial z} + z\frac{\partial S'}{\partial z} - S',$$

$$u'' = -\frac{\partial E''}{\partial x} - z_1\frac{\partial S''}{\partial x}, \qquad w'' = \frac{\partial E''}{\partial z_1} + z_1\frac{\partial S''}{\partial z_1} - S''.$$

satisfy equations (1) if σ is given by (3) and if E and S are governed by (7).

These functions may then be expressed by a repeated transform and the solution can in general be written as a linear function of the terms

$$\exp(-z\xi), \quad \exp[-z(\xi^2+p)^{\frac{1}{2}}], \quad \exp(-z_1\xi), \quad \exp[-z_1(\xi^2+p)^{\frac{1}{2}}]$$

of which the first pair reduce to unity for $z = 0$ and the second pair when $z = h$.

6. The limiting forms of E and S $(t \to \infty)$

The steady state solution of the diffusion equations which we have been examining is identical with the solution of the corresponding elastic equations. The excess pore pressure reduces to zero in the steady state; equations (1) and (8) then become the familiar elastic equations for plane and radially symmetric strain. We may then expect the limiting forms of E and S to be closely related to known stress functions of the theory of elasticity. We shall show how E is related to (i) Love's biharmonic stress function χ which is applicable in problems of symmetrical strain in a solid of revolution (**7**), (ii) the harmonic stress function of Boussinesq (**8**) for the solution of problems relating to the semi-infinite body (**9**). Love (**10**) notes that equivalent formulae were given by Hertz (**11**).

Denoting the limiting forms of E and S by E_∞ and S_∞, and writing

$$E_\infty = \frac{\partial L}{\partial z} \qquad (\nabla^4 L = 0),$$

we have, from (3) and (6), $\qquad S_\infty = \eta\nabla^2 L$

if we ignore linear terms. The displacements u_ρ and w become

$$u_\rho = -\frac{\partial^2 L}{\partial\rho\partial z} + \eta z \frac{\partial}{\partial\rho}\nabla^2 L,$$

$$w = -\frac{\partial^2 L}{\partial z^2} + \eta z \frac{\partial}{\partial z}\nabla^2 L - \eta\nabla^2 L,$$

and

$$e = \nabla^2 \frac{\partial L}{\partial z}.$$

If we express e in terms of Love's stress function χ, we have

$$e = -\frac{1-2\nu}{2G}\nabla^2\frac{\partial\chi}{\partial z}.$$

Since e is harmonic, we may write

$$L = -\frac{1-2\nu}{2G}\chi + \omega,$$

where ω is an harmonic function which can be determined by comparing

the expressions for the displacements; we ignore here an arbitrary biharmonic function of e alone since the function may be absorbed in χ. We find finally that

$$L = -\frac{1-2\nu}{2G}\frac{\partial^2\Psi^*}{\partial z^2} + \frac{1-\nu}{2G}\left[4\frac{\partial^2\Psi^*}{\partial z^2} - \nabla^2\left(z\frac{\partial\Psi^*}{\partial z} - \Psi^*\right)\right],$$

where

$$\chi = \frac{\partial^2\Psi^*}{\partial z^2},$$

and the expression in square brackets is harmonic.

A comparison with Boussinesq's stress function ϕ (we follow Green and Zerna's presentation here) is most easily obtained from an examination of the plane strain case. The displacement is given by

$$u = -\frac{\partial^2 L}{\partial x \partial z} + \eta z\frac{\partial}{\partial x}\nabla^2 L,$$

and the expression for w is unchanged in form. If we write

$$L = 2L_1 - z\frac{\partial L_1}{\partial z} \quad (\nabla^2 L_1 = 0)$$

it is easily verified that

$$\sigma_{xz} = 2G(2\eta - 1)z\frac{\partial^4 L_1}{\partial x \partial z^3}$$

and the shearing stress is zero on the plane $z = 0$. For comparison we write side by side our expressions for u and w in terms of L_1 and Boussinesq's expressions in terms of ϕ:

$$u = -\frac{1}{1-2\nu}\left[z\frac{\partial}{\partial z} + 1 - 2\nu\right]\frac{\partial^2 L_1}{\partial x \partial z}, \qquad 2Gu = \left[z\frac{\partial}{\partial z} + 1 - 2\nu\right]\frac{\partial\phi}{\partial x},$$

$$w = -\frac{1}{1-2\nu}\left[z\frac{\partial}{\partial z} - 2(1-\nu)\right]\frac{\partial^2 L_1}{\partial z^2}, \qquad 2Gw = \left[z\frac{\partial}{\partial z} - 2(1-\nu)\right]\frac{\partial\phi}{\partial z},$$

and we may write

$$\phi = -\frac{2G}{1-2\nu}\frac{\partial L_1}{\partial z}.$$

7. Three-dimensional displacement functions in consolidation problems

The comparison with the stress functions of Boussinesq, Hertz, and Love, suggests that we may be able to carry the preceding analysis a stage further by formulating techniques for the treatment of more general types of surface loading on a semi-infinite body $z > 0$. We shall outline briefly a quite general method of attack by making use of a special form of Fourier's double integral. The use of this method in elasticity problems is well-known (**12**) and it will appear that the solution of a consolidation

problem is in general feasible if the corresponding elastic problem can be solved.

It is easily verified that the plane strain equations for E and S and the equations which express the stresses and displacements in terms of these functions can be generalized into three dimensions without change of form, the plane operator ∇^2 being replaced by

$$\nabla^2 \equiv \frac{\partial^2}{\partial x^2}+\frac{\partial^2}{\partial y^2}+\frac{\partial^2}{\partial z^2}.$$

For definiteness we shall consider a problem which frequently arises in applications of the theory; an area D of the plane $z = 0$ is subjected to a normal stress $f(x, y)$, the shearing stress being zero all over this plane. In addition, a boundary value of the pore pressure σ, or its derivative $\partial\sigma/\partial z$, or a linear combination of both will be prescribed; it is sufficiently illustrative here to take this condition to be $\sigma = 0$ on $z = 0$. We adopt as possible solutions for E and S

$$E = \frac{1}{2\pi i}\int_{-\infty}^{\infty}\int_{-\infty}^{\infty}\int_{\mathrm{Br}} (A_1 e^{-\gamma z}+A_2 e^{-z(\gamma^2+p/k)})e^{i(\alpha x+\beta y)+pt}\, d\alpha d\beta dp, \tag{20}$$

$$S = \frac{1}{2\pi i}\int_{-\infty}^{\infty}\int_{-\infty}^{\infty}\int_{\mathrm{Br}} B_1 e^{i(\alpha x+\beta y)-\gamma z+pt}\, d\alpha d\beta dp, \tag{21}$$

where $$\gamma^2 = \alpha^2+\beta^2$$

and Br denotes the Bromwich–Wagner contour. The conditions of zero shear and zero pore pressure on $z = 0$ yield two relations between the functions A_1, A_2, B_1; then from the formulae of section 2 the boundary value of the normal stress σ_{zz} can be expressed by

$$\frac{\sigma_{zz}}{2G} = \frac{1}{2\pi i}\int_{-\infty}^{\infty}\int_{-\infty}^{\infty}\int_{\mathrm{Br}} \gamma^2\Lambda A_2 e^{i(\alpha x+\beta y)+pt}\, d\alpha d\beta dp \tag{22}$$

with $$\Lambda = 1+\eta s-(1+s)^{\frac{1}{2}} \quad (s = p/\gamma^2).$$

Inverting this relation we may write

$$\gamma^2\Lambda A_2 = \frac{1}{4\pi^2 p}\iint_D \frac{f(\zeta,\xi)}{2G} e^{-i(\alpha\zeta+\beta\xi)}\, d\zeta d\xi.$$

For example, if f is constant and D is a rectangle of sides 2λ, 2μ, the origin being at the centre of the rectangle, we find

$$\gamma^2\Lambda A_2 = \frac{f\sin\alpha\lambda\sin\beta\mu}{2\pi^2 G\alpha\beta p}.$$

The functions E and S in this example are found to be defined by

$$\frac{2G}{f}E = \frac{1}{2\pi^3 i}\int_{-\infty}^{\infty}\int_{-\infty}^{\infty}\int_{\mathrm{Br}} \frac{\sin\alpha\lambda\sin\beta\mu}{p\Lambda\gamma^4\alpha\beta}\left[e^{-z\gamma(1+s)^{\frac{1}{2}}} - (1+s)^{\frac{1}{2}}e^{-z\gamma}\right]e^{i(\alpha x+\beta y)+pt}\,d\alpha d\beta dp,$$

$$\frac{2G}{f}S = -\frac{\eta}{2\pi^3 i}\int_{-\infty}^{\infty}\int_{-\infty}^{\infty}\int_{\mathrm{Br}} \frac{\sin\alpha\lambda\sin\beta\mu}{\Lambda\gamma^3\alpha\beta}\,e^{i(\alpha x+\beta y)-z\gamma+pt}\,d\alpha d\beta dp.$$

The solution which we have just sketched is purely operative and we have not considered at any stage the validity of our operations. It is clear, however, that the existence and differentiability of the Fourier integrals in (20) and (21) depend on the behaviour of the Bromwich contour integrals *qua* functions of α and β. Equation (22) shows that the only singularities in the p-plane are poles and branch-points and it is usually possible to effect the integration with respect to p.

The detailed exploration of these techniques is considered in a following paper.

8. Conclusion

The solution of specific problems of the theory we have been considering will lead in general to algebraic work of considerable complexity and very few solutions are available. The use of displacement functions followed by repeated transforms permits an easy and natural incorporation of the boundary and initial conditions. The success of the method depends mainly on the possibility of evaluating certain integrals in the complex plane, the integrands of which possess, in general, a finite number of poles and branch-points.

REFERENCES

1. M. A. Biot, *J. App. Phys.* **12** (1941) 155, 426, and 578.
2. K. Terzaghi, *Theoretical Soil Mechanics* (New York, 1943).
3. M. A. Biot, *J. App. Phys.* **26** (1955) 182.
4. —— ibid. **23** (1956) 91.
5. E. C. Titchmarsh, *The Theory of Fourier Integrals* (Oxford, 1948).
6. G. Doetsch, *Handbuch der Laplace-Transformation* (Basel, 1950).
7. A. E. H. Love, *The Mathematical Theory of Elasticity*, 4th edition, 266 (Cambridge, 1927).
8. J. Boussinesq, *Application des potentials* (Paris, 1885).
9. A. E. Green and W. Zerna, *Theoretical Elasticity*, 171–2 (Oxford, 1954).
10. A. E. H. Love, *Phil. Trans. Roy. Soc.* A, **228** (1929) 377.
11. H. Hertz, *J. Math.* (*Crelle*) **92** (1881).
12. P. Frank and R. v. Mises, *Die Differential und Integralgleichungen der Physik*, 7th edition, vol. 2, 599, 644 (Brunswick, 1927).

MULTHOPP'S INFLUENCE FUNCTIONS AND THEIR AUTOMATIC COMPUTATION

By G. G. ALWAY

(*National Physical Laboratory, Teddington, Middlesex*)

[Received 29 July 1959]

SUMMARY

This paper gives a method for the calculation of the influence functions arising in Multhopp's subsonic lifting surface theory. It is eminently suitable for programming on automatic computers but double length working would be necessary if large values of the arguments and high order functions were required.

1. Introduction

CERTAIN aerodynamic theories initiated by Multhopp (**1**, **2**) involve several functions of two variables whose numerical values are required in practical applications. A few of these functions have been tabulated by Curtis (**3**), to supplement charts given in (**1**), Figs. (1)–(6). Desk machines have now been replaced by automatic computers in the rest of the calculations involved in the theory and a suitable method for forming each value of the functions directly in the machine is needed. The purpose of this paper is to meet this requirement for a reasonably large number of Multhopp's influence functions, and for a wide range of the independent variables.

The functions considered depend essentially on the quantities

$$\left.\begin{aligned} S(p) &= \frac{1}{\pi}\int_0^{\pi} \frac{[\cos p\theta + \cos(p+1)\theta][X-\frac{1}{2}(1-\cos\theta)]}{\{[X-\frac{1}{2}(1-\cos\theta)]^2+Y^2\}^{\frac{1}{2}}}\,d\theta \\ T(p) &= \frac{1}{\pi}\int_0^{\pi} [\cos p\theta + \cos(p+1)\theta]\{[X-\tfrac{1}{2}(1-\cos\theta)]^2+Y^2\}^{\frac{1}{2}}\,d\theta \end{aligned}\right\}, \quad (1)$$

and are given by

$$\left.\begin{aligned} \mathrm{i}(X,Y) &= 1+S(0), \qquad \mathrm{j}(X,Y) = 4S(1) \\ \mathrm{k}(X,Y) &= S(2), \qquad \mathrm{l}(X,Y) = S(3), \qquad \mathrm{m}(X,Y) = S(4) \\ \mathrm{ii}(X,Y) &= \int_{-\infty}^{X} \mathrm{i}(X_0,Y)\,dX_0 = X-\tfrac{1}{4}+T(0) \\ \mathrm{jj}(X,Y) &= \int_{-\infty}^{X} \mathrm{j}(X_0,Y)\,dX_0 = 1+4T(1) \end{aligned}\right\}. \quad (2)$$

$$\left.\begin{aligned} \mathsf{kk}(X,Y) &= \int_{-\infty}^{X} \mathsf{k}(X_0,Y)\,dX_0 = T(2) \\ \mathsf{ll}(X,Y) &= \int_{-\infty}^{X} \mathsf{l}(X_0,Y)\,dX_0 = T(3) \end{aligned}\right\}$$

2. The method of computation

The functions (2) are not linearly independent; each can be expressed as a linear combination of any three others. If i, j, ii are known, suitable expressions for deriving successively the remaining six functions are as follows:

$$12\mathsf{k} = 8\mathsf{i}-3\mathsf{j}+32\mathsf{ii}-8M(4\mathsf{i}+\mathsf{j}-8\mathsf{ii})-128L\mathsf{i}+128Y^2, \tag{3}$$

$$8\mathsf{jj} = 8\mathsf{i}-\mathsf{j}-4\mathsf{k}, \tag{4}$$

$$32\mathsf{l} = -24\mathsf{i}+3\mathsf{j}-4\mathsf{k}+96\mathsf{ii}-48M(2\mathsf{i}+2\mathsf{k}-\mathsf{jj})-96L\mathsf{j}, \tag{5}$$

$$96\mathsf{kk} = 3\mathsf{j}-4\mathsf{k}-8\mathsf{l}, \tag{6}$$

$$15\mathsf{m} = -12\mathsf{i}+4\mathsf{k}-\mathsf{l}+12\mathsf{jj}-12M(\mathsf{j}+4\mathsf{l}-8\mathsf{kk})-192L\mathsf{k}, \tag{7}$$

$$48\mathsf{ll} = 4\mathsf{k}-\mathsf{l}-3\mathsf{m}, \tag{8}$$

where
$$M = 2X-1, \qquad L = X^2+Y^2-X+\tfrac{3}{8}. \tag{9}$$

The proof of these formulae is given in Appendix A.

Each of the influence functions can be expressed as a linear combination of three complete elliptic integrals. If the following three elliptic integrals are chosen, relatively simple expressions result for i, j, ii.

Let

$$\left.\begin{aligned} A &= \frac{2}{\pi}\int_0^{\frac{1}{2}\pi} \frac{[1-(P-Q)^2]\cos^2\alpha\,d\alpha}{\{4PQ\cos^2\alpha+[(P+Q)^2-1]\sin^2\alpha\}^{\frac{1}{2}}} \\ B &= \frac{2}{\pi}\int_0^{\frac{1}{2}\pi} \frac{d\alpha}{\{4PQ\cos^2\alpha+[(P+Q)^2-1]\sin^2\alpha\}^{\frac{1}{2}}} \\ C &= \frac{2}{\pi}\int_0^{\frac{1}{2}\pi} \frac{(P^2-Q^2)\sin^2\alpha\,d\alpha}{[4PQ\cos^2\alpha+(P+Q)^2\sin^2\alpha]\{4PQ\cos^2\alpha+[(P+Q)^2-1]\sin^2\alpha\}^{\frac{1}{2}}} \end{aligned}\right\}, \tag{10}$$

where $P = [(X-1)^2+Y^2]^{\frac{1}{2}}$, $Q = [X^2+Y^2]^{\frac{1}{2}}$; then, as is proved in Appendix B:

$$\mathsf{i} = 1+A+(2X-1)B+C, \tag{12}$$

$$\mathsf{j} = 8(1-X)A-16Y^2C, \tag{13}$$

$$\mathsf{ii} = (X-\tfrac{1}{4})+(\tfrac{1}{2}X+\tfrac{1}{4})A+[2Y^2+(2X-1)(X-\tfrac{1}{4})]B+(Y^2+X-\tfrac{1}{4})C. \tag{14}$$

Bartky (4) gives a method of calculating complete elliptic integrals

which is eminently suitable for an automatic computer. This iterative method is an extension of Landen's classical transformation. Bartky's result is that if

$$I(i) = \int_0^{\frac{1}{2}\pi} \frac{(a_i m_i \cos^2\theta + b_i r_i n_i \sin^2\theta)\, d\theta}{(m_i \cos^2\theta + r_i n_i \sin^2\theta)(m_i^2 \cos^2\theta + n_i^2 \sin^2\theta)^{\frac{1}{2}}}$$

and

$$\left.\begin{aligned} m_{i+1} &= \tfrac{1}{2}(m_i + n_i), & n_{i+1} &= (m_i n_i)^{\frac{1}{2}} \\ a_{i+1} &= \tfrac{1}{2}(a_i + b_i), & b_{i+1} &= \frac{a_i + r_i b_i}{1 + r_i} \\ r_{i+1} &= \frac{n_{i+1}}{4m_{i+1}}\left(r_i + \frac{1}{r_i} + 2\right) \end{aligned}\right\} \qquad (15)$$

then $I(i) = I(i+1)$

If we now put $q_i^2 = r_i m_i n_i$ and assume r_i, m_i, n_i are all positive, we can deduce that

$$\left.\begin{aligned} q_{i+1} &= \frac{1}{2}\left(q_i + \frac{m_i n_i}{q_i}\right) \\ q_{i+1} b_{i+1} &= \frac{1}{2}\left(\frac{m_i n_i}{q_i} a_i + q_i b_i\right) \end{aligned}\right\}. \qquad (16)$$

Further, $q_{i+1} = m_{i+1}$ if $q_i = m_i$.

To adapt this result for the present purpose of computing A, B, C, we write

$$\left.\begin{aligned} m_0 &= 2[PQ]^{\frac{1}{2}}, & n_0 &= [(P+Q)^2 - 1]^{\frac{1}{2}} \\ a_0 &= 1 - (P-Q)^2, & b_0 &= 0, \quad c_0 = 0 \\ d_0 &= P - Q, & q_0 &= P + Q \end{aligned}\right\}, \qquad (17)$$

and let

$$\left.\begin{aligned} m_{i+1} &= \tfrac{1}{2}(m_i + n_i), & n_{i+1} &= (n_i m_i)^{\frac{1}{2}} \\ a_{i+1} &= \frac{1}{2}\left(a_i + \frac{b_i}{m_i}\right), & b_{i+1} &= \tfrac{1}{2}(n_i a_i + b_i) \\ c_{i+1} &= \frac{1}{2}\left(c_i + \frac{d_i}{q_i}\right), & d_{i+1} &= \frac{1}{2}\left(\frac{m_i n_i}{q_i} c_i + d_i\right) \\ q_{i+1} &= \frac{1}{2}\left(q_i + \frac{m_i n_i}{q_i}\right) \end{aligned}\right\}. \qquad (18)$$

The iteration proceeds until $m_r = n_r = q_r$ to the accuracy of the calculation. Then

$$A = \frac{a_{r+1}}{m_r}, \qquad B = \frac{1}{m_r}, \qquad C = \frac{c_{r+1}}{m_r}, \qquad (19)$$

for $a_{r+1} = a_{r+2}$ and $c_{r+1} = c_{r+2}$ when $m_r = n_r = q_r$.

3. Comments on the method

Some of the coefficients in the relations used increase as $|X|$ and Y increase resulting in loss of precision by cancellation. Higher-order func-

tions (i.e. those with larger p) are affected more than lower-order ones. The cancellation can be overcome by using multiple-length arithmetic but a large range of applications is adequately covered by single-length working. When $|X|$ and Y are as large as 3, for example, only three decimals are lost in forming $\|$.

The convergence of the iterative process (18) is rapid and three or four cycles of calculation are usually sufficient to give six decimal places correctly.

Errors will be introduced when P or Q are small, that is, very close to $Y = 0$, $X = 0$ or $Y = 0$, $X = 1$. For then m_0 is small. Theoretically the method also breaks down when $Y = 0$ and X lies between 0 and 1, for then $n_0 = 0$ and so the final $m_r = 0$. It has been found, however, that correct values may be obtained if the rounding error in the formation of square roots is such that the calculated root is always strictly positive, for then $n_i \neq 0$ and the process converges. To ensure this and also to avoid trouble with the scaling of numbers the computation of the iterative process is best arranged as follows. The multiplication routine should produce a double-length product; the division routine should work with a double-length dividend and a single-length divisor to give a single-length quotient; the square root routine should produce a single-length root from a double-length argument. Then if the precision of quantities b_i and d_i is double-length and of the remaining quantities single-length, no further thought need be given to the size of the numbers occurring in the iterative process. Moreover, it will be found that difficulties do not arise when Y is small. For instance with $Y = 0$ and $X = 1{\cdot}000004$, we obtain $\mathfrak{i}$ with an error of only 4×10^{-6}.

Acknowledgements

The work described above has been carried out as part of the research programme of the National Physical Laboratory, and this paper is published by permission of the Director of the Laboratory.

APPENDIX A

THE LINEAR DEPENDENCE RELATIONS

Equations (4), (6), (8) may be proved by integration by parts as follows. Putting

$$R(\theta) = X - \tfrac{1}{2}(1 - \cos\theta), \qquad W(\theta) = (R^2 + Y^2)^{\frac{1}{2}}, \tag{20}$$

we have

$$\int_0^\pi \cos n\theta W(\theta)\, d\theta = \left[\frac{\sin n\theta}{n} W(\theta)\right]_0^\pi + \frac{1}{2}\int_0^\pi \frac{\sin n\theta \sin\theta R(\theta)\, d\theta}{n\, W(\theta)}, \tag{21}$$

where the first term on the right is zero if n is a positive integer. Further we have identically

$$\frac{1}{2}\frac{\sin n\theta \sin\theta}{n}+\frac{1}{2}\frac{\sin(n+1)\theta\sin\theta}{n+1}=\frac{\cos(n-1)\theta-\cos(n+1)\theta}{4n}+\frac{\cos n\theta-\cos(n+2)\theta}{4(n+1)}$$

$$=\frac{\cos(n-1)\theta+\cos n\theta}{4n}-\frac{\cos n\theta+\cos(n+1)\theta}{4n(n+1)}-\frac{\cos(n+1)\theta+\cos(n+2)\theta}{4(n+1)}.$$

The sum of the two equations derived from (21) with $n = 1$ and $n = 2$ now gives equation (4). Similarly we deduce equation (6) from $n = 2$ and $n = 3$, and equation (8) from $n = 3$ and $n = 4$.

To prove the remaining formula we make use of the identity

$$\cos m\theta R(\theta)W(\theta) = \cos m\theta[W(\theta)]^2\frac{R(\theta)}{W(\theta)}.$$

Substituting from (20) for $R(\theta)$ on the left-hand side and for $[W(\theta)]^2$ on the right-hand side we deduce

$$\tfrac{1}{2}M\cos m\theta\, W(\theta)+\tfrac{1}{4}[\cos(m+1)\theta+\cos(m-1)\theta]W(\theta)$$

$$= L\cos m\theta\frac{R(\theta)}{W(\theta)}+\tfrac{1}{4}M[\cos(m+1)\theta+\cos(m-1)\theta]\frac{R(\theta)}{W(\theta)}+$$

$$+\tfrac{1}{16}[\cos(m+2)\theta+\cos(m-2)\theta]\frac{R(\theta)}{W(\theta)}. \quad (22)$$

The integral with respect to θ from 0 to π of the sum of the two equations derived from (22) with $m = 0$ and $m = 1$ is

$$\tfrac{1}{2}M(\mathrm{ii}-X+\tfrac{1}{4})+\tfrac{1}{4}[\mathrm{ii}-X+\tfrac{1}{4}+\tfrac{1}{4}(\mathrm{jj}-1)] = L(\mathrm{i}-1)+\tfrac{1}{4}M(\mathrm{i}-1+\tfrac{1}{4}\mathrm{j})+\tfrac{1}{16}(\tfrac{1}{4}\mathrm{j}+\mathrm{k}).$$

Substituting in this equation for jj from (4) we obtain (3). Similarly (5) may be obtained from $m = 1$ and $m = 2$ by substituting for kk from (6), and (7) from $m = 2$ and $m = 3$ by substituting for ll from (8).

APPENDIX B

THE TRANSFORMATION TO ELLIPTIC INTEGRALS

We use a transformation similar to that given by Curtis (5) whose equation (3) is equivalent to our (29) below. His method does not appear to be suitable for deriving all the equations we need. Our transformation is

$$\cos\theta = \frac{(P-Q)-(P+Q)\cos\alpha}{(P+Q)-(P-Q)\cos\alpha}, \quad (23)$$

where α ranges from π to 0 as θ ranges from 0 to π. This relation gives

$$-\sin\theta\, d\theta = \frac{4PQ\sin\alpha\, d\alpha}{[(P+Q)-(P-Q)\cos\alpha]^2}, \quad (24)$$

$$\sin^2\theta = \frac{4PQ\sin^2\alpha}{[(P+Q)-(P-Q)\cos\alpha]^2}, \quad (25)$$

$$[W(\theta)]^2 = \frac{PQ\{4PQ\cos^2\alpha+[(P+Q)^2-1]\sin^2\alpha\}}{[(P+Q)-(P-Q)\cos\alpha]^2}. \quad (26)$$

To simplify our subsequent equations we put

$$\left.\begin{aligned} d &= P-Q, \qquad f = P+Q \\ G(\alpha) &= 4PQ\cos^2\alpha+[(P+Q)^2-1]\sin^2\alpha \\ H(\alpha) &= G(\alpha)+\sin^2\alpha = f^2-d^2\cos^2\alpha \end{aligned}\right\}. \quad (27)$$

Equations (24), (25), (26) yield immediately

$$\frac{d\theta}{d\alpha} = -\frac{2W(\theta)}{[G(\alpha)]^{\frac{1}{2}}} \tag{28}$$

and thence

$$\frac{1}{2\pi}\int_0^{\pi}\frac{d\theta}{W(\theta)} = -\frac{1}{2\pi}\int_{\pi}^{0}\frac{2\,d\alpha}{[G(\alpha)]^{\frac{1}{2}}} = \frac{2}{\pi}\int_0^{\frac{1}{2}\pi}\frac{d\alpha}{[G(\alpha)]^{\frac{1}{2}}} = B. \tag{29}$$

Equation (28) can also be used to prove that

$$\frac{1}{2\pi}\int_0^{\pi}\frac{\cos\theta\,d\theta}{W(\theta)} = -\frac{1}{2\pi}\int_{\pi}^{0}\frac{d-f\cos\alpha}{f-d\cos\alpha}\frac{2\,d\alpha}{[G(\alpha)]^{\frac{1}{2}}} = \frac{1}{2\pi}\int_0^{\pi}\frac{d+f\cos\beta}{f+d\cos\beta}\frac{2\,d\beta}{[G(\beta)]^{\frac{1}{2}}}, \tag{30}$$

where $\beta = \pi - \alpha$. Taking the mean of the last two expressions we derive

$$\frac{1}{2\pi}\int_0^{\pi}\frac{\cos\theta\,d\theta}{W(\theta)} = \frac{1}{2\pi}\int_0^{\pi}\frac{2fd(1-\cos^2\alpha)}{f^2-d^2\cos^2\alpha}\frac{d\alpha}{[G(\alpha)]^{\frac{1}{2}}} = C. \tag{31}$$

A final application of equation (28) gives

$$\frac{1}{\pi}\int_0^{\pi}\frac{\sin^2\theta\,d\theta}{W(\theta)} = -\frac{1}{\pi}\int_{\pi}^{0}\frac{8PQ\sin^2\alpha}{(f-d\cos\alpha)^2}\frac{d\alpha}{[G(\alpha)]^{\frac{1}{2}}} = \frac{1}{\pi}\int_0^{\pi}\frac{8PQ\sin^2\beta}{(f+d\cos\beta)^2}\frac{d\beta}{[G(\beta)]^{\frac{1}{2}}} \tag{32}$$

Taking the mean of the last two expressions, we derive

$$\frac{1}{\pi}\int_0^{\pi}\frac{\sin^2\theta\,d\theta}{W(\theta)} = \frac{1}{\pi}\int_0^{\pi}8PQ\sin^2\alpha\,\frac{(f^2+d^2\cos^2\alpha)}{(f^2-d^2\cos^2\alpha)^2}\frac{d\alpha}{[G(\alpha)]^{\frac{1}{2}}}. \tag{33}$$

Now

$$\frac{d}{d\alpha}\left[\frac{d^2\cos\alpha\sin\alpha[G(\alpha)]^{\frac{1}{2}}}{H(\alpha)}\right]$$
$$= \frac{1}{[G(\alpha)]^{\frac{1}{2}}[H(\alpha)]^2} - \{2\cos^2\alpha\sin^2\alpha d^4G(\alpha) + (2\cos^2\alpha - 1)d^2G(\alpha)H(\alpha) -$$
$$-\cos^2\alpha\sin^2\alpha d^2(1-d^2)H(\alpha)\}. \tag{34}$$

The expression in the curly brackets on the right of (34) is a polynomial in $\cos^2\alpha$ of the third degree which can be expressed in terms of the independent quantities $[H(\alpha)]^2\cos^2\alpha$, $[H(\alpha)]^2$, $H(\alpha)\sin^2\alpha$, $\sin^2\alpha(f^2+d^2\cos^2\alpha)$ in the form

$$[1-(1-d^2)\cos^2\alpha][H(\alpha)]^2 - \sin^2\alpha f^2d^2H(\alpha) - (f^2-d^2)\sin^2\alpha(f^2+d^2\cos^2\alpha).$$

Using this expression, integrating (34) with respect to α from 0 to $\frac{1}{2}\pi$ and substituting from equations (29), (31), (33) we obtain

$$\frac{1}{\pi}\int_0^{\pi}\cos\theta\,\frac{R(\theta)\,d\theta}{W(\theta)} = A. \tag{35}$$

We are now in a position to prove the relations connecting i, j, ii with A, B, C, namely (12), (13), (14). Equations (29), (31), (35) give (12). Next, we have

$$\frac{d}{d\theta}[\sin\theta W(\theta)] = \frac{1}{W(\theta)}[-\tfrac{1}{4}M + (X^2+Y^2-X)\cos\theta + \tfrac{3}{4}M\cos^2\theta + \tfrac{1}{2}\cos^3\theta].$$

Integrating this result with respect to θ from 0 to π we obtain an expression for $\int_0^{\pi}\frac{\cos^3\theta}{W(\theta)}d\theta$ which, where used in conjunction with (31), (35) gives (13) and also with (29), (31), (35) gives (14).

REFERENCES

1. H. Multhopp, *Methods for Calculating the Lift Distribution of Wings*, A.R.C., R. and M. 2884 (1955).
2. H. C. Garner, *Multhopp's Subsonic Lifting Surface Theory of Wings in Flow Pitching Oscillations*, ibid. 2885 (1956).
3. A. R. Curtis, *Tables of Multhopp's Influence Functions*, N.P.L. Mathematics Division report Ma./21/0505 (1952).
4. W. Bartky, 'Numerical calculation of a generalized complete elliptic integral', *Rev. Mod. Phys.* **10** (1938) 264.
5. A. R. Curtis, 'Some elliptic integrals', *Math. Gazette* **38** (1954) 199.

AN APPROXIMATE SOLUTION OF THE ONE-DIMENSIONAL TRANSPORT EQUATION

By M. G. SMITH

(*Armament Research and Development Establishment, Fort Halstead, Sevenoaks, Kent*†)

[Received 25 April 1958; revise received 4 September 1958]

SUMMARY

An approximate method for obtaining a solution of the simplest form of the transport equation is described. The approximation is of the 'diffusion' type, but it incorporates fitting certain parameters by least squares, and so, it is hoped, gives better solutions than the straightforward approximation of this type.

A numerical solution is exhibited for a simple case, and this shows features characteristic of 'diffusion' solutions, but gives a good qualitative and quantitative solution.

The method can be extended to obtain an approximate solution of the transport equation in other coordinate systems.

1. Introduction

THE simplest case of the transport equation, the one we will designate 'one-dimensional', is

$$\mu \frac{\partial i}{\partial z} + i = \tfrac{1}{2}\varpi \sum_{r=0}^{\infty} a_r P_r(\mu) \int_{-1}^{1} i(z, \mu') P_r(\mu')\, d\mu'. \tag{1.1}$$

Here i is the intensity of radiation at a point in a semi-infinite isotropic distribution of scattering particles in a given direction. The point is defined by the single space coordinate z (a pure number measuring the depth below the surface in multiples of the mean free path of the particle distribution), and the direction in which the intensity is measured by θ, the angle between the given direction and the normal to the surface $z = 0$. As usual, $\mu = \cos\theta$.

The optical properties of the scattering material are given by the 'albedo' for scattering ϖ ($\leqslant 1$), which measures the fraction of radiation scattered, and the scattering function

$$f(\Theta) = \sum_{r=0}^{\infty} a_r P_r(\cos\Theta), \tag{1.2}$$

which measures the density of radiation scattered in a direction at an angle Θ from incident unit intensity of radiation.

† Present address: Mathematics Department, Sir John Cass College, University of London.

The usual boundary conditions are that the intensity be specified over the forward hemisphere at $z = 0$, and over the backward hemisphere at some other point $z = z_0$.

Using the Wiener–Hopf technique (1), an analytical solution is possible when the latter boundary condition is given at infinity. In general, however, the complexity of the analytic solutions is so great that it is necessary to find numerical solutions also. To obtain any reasonable degree of accuracy in solution, the time and space required is such that it is only really feasible using a modern high-speed computer.

For this reason there has always been considerable interest in approximate methods. The most important and successful is that of Chandrasekhar (see **2**), which replaces the integral on the right-hand side by a quadrature formula. Solving a system of linear differential equations, and using the properties of the Legendre function, a solution accurate to any desired order is obtained. As the corresponding treatment for the equation when expressed in spherical polar coordinates is not so convenient, a method was sought that could be applied to more general forms of the transport equation.

Another method involves solving what is, in fact, a different physical problem by the use of the diffusion equation. This method gives solutions which are least accurate near the boundaries—usually the places of greatest interest.

The method proposed here is based largely on the latter method, but should in general give a better answer.

2. The integral equations

We shall consider, for simplicity, the case when only the first two terms appear in the summation on the right-hand side. Bearing in mind the normalization condition implicit in the definition of the scattering function this then becomes

$$\tfrac{1}{2}\varpi\left\{\int_{-1}^{1} i(z,\mu')\,d\mu' + \beta\mu\int_{-1}^{1} i(z,\mu')\mu'\,d\mu'\right\}, \tag{2.1}$$

where β is a positive constant. This represents an ovoid scattering pattern, that is, one scattering more radiation forward, and less backward, than in the isotropic case.

We shall take as boundary conditions:

$$i(0,\mu) = 1 \quad \text{if} \quad 0 \leqslant \mu \leqslant 1$$

and

$$i(z_0,\mu) = 0 \quad \text{if} \quad -1 \leqslant \mu \leqslant 0.$$

Because these conditions are only specified on half boundaries it is convenient to extend the notation. We put

$$\begin{aligned} i(z,\mu) &= I(z,\mu) \quad \text{if} \quad 0 \leqslant \mu \leqslant 1 \\ &= J(z,-\mu) \quad \text{if} \quad -1 \leqslant \mu \leqslant 0, \end{aligned}$$

and write further

$$p(z) = \int_0^1 \{I(z,\mu') + J(z,\mu')\}\, d\mu'$$

and

$$q(z) = \int_0^1 \{I(z,\mu') - J(z,\mu')\}\mu'\, d\mu'.$$

Then equation (1.1) becomes

$$0 \leqslant z \leqslant z_0 \quad \text{and} \quad 0 \leqslant \mu \leqslant 1,$$

$$\mu \frac{\partial I}{\partial z} + I = \tfrac{1}{2}\varpi[p(z) + \beta\mu q(z)], \tag{2.2}$$

and

$$\mu \frac{\partial J}{\partial z} - J = \tfrac{1}{2}\varpi[-p(z) + \beta\mu q(z)]. \tag{2.3}$$

The corresponding boundary conditions are

$$I(0,\mu) = 1 \tag{2.4}$$

and

$$J(z_0,\mu) = 0 \quad \text{for all } \mu. \tag{2.5}$$

Integrating (2.2) and (2.3) as if the right-hand sides of the equations were known functions, we obtain integral equations for $I(z,\mu)$ and $J(z,\mu)$, viz.

$$I(z,\mu) = e^{-z/\mu} + \frac{\varpi}{2\mu}\int_0^z e^{(t-z)/\mu}\{p(t) + \beta\mu q(t)\}\, dt \tag{2.6}$$

and

$$J(z,\mu) = \frac{\varpi}{2\mu}\int_z^{z_0} e^{(z-t)/\mu}\{p(t) - \beta\mu q(t)\}\, dt. \tag{2.7}$$

Now

$$\int_0^1 \mu^{1-n} e^{-a/\mu}\, d\mu = E_n(a),$$

whence, by the definition of $p(z)$ and $q(z)$, we find that

$$p(z) = E_2(z) + \tfrac{1}{2}\varpi\int_0^{z_0} [p(t)E_1\{|t-z|\} + \beta\,\mathrm{sgn}(z-t)q(t)E_2\{|t-z|\}]\, dt, \tag{2.8}$$

$$q(z) = E_3(z) + \tfrac{1}{2}\varpi\int_0^{z_0} [\mathrm{sgn}(z-t)p(t)E_2\{|t-z|\} + \beta q(t)E_3\{|t-z|\}]\, dt, \tag{2.9}$$

a pair of simultaneous integral equations for $p(z)$ and $q(z)$. If $\varpi = 1$, then, from (2.7)

$$J(z_0-z,\mu) = \frac{1}{2\mu}\int_{z_0-z}^{z_0} e^{(z_0-z-t)/\mu}\{p(t)-\beta\mu q(t)\}\,dt$$

$$= \frac{1}{2\mu}\int_0^z e^{(u-z)/\mu}\{p(z_0-u)-\beta\mu q(z_0-u)\}\,du,$$

and therefore

$$I(z,\mu)+J(z_0-z,\mu) = e^{-z/\mu}+\int_0^z e^{(t-z)/\mu}[\{p(t)+p(z_0-t)\}+ +\beta\mu\{q(t)-q(z_0-t)\}]\,dt.$$

It is easy to see that this integral equation is satisfied identically by

$$I(z,\mu)+J(z_0-z,\mu) = 1. \tag{2.10}$$

3. Differential relations

If we integrate (2.2) and (2.3) between $\mu = 0$ and $\mu = 1$ and subtract, we obtain

$$\frac{dq}{dz}+(1-\varpi)p = 0, \tag{3.1}$$

and if we multiply (2.2) and (2.3) by μ, integrate and add, we obtain

$$\frac{dr}{dz}+\left(1-\frac{\beta\varpi}{3}\right)q = 0, \tag{3.2}$$

where by analogy we have put

$$r(z) = \int_0^1 \{I(z,\mu')+J(z,\mu')\}\mu'^2\,d\mu'.$$

We may obviously continue this process to obtain differential equations for the higher moment functions. There will, however, always be one less equation than there are moment functions.

4. The approximate solution

We shall now assume that

$$r(z) = \lambda p(z), \tag{4.1}$$

and substitute this into (3.2). There is no obvious immediate physical interpretation of this assumption, though it implies a diffusion-like solution. The justification lies in its utility.

Eliminating $q(z)$ between (3.1), (3.2), and (4.1), we find

$$\lambda\frac{d^2p}{dz^2}-\gamma(1-\varpi)p = 0 \tag{4.2}$$

where $\gamma = 1-\frac{1}{3}\beta\varpi$. If then $\varpi \neq 1$,

$$p(z) = Ae^{\alpha z}+Be^{-\alpha z}, \tag{4.3}$$

and

$$q(z) = \frac{\lambda\alpha}{\gamma}\{Be^{-\alpha z}-Ae^{\alpha z}\}, \tag{4.4}$$

where

$$\lambda\alpha^2-\gamma(1-\varpi) = 0. \tag{4.5}$$

Now whatever values are given to A, B, and α, if (4.3) and (4.4) are substituted into (2.6) and (2.7) we have values for $I(z,\mu)$ and $J(z,\mu)$ which satisfy the boundary conditions.

Thus we will choose A, B, and α to give a good solution of the pair of integral equations (2.8) and (2.9) in the sense of Gauss.

Let $\bar{p}(z)$ and $\bar{q}(z)$ be the functions obtained by substituting (4.3) and (4.4) into the right-hand sides of (2.8) and (2.9). Now

$$\int_0^{z_0} \operatorname{sgn}(z-t)q(t)E_2\{|z-t|\}\,dt = -\frac{\lambda}{\gamma}\int_0^{z_0} \operatorname{sgn}(z-t)\frac{dp}{dt}E_2\{|z-t|\}\,dt$$

$$= -\frac{\lambda}{\gamma}\left[-\int_0^{z_0} p(t)E_1\{|t-z|\}\,dt+2p(z)-p(z_0)E_2(z_0-z)-p(0)E_2(z)\right],$$

after an integration by parts. Hence

$$\bar{p}(z) = \left(1+\frac{\varpi\lambda\beta}{2\gamma}p(0)\right)E_2(z)+\frac{\varpi\lambda\beta}{2\gamma}p(z_0)E_2(z_0-z)-\frac{\varpi\beta\lambda}{\gamma}p(z)+$$

$$+\tfrac{1}{2}\varpi\left(1+\frac{\beta\lambda}{\gamma}\right)\int_0^{z_0} p(t)E_1\{|z-t|\}\,dt, \tag{4.6}$$

and similarly

$$\bar{q}(z) = \left(1+\frac{\varpi\lambda\beta}{2\gamma}p(0)\right)E_3(z)-\frac{\varpi\lambda\beta}{4\gamma}p(z_0)E_3(z_0-z)+\frac{\varpi}{2(1-\varpi)}\left(1+\frac{\beta\lambda}{\gamma}\right)\times$$

$$\times[q(z_0)E_2(z_0-z)+q(0)E_2(z)-2q(z)]+\frac{\varpi}{2(1-\varpi)}\left(1+\frac{\beta\lambda}{\gamma}\right)\int_0^{z_0} q(t)E_1\{|z-t|\}\,dt. \tag{4.7}$$

The integrals $F_n\left(z,\frac{1}{a}\right) = \int_0^z e^{at}E_n(t)\,dt$ (see **2** and **3**)

can be determined, and so

$$\int_0^{z_0} e^{\alpha t}E_1\{|t-z|\}\,dt = \frac{2}{\alpha}\tanh^{-1}\alpha e^{\alpha z}+\frac{e^{\alpha z}}{\alpha}[E_1\{(1+\alpha)z\}-E_1\{(1-\alpha)(z_0-z)\}]+$$

$$+\frac{e^{\alpha z_0}}{\alpha}E_1(z-z_0)-\frac{1}{\alpha}E_1(z). \tag{4.8}$$

Thus if (4.3) and (4.4) are substituted into (4.6) and (4.7) the term in $\bar{p}(z)$ which for large z is of order $e^{\alpha z}$ is

$$A\varpi\left\{\left(1+\frac{\beta\lambda}{\gamma}\right)\frac{\tanh^{-1}\alpha}{\alpha}-\frac{\beta\lambda}{\gamma}\right\}e^{\alpha z}=A\varpi\left[1-\left\{1+\frac{\beta(1-\varpi)}{\alpha^2}\right\}\left\{1-\frac{\tanh^{-1}\alpha}{\alpha}\right\}\right]e^{\alpha z}.$$

Similarly the term in $\bar{q}(z)$ of order $e^{\alpha z}$ is

$$-\frac{A\varpi}{\alpha}\left\{1+\frac{\beta(1-\varpi)}{\alpha^2}\right\}\left\{1-\frac{\tanh^{-1}\alpha}{\alpha}\right\}e^{\alpha z}.$$

Thus if α is chosen to be a root of the equation

$$1-\varpi+\varpi\left\{1+\frac{\beta(1-\varpi)}{\alpha^2}\right\}\left\{1-\frac{\tanh^{-1}\alpha}{\alpha}\right\}=0, \tag{4.9}$$

the terms in $p(z)$ and $\bar{p}(z)$ which are dominant for large z will be the same, as will also those in $q(z)$ and $\bar{q}(z)$. Since the left-hand side of the above equation is an even function of α, the coefficients of $e^{-\alpha z}$ will then also agree. It can soon be verified that, for small values of $1-\varpi$, there is a single pair of symmetrically placed real zeros in the strip $-1<\operatorname{re}\alpha<1$. The appropriate value of λ can be determined from equation (4.5). The roots of (4.9) for some values of ϖ and β are tabulated below.

TABLE

Root $\bar{\alpha}$ of the equation

$$1-\varpi+\varpi\left\{1+\frac{\beta(1-\varpi)}{\alpha^2}\right\}\left\{1-\frac{\tanh^{-1}\alpha}{\alpha}\right\}=0$$

β \ ϖ	1·00000	0·96875	0·93750	0·90625
0·25000	0·000000	0·289885	0·405289	0·490590
0·21875	0·000000	0·291471	0·407425	0·493074
0·18750	0·000000	0·293048	0·409549	0·495546
0·15625	0·000000	0·294617	0·411663	0·498005
0·12500	0·000000	0·296177	0·413765	0·500451
0·09375	0·000000	0·297729	0·415857	0·502885
0·06250	0·000000	0·299274	0·417938	0·505307
0·03125	0·000000	0·300810	0·420009	0·507718
0·00000	0·000000	0·302338	0·422070	0·510116

β \ ϖ	0·87500	0·84375	0·81250	0·78125
0·25000	0·559727	0·618149	0·668674	0·712986
0·21875	0·562443	0·621014	0·671624	0·715968
0·18750	0·565145	0·623865	0·674559	0·718935
0·15625	0·567833	0·626701	0·677479	0·721887
0·12500	0·570508	0·629523	0·680385	0·724824
0·09375	0·573170	0·632332	0·683277	0·727746
0·06250	0·575819	0·635127	0·686154	0·730654
0·03125	0·578456	0·637908	0·689018	0·733547
0·00000	0·581079	0·640676	0·691868	0·736426

The coefficients A and B are now determined from the condition that the mean square deviation of $\tilde{p}(z)$ from $p(z)$, and of $\tilde{q}(z)$ from $q(z)$ shall be a minimum.

Let
$$H(A, B) = \int_0^{z_0} [\{\tilde{p}(z)-p(z)\}^2+\{\tilde{q}(z)-q(z)\}^2]\, dz \tag{4.10}$$

where $p(z)$ and $q(z)$ are given by (4.3) and (4.4). Then

$$\frac{\partial H}{\partial A} = 0, \qquad \frac{\partial H}{\partial B} = 0$$

are a pair of simultaneous equations to determine A and B.

When these values of α, A, and B are substituted into (4.3) and (4.4) we shall have an optimum solution of the integral equations (2.8) and (2.9). If these functions in their turn are substituted into (2.6) and (2.7) we have finally

$$I(z,\mu) = e^{-z/\mu}\left[1-\tfrac{1}{2}\varpi\left\{\frac{A}{1+\alpha\mu}\left(1-\frac{\beta(1-\varpi)}{\alpha}\mu\right)+\frac{B}{1-\alpha\mu}\left(1+\frac{\beta(1-\varpi)}{\alpha}\mu\right)\right\}\right]+$$
$$+\tfrac{1}{2}\varpi\left[\frac{A}{1+\alpha\mu}\left(1-\frac{\beta(1-\varpi)}{\alpha}\mu\right)e^{\alpha z}+\frac{B}{1-\alpha\mu}\left(1+\frac{\beta(1-\varpi)}{\alpha}\mu\right)e^{-\alpha z}\right] \tag{4.11}$$

and

$$J(z,\mu) = \tfrac{1}{2}\varpi\left[\frac{A}{1-\alpha\mu}\left(1+\frac{\beta(1-\varpi)}{\alpha}\mu\right)e^{\alpha z}+\frac{B}{1+\alpha\mu}\left(1-\frac{\beta(1-\varpi)}{\alpha}\right)e^{-\alpha z}\right]-$$
$$-\tfrac{1}{2}\varpi\left[\frac{A}{1-\alpha\mu}\left(1+\frac{\beta(1-\varpi)}{\alpha}\mu\right)e^{\alpha z_0}+\frac{B}{1+\alpha\mu}\left(1-\frac{\beta(1-\varpi)}{\alpha}\right)e^{-\alpha z_0}\right]e^{(z-z_0)/\mu}. \tag{4.12}$$

If the region extends to infinity ($z_0 = \infty$), the appropriate solution would require that $A \equiv 0$, since the intensity is bounded.

5. The case of no absorption

When $\varpi = 1$, equations (4.2), (3.2), and (4.1) give

$$p(z) = Az+B \tag{5.1}$$

and
$$q(z) = -\frac{\lambda}{\gamma}A. \tag{5.2}$$

Then, if we define $\tilde{p}(z)$ and $\tilde{q}(z)$ as before,

$$\tilde{p}(z) = Az+B+E_2(z)+\tfrac{1}{2}A\left[\left\{1+\frac{\lambda\beta}{\gamma}\right\}\{E_3(z)-E_3(z_0-z)\}-z_0E_2(z_0-z)\right]-$$
$$-\tfrac{1}{2}B\{E_2(z)+E_2(z_0-z)\}, \tag{5.3}$$

and

$$\bar{q}(z) = -\tfrac{1}{3}A\left\{1+\frac{\lambda\beta}{\gamma}\right\}+$$
$$+E_3(z)+\tfrac{1}{2}A\left[\left\{1+\frac{\lambda\beta}{\gamma}\right\}\{E_4(z)+E_4(z_0-z)\}+z_0E_3(z_0-z)\right]-$$
$$-\tfrac{1}{2}B\{E_3(z)-E_3(z_0-z)\}. \quad (5.4)$$

The terms in $\bar{p}(z)$ and $p(z)$ which do not decay exponentially agree whatever the value of λ. The constant in $\bar{q}(z)$ is the same as that in $q(z)$ if

$$\lambda = \tfrac{1}{3}. \quad (5.5)$$

(It can easily be verified from (4.5) and (4.9) that $\lambda \to \frac{1}{3}$ as $\varpi \to 1$. This is in fact the well-known Milne–Eddington approximation.)

As before, A and B are determined so as to minimize

$$H(A, B) = \int_0^{z_0} [\{\bar{p}(z)-p(z)\}^2+\{\bar{q}(z)-q(z)\}^2]\, dz.$$

Now $E_2(z)+E_2(z_0-z)$ and $E_4(z)+E_4(z_0-z)$ are even functions of $z-\frac{1}{2}z_0$, and $E_3(z)-E_3(z_0-z)$ is an odd function of $z-\frac{1}{2}z_0$, and so

$$\int_0^{z_0} \{E_2(z)+E_2(z_0-z)\}\{E_3(z)-E_3(z_0-z)\}\, dz$$
$$= \int_0^{z_0} \{E_3(z)-E_3(z_0-z)\}\{E_4(z)+E_4(z_0-z)\}\, dz = 0,$$

and $$\int_0^{z_0} \{E_2^2(z)+E_3^2(z)\}\, dz = \int_0^{z_0} \{E_2^2(z_0-z)+E_3^2(z_0-z)\}\, dz.$$

Hence the equation $$\frac{\partial H}{\partial B} = 0$$

reduces to $$\tfrac{1}{2}(Az_0)+B = 1, \quad (5.6)$$

which is equivalent to equation (2.10).

6. Numerical solution

A numerical solution, using the above approximation, has been computed for the case when $\varpi = 1$, $\beta = 0{\cdot}1$, and $z_0 = 2{\cdot}0$, as a solution of the complete equation with these parametric values already existed but is unpublished. It had been computed by solving the integral equations (2.6) and (2.7) by a Picard iteration method.

The comparison of the two solutions is shown in Fig. 1; the approximate solution is drawn as a full line, and the solution of the full equations as a dotted line.

It will be seen that the greatest discrepancy is always near to each

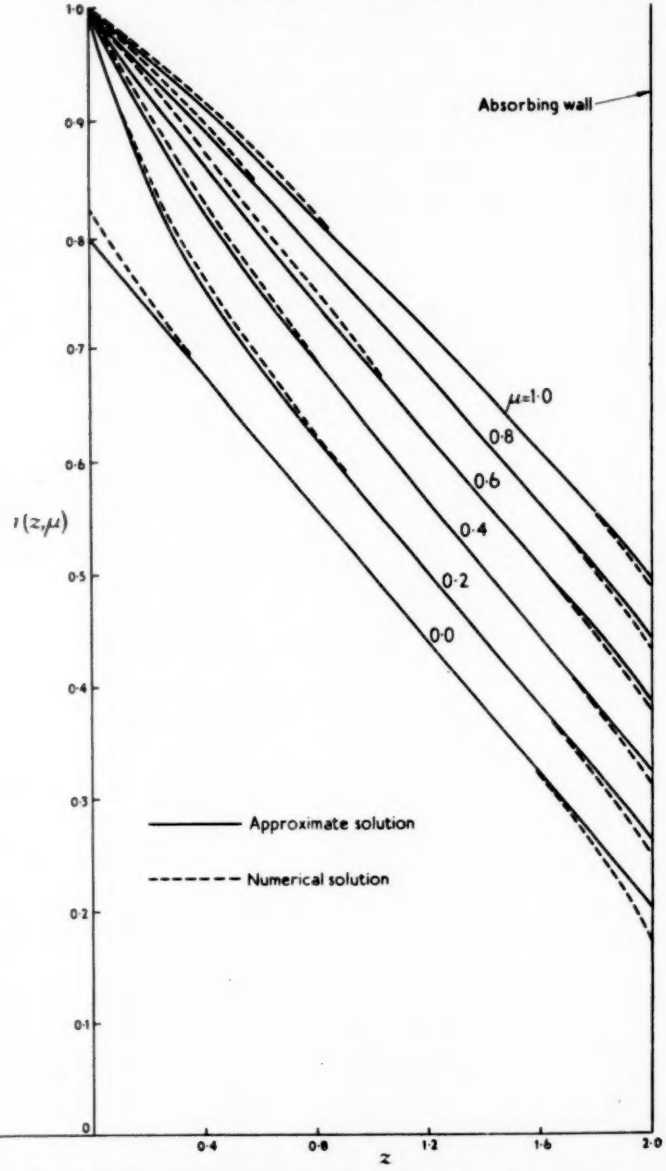

FIG. 1. Solution of the one-dimensional transport equation, with linear scattering, when there is no absorption, and $\beta = 0{\cdot}1$.

boundary, a fault which, as pointed out above, is characteristic of 'diffusion' approximations. The approximations get progressively worse as the direction in which the intensity is measured moves from the forward direction towards the side. Even at its worst, however, the approximation gives both a good qualitative and quantitative description of the solution.

The author wishes to thank Miss K. M. Stocks of the Armament Research and Development Establishment, for her help with the computations.

REFERENCES

1. I. N. Sneddon, *Fourier Transforms* (McGraw-Hill, 1951), pp. 262–6.
2. S. Chandrasekhar, *Radiative Transfer* (Oxford, 1950).
3. V. Kourganoff, *Basic Methods in Transfer Theory* (Oxford, 1952).

THE QUARTERLY JOURNAL OF MECHANICS AND APPLIED MATHEMATICS

VOLUME XIII PART 1 FEBRUARY 1960

CONTENTS

The Editorial Board gratefully acknowledge the support given by: Blackburn & General Aircraft Limited; Bristol Aeroplane Company; Courtaulds Scientific and Educational Trust Fund; English Electric Company; Hawker Siddeley Group Limited; Imperial Chemical Industries Limited; Metropolitan-Vickers Electrical Company Limited; The Shell Petroleum Co. Limited; Vickers-Armstrongs (Aircraft) Limited.